CAPITAL UNIVERSITY OF SCIENCE AND TECHNOLOGY, ISLAMABAD

Sliding Mode Fault Tolerant Control of Air Path Actuators in a Turbocharged Diesel Engine

by

Ghulam Murtaza

A thesis submitted in partial fulfillment for the
degree of Doctor of Philosophy

in the

Faculty of Engineering
Department of Electrical Engineering

2018

Sliding Mode Fault Tolerant Control of Air Path Actuators in a Turbocharged Diesel Engine

By

Ghulam Murtaza

(PE 141006)

Prof. Dr. Kamran Iqbal

University of Arkansas at Little Rock, Arkansas, USA

Dr. Halim Alwi, Lecturer

Department of Engineering, University of Exeter, UK

Dr. Aamir Iqbal Bhatti

(Thesis Supervisor)

Dr. Noor Muhammad Khan

(Head, Department of Electrical Engineering)

Dr. Imtiaz Ahmed Taj

(Dean, Faculty of Engineering)

DEPARTMENT OF ELECTRICAL ENGINEERING

CAPITAL UNIVERSITY OF SCIENCE AND TECHNOLOGY

ISLAMABAD

2018

Copyright © 2018 by Ghulam Murtaza

Dedicated to my parents

CERTIFICATE OF APPROVAL

This is to certify that the research work presented in the thesis, entitled **"Sliding Mode Framework Based Fault Tolerant Control for Air Path Actuators of a Turbocharged Diesel Engine"** was conducted under the supervision of **Dr. Aamir Iqbal Bhatti**. No part of this thesis has been submitted anywhere else for any other degree. This thesis is submitted to the **Department of Electrical Engineering, Capital University of Science and Technology** in partial fulfillment of the requirements for the degree of Doctor in Philosophy in the field of **Electrical Engineering**. The open defence of the thesis was conducted on **October 26, 2018**.

Student Name: Mr. Ghulam Murtaza (PE141006)

The Examining Committee unanimously agrees to award PhD degree in the mentioned field.

Examination Committee :

(a)	External Examiner 1:	Dr. Javaid Iqbal Associate Professor CE&ME, NUST, Islamabad
(b)	External Examiner 2:	Dr. Abdul Khaliq Professor SSCIT, Islamabad
(c)	Internal Examiner :	Dr. Fazal ur Rehman Professor CUST, Islamabad

Supervisor Name : Dr. Aamir Iqbal Bhatti
Professor
CUST, Islamabad

Name of HoD : Dr. Noor Muhammad Khan
Professor
CUST, Islamabad

Name of Dean : Dr. Imtiaz Ahmad Taj
Professor
CUST, Islamabad

AUTHOR'S DECLARATION

I, **Mr. Ghulam Murtaza** **(Registration No. PE-141006)**, hereby state that my PhD thesis titled, '**Sliding Mode Framework Based Fault Tolerant Control for Air Path Actuators of a Turbocharged Diesel Engine**' is my own work and has not been submitted previously by me for taking any degree from Capital University of Science and Technology, Islamabad or anywhere else in the country/ world.

At any time, if my statement is found to be incorrect even after my graduation, the University has the right to withdraw my PhD Degree.
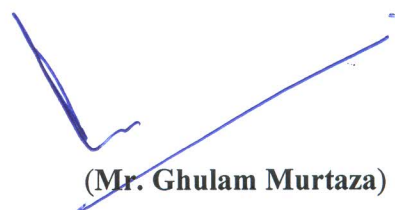
(Mr. Ghulam Murtaza)

Dated: 26 October, 2018

Registration No : PE-141006

PLAGIARISM UNDERTAKING

I solemnly declare that research work presented in the thesis titled "**Sliding Mode Framework Based Fault Tolerant Control for Air Path Actuators of a Turbocharged Diesel Engine**" is solely my research work with no significant contribution from any other person. Small contribution/ help wherever taken has been duly acknowledged and that complete thesis has been written by me.

I understand the zero tolerance policy of the HEC and Capital University of Science and Technology towards plagiarism. Therefore, I as an author of the above titled thesis declare that no portion of my thesis has been plagiarized and any material used as reference is properly referred/ cited.

I undertake that if I am found guilty of any formal plagiarism in the above titled thesis even after award of PhD Degree, the University reserves the right to withdraw/ revoke my PhD degree and that HEC and the University have the right to publish my name on the HEC/ University Website on which names of students are placed who submitted plagiarized thesis.

Dated: 26 October, 2018
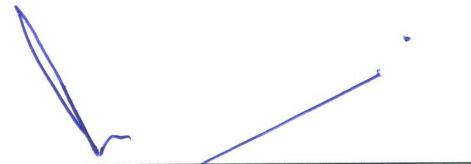
(**Mr. Ghulam Murtaza**)
Registration No. PE-141006

List of Publications

It is certified that following publication(s) have been made out of the research work that has been carried out for this thesis:-

Journal Publications

1. **G. Murtaza**, A. I. Bhatti and Y. A. Butt, "Super twisting controller-based unified FDI and FTC scheme for air path of diesel engine using the certainty equivalence principle," Proceedings of the Institution of Mechanical Engineers, Part D: Journal of Automobile Engineering. Oct 2018, vol. 232, no. 12, pp. 1623-1633. DOI: 10.1177/0954407017732860.

2. **G. Murtaza**, A. I. Bhatti and Y. A. Butt, "Unified FDI and FTC Scheme for Air Path Actuators of a Diesel Engine Using ISM Extended with Adaptive Part," Asian Journal of Control. Nov 2019. (Accepted) DOI: 10.1002/asjc.1871.

Conference Publications

1. **G. Murtaza**, A. I. Bhatti and Y. A. Butt, "Higher order sliding mode based control scheme for air path of diesel engine," in International Conference on Emerging Technologies (ICET), Isb, Pak, Oct 2016, pp. 1-6. IEEE. DOI: 10.1109/ICET.2016.7813217.

2. **G. Murtaza**, A. I. Bhatti, Y. A. Butt and R. Anjum, "FTC for air path actuators of a diesel engine using VGSTA," in International Conference on Emerging Technologies (ICET), Isb, Pak, Dec 2017, pp. 1-6. IEEE. DOI: 10.1109/ICET.2017.8281652.

Acknowledgements

All praises be to Allah Almighty, the most merciful and all powerful.

I am deeply grateful to my supervisor Dr. Aamer Iqbal Bhatti whose persistent guidance and encouragement has always been a source of motivation. I am also especially thankful to my friend, my co-supervisor Dr. Yasir Awais Butt, without his support this couldn't have been possible. Not to forget my family for their continued prayers and support, the unrestricted guidance of the faculty throughout my academic career at CUST, the technical staff and members of CASPR, the management of CUST and all others, too numerous to list, for their ever ready assistance.

Abstract

Exhaust emission control, especially in case of diesel engines, is a challenging research problem as the emission regulating authorities place stringent protocols against emissions. The air management system of a diesel engine, that is fitted with Variable Geometry Turbocharger (VGT) and Exhaust Gas Recirculation (EGR) actuators, is among the sub-systems, whose effective control ensures that emissions are kept to minimum. Both EGR and VGT sub-systems are located in the engine exhaust channel, hence, they are strongly coupled and exposed to high temperatures, un-burnt hydrocarbons and lubricants and thus prone to faults/choking. One way to increase tolerance against faults is to have redundancy. Diesel engines do not have high number of identical actuators to preserve satisfactory operation, but, still have prospects for enhancing the reliability of these control loops by constructing algorithms, that are capable of performing online detection, diagnosis, estimation and compensation of faults. This research investigates the possible options for development of Fault Tolerant Control (FTC) schemes for coordinated control of air management system actuators of diesel engine. The dynamic nature of a control system and real time environment of Fault Detection and Isolation (FDI) and controller re-configuration requires FTC system to be capable of detecting, identifying and accommodating the faults as swiftly as possible. To meet the purpose, unified and systematic design techniques need to be developed to guarantee swift integration of FDI and FTC schemes, such that, the faults are handled in an early design phase by extending the control system with additional modules, i.e., FDI module. The model used in this research is a fully validated industrial scale Mean Value Model of a diesel engine that is equipped with VGT and EGR actuators. It has eight states and three control inputs. Two types of approaches i.e., passive FTC and unified FDI and FTC with further two algorithms of each have been proposed based on the sliding mode framework. The simulation results have shown that the proposed controllers can comfortably meet strict emission regulations even in the event of system faults. Specially fault detection, estimation and compensation capability of unified approaches give them an edge over passive schemes.

Contents

List of Figures

List of Tables

Abbreviations

BSR	Blade Speed Ratio
CESTA	Certainty Equivalence Super Twisting Algorithm
EGR	Exhaust Gas Recirculation
FDI	Fault Detection and Isolation
FTC	Fault Tolerant Control
HOSMC	Higher Order Sliding Mode Control
ISM	Integral Sliding Mode
LPV	Linear Parameter Varying
LUT	Look Up Table
MPC	Model Predictive Control
MIMO	Multiple Input Multiple Output
MVM	Mean Value Model
NMPC	Non-linear Model Predictive Control
OBD	On-Board diagnosis
ODE	Ordinary Differential Equation
PDE	Partial Differential Equation
PLS	Partial Least Squares
PCA	Principal Component Analysis
SISO	Single Input Single Output
SM	Sliding Mode
SMC	Sliding Mode Control
STA	Super Twisting Algorithm
VGSTA	Variable Gain Super Twisting Algorithm
VGT	Variable Geometry Turbocharger

Chapter 1

Introduction

1.1 Background

The concerns of reliability, operational safety and ecological safeguard are of great significance, particularly for safety critical systems like nuclear reactors, space crafts, air planes, banking systems, transportation systems and chemical industries. In case of occurrence of faults, consequences can be grave with regards to loss of human lives, environmental influence and financial losses. Hence, there is a requirement for developing online supervision, fault diagnosis and fault tolerant schemes to enhance the reliability of these safety critical systems. FDI and FTC schemes are drawing more attention lately, for process monitoring and control for the ever growing demand of reliability, safety and enhanced performance of dynamic systems. Early detection and diagnosis of mal-function when the system is working in a controllable region can assist in prevention of anomalous system functions and decrease productivity loss, which helps evading unnecessary interruptions in system operation and catastrophes. Therefore, FDI and FTC are the most important research topics drawing substantial attention from industrial practitioners and research scholars. Design of a diagnosis system is one imperative step towards development of FTC scheme. Both will be discussed in succeeding paragraphs.

1.2   Fault Diagnosis

A fault can be termed as an unanticipated variation in system's functioning, although it possibly will not signify the physical failure or breakdown. Such a mal-function disturbs the system's normal operation, thus, instigating an intolerable deterioration in the system's performance or even leading to complete failure. There is a difference among the terms "fault" and "failure". "Failure" is wide-ranging. It depicts total collapse of a system, whereas, "fault" denotes that a mal-function is bearable at its current stage. Early diagnosis of fault is important to avoid any grave consequences. A monitoring system that detects the faults and identifies their location and implication in a system is called an "FDI system". This system generally performs the following tasks:-

1. **Fault detection**:- Something has gone wrong in the system or everything is functioning fine.

2. **Fault isolation**:- To decide about the exact location of the fault, e.g., which hardware, actuator or sensor has developed a fault.

3. **Fault identification**:- To make an estimate about the extent and nature of the fault.

The comparative significance of these tasks and decisions is subjective, still, the detection is a pre-requisite for all practical systems and isolation of fault also carries equal importance. Identification of the fault, however, may not be needed if re-configuration of the controller is not involved. Hence, fault diagnosis is mostly taken as fault detection and fault isolation. The FDI problem can be decoupled in two main steps, residual generation and residual analysis.

1.3   Fault Tolerant Control

It is demanded from the modern controlled systems to keep functioning within acceptable limits to fulfill the designated tasks even if they are affected by faults

in the controller or in the system that is being controlled. A control system with this type of fault tolerance ability is termed as an FTC. In comparison to the normal system the performance degradation for a fault tolerant system may be smooth, if they are operating in a faulty condition. The main aim however is to retain satisfactory operation of the system and to provide the supervising system with reasonable amount of time to repair the fault. FTC has received increased attention lately, this is encouraged by the requirement to achieve high standards of dependability, maintainability and performance in the situations where the controlled system can have possibly damaging effects because of faults. For example, in case of automobiles and air planes the safety is of paramount importance, control system must be able to withstand minor system faults or the consequences may be disastrous. Similarly for nuclear and chemical plants, the effects of an incorrect control action resulting from a component mal-function can be catastrophic. An FTC system is intended to preserve a certain amount of its control integrity in the occasion of a presumed set of possible faults. This can be accomplished by designing a control system with built in capability of automatic re-configuration, in cases where a mal-function is detected and isolated. Fault diagnosis is vital for any FTC scheme, as controller re-configuration is only possible if the fault is correctly detected, isolated so that the information is sent to a monitoring system to make a proper decision. FTC can be categorized into active FTC and passive FTC [1].

Addition of FDI module and re-configurable controller within the overall framework is the key distinguishing attribute of active FTC system against a passive FTC system. The main concerning factor in any active FTC system is the narrow time slot available for the FDI module to generate desired information and for the control system re-configuration.

1.4 FDI - FTC Integration

The researchers mostly targeted FDI and FTC sub-systems as two distinct entities. Most of the FDI methodologies are aimed to monitor the system or to diagnose the faults in the system, not as an integral part of FTC systems. Consequently, some existing FDI methodologies may not meet the controller re-configuration requirements. Conversely, most of the research on FTC systems is conducted with a supposition that a perfect FDI module already exists. A detailed study on the subject has been carried out in [1] and the references therein. The design and analysis with the complete system structure and interaction among FDI and FTC sub-systems has still a wide scope of further research. For example:-

1. What are the requirements for FDI from the perspective of FTC design?

2. What all details can be delivered by FDI methodologies for overall FTC system strategies?

3. Ways to systematically analyze the interactions among FDI and FTC sub-systems?

4. How to plan FDI and FTC sub-systems in an integrated manner for online applications?

To shape a purposeful FTC system, it is vital to inspect and scrutinize all sub-systems carefully to guarantee functioning can be ensured in coordination. Specifically, from a re-configurable control perspective, it is desired to know the type of input required from an FDI sub-system to attain a realistic control scheme and from an FDI perspective, it is desired to recognize the type of information that can be generated. The trade-off among these two sub-systems should be optimized, or else, the system will not perform as anticipated. A delayed or wrong input from FDI may end up in performance degradation or in extreme case total instability. A smooth integration of an FDI sub-system with an appropriate re-configurable control methodology still offers substantial challenges in practical applications and require some more investigation.

One serious issue in this integration is the narrow time slot available for FDI subsystem to detect the fault and for re-configuration mechanism to re-configure the controller. In the FDI module, system fault has to be detected and identified swiftly and parameters of the fault should be estimated online. Based on the fault data on post fault system model, re-configurable control law has to be synthesized automatically to preserve stability and preferred system dynamics during steady and transient state conditions. Additionally, in post-fault system the parameters of the control law are required to be re-calculated, the structure of the new controller may also be changed, thus requiring closed loop stability to be re-established.

1.5 FTC Schemes and Diesel Automotive

Automotive progresses in the last three decades have only been possible through growing use of mechatronic modules in the chassis and the power-train. Mechatronic modules are considered as a combination of mechanical and electronic, the combination is among the hardware and the software. This enhancement has significantly impacted the design and functioning of the power-train which comprises of engine and drive-train. The mechatronic components have substituted formerly mechanical, pneumatic and hydraulic parts with sensors having electrical-outputs, actuators having electrical-inputs and digital-electronics for control. This advancement has opened the access to internal system dynamics and hence enabled new potentials for FDI followed by FTC schemes. Earlier the supervision system of diesel engines involved limit checking of some parameters like pressures, temperatures and voltages against thresh holds. The invention of analog-control in 1967 and later digital-control in 1979 then gave new avenues for onboard diagnostics and testing facilities. In 1988 an OBD was required by emission regulation authorities in USA and 2000 in Europe to keep a check on the components of an engine that are related to emissions [2]. Thereafter the permissible percentage of emissions have been decreased in a period of 4 to 5 years.

Today necessity of lesser emissions, while retaining or refining the performance parameters demand the air properties be flawlessly controlled and coordinated to match the engine operational conditions. Air system is responsible for provision of air to the combustion chambers, it is one of the critical feature of recent diesel engines and can influence emissions, fuel economy and performance. Air management system ensures the air provision to the intake manifold at all operating conditions and fulfills some other requirements, like:- sufficient oxygen to guarantee 100 % combustion, appropriate amount of EGR to maintain the lower combustion temperature and oxygen concentration, control of air temperature and pressure. To regulate these intake air properties flawlessly, necessitated the involvement of additional hardware for example, various variabilities like variable-intake systems, variable-valve trains variable-exhaust gas recirculation, variable-turbo charger controls etc have been introduced. These changes gradually transitioned the image of diesel engines from smoky, slow, noisy, dirty, smelly and heavy to the responsive, cleaner and exciting to drive. At the same time this added intricacy requires more refined control algorithms with precise sensors and sophisticated FTC techniques to guarantee that everything performs as predicted even in presence of minor faults in the system.

Diesel engines are extensively employed as principal power plant for heavy duty trucks, off road vehicles, buses and machinery. The focus in legislation, EURO V and VI, has been on emissions of nitrogen oxides (NO_x) and particulate matter (PM) owing to their substantial role in global emission inventories. Air system (as shown in Figure 1.1) is among the sub-systems that has been re-designed to synthesize advanced control strategies that could help reduce emissions. Air system consists of two actuators, EGR and VGT, whose coordinated control can ensure desired oxygen level and low temperature in the combustion chambers, thus, avoiding higher temperature and oxygen concentration, that may result in NO_x production or lower oxygen concentration that increases PM emission. Any fault in this system could result in increased emissions. It is therefore desirable to have fault tolerant strategy in place that can ensure satisfactory system performance even in case of minor faults. The primary task to be attempted in attaining
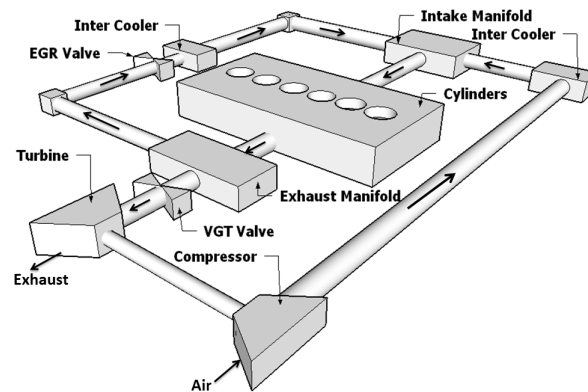
FIGURE 1.1: Air path of a turbocharged diesel engine

fault tolerance is to synthesize a controller with appropriate configuration that can ensure stability and adequate performance, in both cases, when all system modules are working and when sensors, actuators or other components mal-function.

1.6   Diesel Engine Air System Faults

As already highlighted, the air system is responsible for introducing air and exhaust gas fraction into the intake manifold to guarantee the fuel combustion with minimal exhaust emissions. The detailed functioning of the air system will be explained later in Section 4.2. The system consists of VGT and EGR actuators, these actuators control the quantity of exhaust entering the turbo charger and intake manifold respectively, as shown in Figure 1.2.
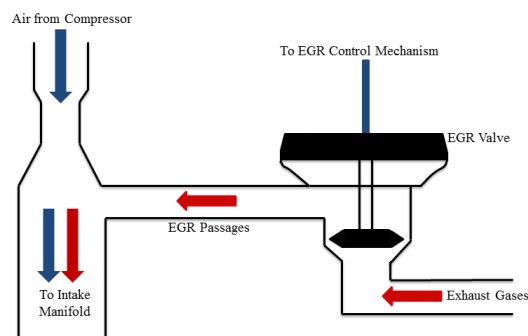
FIGURE 1.2: EGR actuator - exhaust gas flow

FIGURE 1.3: Chocked EGR actuator [3]

Exposure to high exhaust temperatures and unburned hydrocarbons sometimes result in system mal-functions. The faults are, actuator getting chocked with soot or tar as shown in Figure 1.3, leakages in the system resulting in exhaust gas escape, faulty actuation mechanisms that result in offset in actuator positions, wearing of actuator components due to erosion or corrosion and components getting coated with exhaust PM. These faults introduce a permanent error in actuators which can affect tracking of set-points during steady and transient states, resulting in enhanced emissions. It is hence desired to implement a control scheme that can tolerate such faults.

1.7   Motivation of the Work

The debate about the diesel engine air management and its various sub-systems brings forth certain noteworthy arguments concerning its control. These are discussed as follows:-

1. The coupling between the air management system's exhaust and intake paths, because of the VGT and EGR sub-systems, creates a significant inter-dependence among the sub-systems. Hence fault in any of the sub-system would result in deviation from the desired performance.

2. The working of the air-path sub-systems is heavily dependent on the performance of their actuation mechanisms. The actuators, i.e., EGR and

VGT control the quantity of engine exhaust going into EGR and VGT sub-systems respectively. Any deviation, because of actuation faults, in quantity of exhaust flowing through these actuators, would result in set-point tracking errors and eventually increased emissions.

These complications are the core of the research work offered in this thesis. Traditionally, FDI module and control module have often been separately designed. It seems straight forward task to merge various sub-systems in FTC system, unfortunately, in reality this is not as simple. The key reason of this difficulty is, each individual sub-system, operating flawlessly on its own, fails to provide desired results instantaneously for remaining sub-systems. How to integrate various sub-systems effectively for real-world problems still remains a vital subject for research. The main objective in this integration is the mitigation of adverse interactions between each sub-system [1]. The dynamic nature of a control system and real time environment of FDI and controller re-configuration requires FTC system to be capable of detecting, identifying and accommodating the faults as swiftly as possible. There has to be a firm time limit in making and implementing decisions for controller re-configuration to prevent exposing a system to potentially unsafe circumstances. Hence, from theoretical perspective, unified and systematic control strategies are to be worked out for diesel engine air management system, to guarantee integration of FDI and FTC schemes as quickly as possible to ensure desired system performance under all situations.

1.8 Objectives

In order to meet the above discussed requirements, following is essentially required:-

1. Proposing robust controllers with simpler structures for diesel engine air management system actuators, that have the capability to withstand minor system faults by virtue of inherent robustness properties.

2. Proposing unified diagnosis and control design methodologies for air system actuators, that have both FDI and FTC modules integrated in a controller, so as to achieve timely fault information and circumvent the shortcomings of controller re-configuration.

1.9   Contributions

The contribution can be divided into following segments:-

1. Passive FTC schemes have been proposed for diesel engine air management system actuators, the schemes have the capability to withstand minor system faults with no requirement of on-line fault detection, diagnosis or controller re-configuration. The proposed controllers manage the actuator positioning tasks in accordance with the engines operating point. The robustness properties of the controllers ensure nullifying the fault effects. The portion of the thesis earmarked for the development of passive FTC scheme for actuators is further divided into two sub-segments on the basis of different control methods that have been developed and evaluated in terms of robustness against faults [4, 5]. Two type of algorithms used for the purpose are STA and VGSTA.

2. The proposed passive FTC schemes are capable of tolerating minor additive or multiplicative faults with regards to actuators or process, as the designed controllers are robust. But for faults of larger magnitude these proposed passive schemes fail to provide desired objectives. To overcome these shortcomings, unified schemes have been proposed. These schemes use FDI module with FTC, thus, helping in fault detection, estimation and compensation. Especially the unification of FDI and FTC schemes give the desired objectives swiftly without any requirement of controller re-configuration. Additional advantage of proposed unified schemes is, they do not require any upper bound on faults. Closed loop stability of the unified schemes have been established. The segment of the thesis dedicated to the development

of unified FDI and FTC schemes for control of actuators is further divided into two sub-segments on the basis of different control methods that have been developed and evaluated in terms of fault detection, estimation and compensation [6, 7]. Two type of controllers developed for the purpose are CESTA and ISM extended with an adaptive part.

1.10 Outline of the Thesis

The thesis is organized as follows:-

1. **Chapter 1, Introduction:** Introduces some background related to our work. Basic concept of FDI and FTC schemes, issues in their integration and their significance related to diesel engine emission control is explained. In the end motivation, objective and contributions are highlighted.

2. **Chapter 2, Literature Review:** This chapter sheds some light on FDI and FTC methodologies. Additionally, it gives a summary of the previous work reported in the literature on the control and FTC of diesel engine air management system actuators. The shortfalls in the reported work are discussed, followed by research gap identification.

3. **Chapter 3, SMC - Review of Concepts:** This chapter is on review of basic concepts on SMC techniques. The concepts which are relevant to this research are briefly discussed.

4. **Chapter 4, Diesel Engine Modelling:** Chapter focuses on working and modelling of various sub-systems of a turbo charged diesel engine. Reduced state control oriented model for a diesel engine is also discussed. A non-linear input transformation is explained, that gives actuator positions against flow rates.

5. **Chapter 5, Passive FTC - Diesel Engine Air Path**: This chapter give details on proposed passive FTC schemes for diesel engine air management

system actuators. Two schemes are discussed in detail including stability analysis. Simulation results are presented, which suggest our schemes make the system robust to minor faults. Discrepancies in the proposed schemes are also discussed.

6. **Chapter 6, Unified FDI and FTC - Diesel Engine Air Path:** Chapter highlights the importance of FDI schemes and their unification with FTC schemes. The discrepancies of passive FTC schemes are mitigated by this unification. Two schemes are proposed and discussed in detail along with stability analysis. Simulation results are presented, which suggest our schemes have eliminated the effects of minor system faults.

7. **Chapter 7, Summary, Conclusion and Recommendations:** This chapter concludes the manuscript and highlights some future research directions.

1.11 Chapter Summary

FDI and FTC of diesel engines is an active research area that has attracted more focus recently. A brief review of FDI and FTC schemes have been discussed. Their integration issues have been deliberated. Significance of FTC schemes with regards to diesel engines have been explained. Lastly some of the contributions of this thesis have been highlighted and thesis outline has been discussed.

Chapter 2

Literature Review

This chapter will be covered in two portions, first portion will focus on basics of FDI and FTC schemes highlighting various techniques that are being used along with references. Second portion will discuss diesel engine air management system control techniques that are already available in literature, followed by research gap identification.

2.1   FDI and FTC

A lot of work has been done on fault diagnosis, spanning from analytical approaches to statistical methods and artificial intelligence, which is also supplemented by the advancement in modern control theory that has offered influential methods of mathematical modelling, parameter identification and state estimation. Design of a diagnosis system is one imperative step towards development of FTC scheme. In FTC systems, faults are handled such that system can still perform in satisfactory manner and results are within acceptable limits. This is preferred over total breakdown of a system caused by faults. The arrangements for managing faults are different for each occurring fault. The main challenge for the FTC scheme is to ensure system's adequate operation and dependability in most hostile operating conditions like, the existence of disturbances, modelling errors, noise and faults.

2.1.1 Fault Detection and Isolation

Basics of FDI system have already been explained in Section 1.2, the two main tasks being performed by FDI system are as follows [8], details will be covered in succeeding paragraphs.

1. **Residual generation**:- For detection, diagnosis and isolation of the fault, it is necessary to generate residual signals which are sensitive to a set of possible faults. The residual is a signal which should normally be zero or near to zero in case there is no fault in the system, but is considerably higher then zero if a fault occur. Using the available data from the supervised system, a residual signal can be produced in many different ways. This auxiliary signal is designed in a way that it reflects the commencement of a probable fault in the monitored system. This implies that, ideally, the residual signal is independent of system's inputs and outputs.

2. **Residual analysis**:- The residuals are studied for probable set of faults. A rule to detect a fault is then applied to conclude if any fault has affected the system. Fault detection method may involve a simple check on the basis of some threshold, which is applied on residuals instantaneous values or moving averages. It may involve complex methods of theory of statistics.

2.1.1.1 The Residual Generation in FDI

The generation of the residual signals is a vital concern in FDI design. A diverse range of techniques are available for residual generation [1, 8–11] as shown in Table 2.1. As mentioned earlier, most of the research in this field is focused on system monitoring, detecting and isolation, rather than control applications. Relatively fewer results are available on methodical study on the tasks of FDI in overall FTC frame-work. Similarly, not much information is available regarding methodologies to propose FDI for re-configurable control in the context of FTC systems.

TABLE 2.1: Residual generation techniques. [1]

Techniques	Model based	Quantitative	State estimation	Observers
				Kalman filters
			Parameter estimation	LS/RLS
				Regression analysis
			State-parameter estimation	Extended Kalman filters
				Two stage Kalman filters
			Parity space	State space
				Input output
		Qualitative	Causal models	Graphs
				Fault trees
				Qualitative physics
			Abstraction hierarchy	Structural
				Functional
	Data based	Quantitative	Statistical	PCA/PLS
				Statistical classifiers
			Non statistical	Neural networks
		Qualitative	Expert systems	
			Fuzzy logic	
			Pattern recognition	
			Time frequency analysis	
			Trend analysis	

Since most approaches to design a control are based on system model, hence, our focus will mainly be on those FDI methodologies that rely on quantitative models. Some of the techniques will be discussed briefly in this Section, as follows:-

1. **Knowledge Based**:- Prior system knowledge from a fundamental understanding of the process or from the experience with the process is used to determine that a fault has been developed. This is the most commonly used technique in real applications. It is mostly used in support of other approaches. The former knowledge based on system's physical performance and experience can be used to interpret the reliability of the strategy and for calibrating the algorithms [12]. Fuzzy logic based techniques can be classified in this category.

2. **Hardware Redundancy**:- Identical (redundant) hardware modules are used. The fault easily gets detected as soon as there is a deviation in the results of one of the two components [8]. The main advantage of this strategy

is the reliability and ease of implementation. The issues of fault isolation and development of FTC algorithm are resolved automatically. The disadvantage is the cost of redundant components, which may increase the cost of physical implementation due to increase in the physical hardware needed to implement the devised FTC algorithm.

3. **Signal Based**:- It is presumed that there are signals in the system that convey useful information about the probable faults. These signals are then examined to yield evidence regarding the fault detection and development of FTC schemes. Signal processing techniques are employed to extract fault information from signals. The approach could be valuable if reliable measurements are obtainable and if the fault behavior has a clear signature [13].

4. **Data Based**:- They can be divided into quantitative and qualitative approaches. The quantitative approaches fall in non-statistical techniques and statistical techniques. Neural networks are the example of non statistical techniques. PCA, PLS and statistical pattern classifiers are examples of statistical feature extraction approaches.

   (a) **Neural Networks**:- Neural network can be used to train a black-box model without having a comprehensive knowledge of the processes involved. The model is then equated with the actual physical process to ascertain amount of tolerance condition. The technique does not need physical knowledge of the process, the network generalization banks on the data quality and range (the model is preferably trained in all possible operating conditions). Neural networks employed for FDI can be segregated along two axis:- the network architecture like radial basis, sigmoidal etc and the learning technique like unsupervised and supervised learning. Amongst the advantages that make neural networks attractive are, it requires less formal statistical training to discreetly identify intricate non-linear relations and the limited memory footprint on the micro-controllers. The main shortfall of this technique is that

the network has to be trained every time the process changes on a data base that is not always available or could be provided in a short period of time, convolutional neural networks are however independent of prior knowledge. A comprehensive study of neural networks for fault diagnosis in steady state processes was carried out in [14][15].

(b) **Statistical Approaches**:- Multivariate statistical techniques like PCA and PLS have extensively been used for fault diagnosis. A huge amount of literature is available on the subject [16–19]. One of the major limitations of PCA is, it's model is time invariant, whereas on the contrary most real processes are time varying. Hence, recursive updating of model is essentially required for successful implementation of this technique.

Statistical pattern recognition framework has also been used for fault diagnosis, considering it to be a classification problem [20]. The instantaneous estimates of the classifier utilizing information regarding the system's failure modes statistical properties are combined to diagnose the faults.

5. **Model Based**:- Differences between system's theoretical model and the physical process are examined to study the fault conditions [8, 13]. System's model is taken as a virtual redundant component. The main advantages of the technique are, easy implementation and low cost. The disadvantage of this technique is that no physical process can be modelled exactly, as parameter uncertainties, modelling errors and unknown disturbances will affect the residual terms. In addition, a second stage analysis is required for fault detection and and estimation. This can be termed as a problem of extracting useful information from the residual signals. Model based strategies can be broadly categorized into quantitative and qualitative approaches. The quantitative approaches fall in further four categories:-

(a) **State Estimation**:- This is by far the most popular way of generating
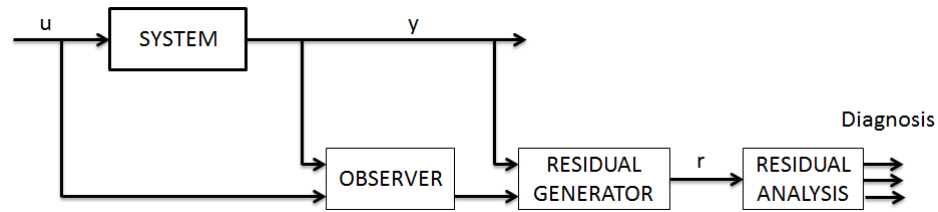
FIGURE 2.1: Observer based residual generation

residuals in engineering problems. The estimators or observers are employed to reconstruct some states of the system, as shown in Figure 2.1, in order to be compared with the available measurements. This comparison produces residual signals. Output error is the most obvious term that can be used as residual but combination of other signals can also be used. This approach can be used in linear as well as in non-linear systems [21–24].

(b) **Parity Equation**:- Parity equations are re-organized and transformed alternates of state space models or input output models. The concept is to compare the plant model's parity with output of sensors and known process inputs. The idea behind this technique is to reorganize the model's structure so that the best fault isolation is obtained. Fault isolation requires the capability to produce residual vectors which are orthogonal to each other for dissimilar faults. A full derivation of this structure equivalence can be found in [25, 26].

(c) **Parameter Estimation**:- Parameters from the physical processes are calculated and are compared against parameters calculated from process models or against known reference values. To produce residuals using this technique, an on-line parameter identification algorithm should be used [12, 27].

(d) **Frequency Domain (Factorization) Approaches**:- Residuals can be produced in the frequency domain by factorization of the supervised system's transfer function. Systematic formulation and solution of the problem is available at [28, 29].

2.1.1.2   Residual Evaluation in FDI

After the generation of residual signals, next step is to evaluate them, as, successful implementation of FTC schemes require reliable residual evaluation. Two methods are mostly used in this regard:-

1. Statistical methods.

2. Norm based residual evaluation or thresh hold calculation.

The details of these methods are covered in [30]. Residuals are assessed in order to take the following decisions:-

1. Presence of fault, if any.

2. Type of fault, if it is present.

The second decision relies on the point whether a single fault or more than one fault can affect the system. Multiple faults occur seldom, they only affect the system if there is some severe defect. Multiple faults are harder and more complex to detect and isolate as they have a coupled effect and they may affect residuals simultaneously. It is therefore necessary to plan residual generation such that a different set of residual is generated for each fault. Such residuals are known as structured [31]. In case of more than one fault it should be ensured that overlapping of subsequent fault effects do not lead to incorrect decisions. Structured residuals can be defined in several different ways that can be used for correct residual evaluation.

2.1.2   Fault Tolerant Control

Basics of FTC system have already been explained in Section 1.3. Two types of FTC techniques will be discussed here [1]:-

2.1.2.1 Active FTC Technique

Active FTC technique is characterized by the controller re-configuration supported by FDI schemes. Active FTC schemes respond to the system component mal-functions actively by re-configuring the control efforts such that the system's stability and acceptable performance can be preserved. In some situations, slightly degraded system performance may be accepted. Active FTC systems are also known as self repairing, re-configurable, re-structurable or self designing. In these systems, the controller handles the fault effects either by choosing a precomputed controller or by designing a new controller on-line. To attain an effective and successful control system re-configuration, both techniques heavily rely on real time FDI structures to deliver the latest information regarding actual system status. Therefore, main objective in an FTC scheme is to synthesize a controller with appropriate structure to maintain desired system performance in both scenarios, when all system components are working fine and when some components like actuators, sensors etc mal-function. It is pertinent to highlight that the stress on system response in these two scenarios is considerably diverse. During usual operations, the quality of the system behavior is more desired. However, in the event of a fault, the emphasis should be on, how the system retains an acceptable performance. Main attributes considered for the design of active FTC systems are:-

1. A controller that can be re-configured without much difficulty.

2. An FDI module which is sensitive to faults and robust against modelling uncertainties and external disturbances.

3. A re-configuration mechanism that can recover the system pre-fault performance in the uncertain environment inside the constraints of controller and system states.

2.1.2.2 Passive FTC Technique

Passive FTC exploits the robustness of controllers without demanding structural alterations. Implementation of passive techniques is often simple but not typically appropriate for larger fault cases. Controllers are kept fixed, however, they are synthesized to possess robustness to handle certain presumed faults. Technique do not need FDI module or controller re-configuration, thus fault tolerant capabilities are limited. These controllers are also known as reliable control-systems or control-systems with integrity [1].

2.1.3 Controller Re-configuration

Once the mal-function is successfully detected and isolated next step is controller re-configuration to avert failure at the system level. The controller parameters must be adjusted to handle changed system dynamics. Control re-configuration is a building block for increased dependability of the systems under feedback control. Existing re-configurable control design techniques can be classified on the basis of under mentioned criteria [1]:-

1. Various tools for mathematical design.

2. Design techniques.

3. Re-configuration mechanisms.

4. Type of involved systems.

Re-configuration can be achieved by various different algorithms, like [1, 8]:-

1. Adaptive control

2. Robust control techniques

3. Linear matrix inequality

4. Eigen structure assignment

5. Linear parameter varying

6. Intelligent control

7. Pseudo inverse method

8. Linear-quadratic regulator

9. Model following

10. Model predictive control

11. Robust control techniques

12. Disturbance decoupling

13. Generalized internal model control

Such classifications and algorithms are discussed in detail in [1] and the references therein. A vital measure for the appropriateness of a control technique for controller re-configuration is its capacity to be applied to preserve an adequate performance, though slightly degraded, in faulty system in an online real-time setting. Under mentioned necessities should be met in this regard:-

1. Control re-configuration has to be be accomplished under real-time constraints.

2. Re-configurable controller has to be developed automatically with minimum human interactions.

3. The solution has to be provided even if it is not optimal.

In practice, a blend of various techniques may be more suitable to attain a best overall re-configuration mechanism.

2.2   Significance of Robustness

Model based FDI and FTC schemes use system's mathematical models. A 100% precise mathematical model of a physical system is however not possible. Various parameters of the system vary with time in an unpredictable fashion. The physiognomies of the disturbances and noise are also not known and hence cannot be incorporated in the model precisely. A disparity will always exist among the physical process and its mathematical model, even if the system is not affected by the faults. Apart from the models employed for designing a control algorithm, these shortcomings create the basic approach complications for FDI and FTC applications. They act as a cause of false alarm that can affect the scheme's performance. Hence, the affect of modeling inaccuracies is the utmost important aspect in the model based FDI and FTC concept, and the problem's elucidation is crucial for its real world relevance.

To overcome the problems presented by modelling uncertainties, robustness has to be introduced in a model based FDI/FTC scheme, such that, it becomes insensitive or even invariant to these uncertainties [8]. At times, a mere lessening of sensitivity to modelling uncertainty does not resolve the issues as reduction in sensitivity may be related with a decrease of the sensitivity with regards to faults [22]. Hence, a more appropriate design for the robust FDI problem is to increase robustness to modelling uncertainties, whilst retaining fault sensitivity. An FDI scheme intended to offer adequate sensitivity to faults and suitable robustness against modelling uncertainties, is termed as a robust FDI scheme [22]. The significance of robustness in FDI schemes based on the mathematical model has been widely acknowledged by both academia and industry. A vital requirement from FDI scheme is to diagnose the presence of soft faults in a system before their manifestation, as, such problems necessitate intervention of human operator or automatic system. The hard and abrupt faults, however are easily detectable, as they affect FDI system sizably as compared to the modelling uncertainties and can be easily detected by introducing an appropriate threshold on the residual. Soft faults do not affect the residuals, hence can remain concealed as a result of
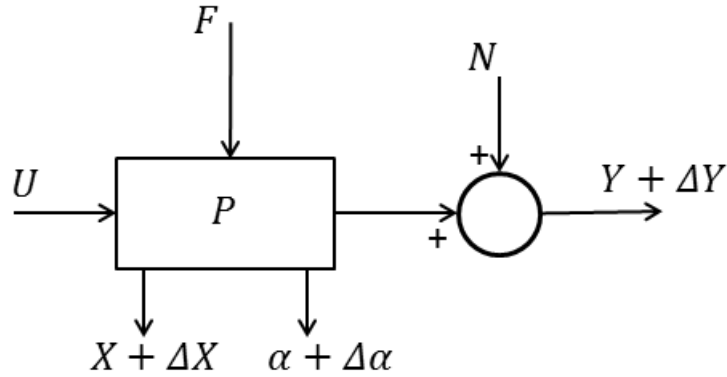
FIGURE 2.2: Process in open loop

modelling uncertainties. This calls for the requirement of robustness in FDI systems. Significance of robustness in model based schemes is covered in detail in [8] and references therein.

2.3 Significance of Model Based Schemes

Modern systems are highly complex with regards to the large number of subsystems and stringent output requirements. They depend upon sophisticated control techniques to meet improved performance requirements. An orthodox feedback control for a highly non-linear system may result in an undesired performance, especially in the event of system faults. To alleviate these weaknesses, new model based control development techniques are being researched so as to detect and tolerate component faults while maintaining performance within the limits of acceptability. This is mainly important for systems like aircrafts, vehicles, nuclear and chemical plants, where consequences of a minor fault may put human lives in danger. For these systems, specially, the requirement on safety, reliability and fault handling is particularly high. It is therefore desirable to have model based control-systems that can detect and tolerate faults to increase the availability and reliability while maintaining the desired performance.

Consider a system operating in open loop as shown in Figure 2.2. For some input $U(t)$ the system gives output $Y(t)$. If the system is affected by some fault (due

to internal or external reasons), some examples for external reasons are variations in dust, wind speed, density, temperature, humidity etc. Examples for internal reasons are poor lubrication, erosion, wear, short circuits, system leakages, actuator chocking etc. The faults $F(t)$ initially effect internal system parameters $\alpha(t)$ by $\Delta\alpha(t)$ or internal states $X(t)$ by $\Delta X(t)$ and eventually the system's output $Y(t)$ is changed by $\Delta Y(t)$. The effect of noise and disturbances $N(t)$ also need consideration with regards to influencing the system's output $Y(t)$. If the system is operating in open loop configuration, the fault generally ends up in a permanent offset in output i.e., $\Delta Y(t)$. However, in closed loop configuration case (Figure 2.3) it is a different response, as it depends on the type of applied control algorithm, like if a PI controller is used, the output displays only a disappearing minor deviation. But then the input variable $U(t)$ displays a permanent offset $\Delta U(t)$ for proportionately acting processes. If merely output $Y(t)$ is being observed, the fault will go unnoticed, as, the closed loop compensates the effects of disturbances $N(t)$, parameter variations $\Delta\alpha(t)$ and state variations $\Delta X(t)$ with respect to the control variable $Y(t)$. This implies that closed loop compensates the faults $F(t)$. Only if the fault is of larger size that can force the input $U(t)$ to saturate, a permanent deviation in output $\Delta Y(t)$ will be observed. Hence, to ensure effective detection, isolation and compensation of faults, model based non-linear FDI and FTC schemes are preferred for processes in closed loop where various system attributes can be monitored alongside output $Y(t)$. If the tolerance limit of some parameter is surpassed, an alarm is raised.
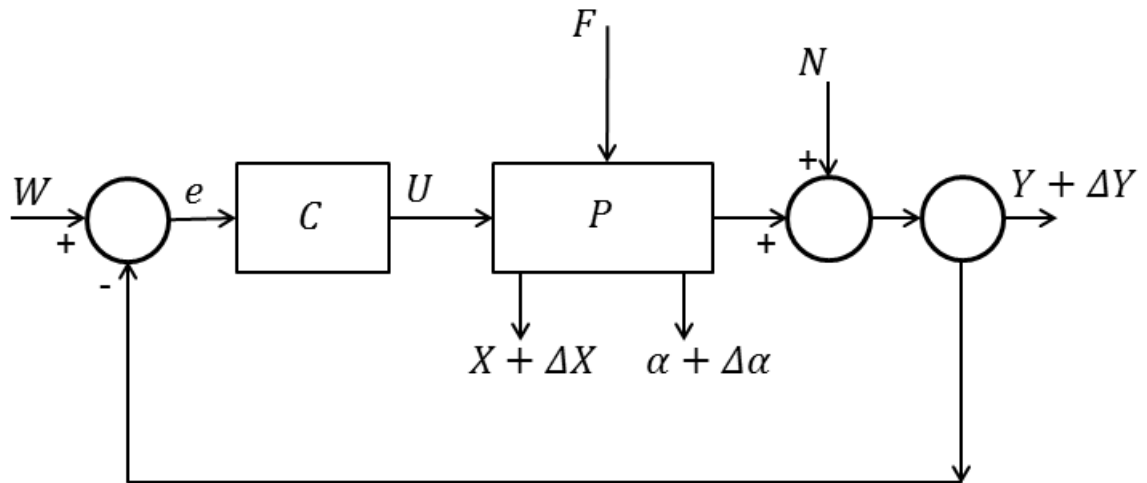
FIGURE 2.3: Process in closed loop

2.4 Diesel Engine Air Management System Control

Emission control, especially in case of diesel engines, is a very difficult research problem [32]. This complication is a result of intricate and inter-dependent processes that are necessary for conversion of chemical into kinetic energy and partially due to highly inter-related sub-systems whose integrated and cohesive action yields torque, for driving an automobile. The air management system is among the sub-systems, whose control is essential for warranting that emissions are retained within the specified low boundaries, while sufficient oxygen is available in the combustion chambers for fuel burning. A lot of work has been done for control development of air path of diesel engines. It is explained in a systematic way in this Chapter.

2.4.1 PID Based Approaches

Various methods for emission reduction through the efficient control of air management system actuators have been published. Control techniques centering on PID based approaches were proposed in [33, 34]. In [33] normalized air to fuel ratio

(normalized with respect to the stoichiometric air to fuel ratio) and exhaust gas fraction were made to track their set-points being coupled to emissions. An efficient tuning strategy for the PID controllers was also proposed. Normalized air to fuel ratio and exhaust gas fraction were controlled by EGR valve and VGT valve respectively, which handled the sign reversal in the system. In [34] the control goals of reducing the consumption of fuel and to retain safe turbocharger function were set to meet the authorized emission criterion. The objectives were attained from tracking of normalized oxygen to fuel ratio and exhaust gas fraction in intake manifold, same were selected as both performance and feedback variables. A novel approach for pumping work minimization was developed. The suggested performance variables were sturdily coupled with the emissions that made adjustment of set-points easier. Controller objectives were seized in a cost-function, which made it possible to tune the gains automatically despite the objectives being conflicting. PID controllers, however, offer low robustness as compared to the robust controllers when the system encounters multiple challenges from the operating environment. The algorithms may handle minor system faults, but absence of FDI structure prevents any possibility of fault detection and estimation.

2.4.2 Control Lyapunov Function Based - Feedback Linearization

Non-linear control design on the basis of control Lyapunov function was proposed in [35–37]. Input/output linearization strategy was employed. A control Lyapunov function was synthesized by applying input/output linearization to a third order engine model. The set-points to be tracked were taken as compressor flow and exhaust manifold pressure and the performance parameters i.e., normalized air to fuel ratio and exhaust gas fraction were transformed into these set-points. Controller was validated on a full order system model and experimental platform. It was established that intrinsic non-linearities in a system could be handled by non-linear control methods. In [35] the design was enhanced with an integral action on compressor flow rate so as to nullify the effects of modelling errors and

to track the output variables with increased accuracy. All the approaches were based on the general assumption that system is fault free, thus, fault handling was not addressed, additionally, the control schemes are conservative.

2.4.3 Model Predictive Control

Techniques based on MPC approach have been proposed by several researchers in [38–43]. In [38] the problem was presented as an optimal control problem with the constraints on inputs to handle it in a model based environment. In order to calculate the explicit solution of the control law offline, explicit MPC was used. The solution was then used to construct LUTs for online controller selection. In [39] NMPC was applied to control the set-points of normalized air to fuel ratio and exhaust gas fraction, the aim was to attain lower exhaust emissions and fuel consumption with no smoke generation. It was shown that NMPC achieved the desired control objectives with constraint satisfaction. In [40] explicit MPC was proposed that allowed sub-controllers to track time varying set-points. The approach required a lesser computational footprint that was appropriate for online implementation. In [41] NMPC strategy was used on LPV model. In order to get a non-linear model of high quality, data based LPV modelling with real data from engine test bench was used. It was shown that NMPC is a better approach than MPC as far as tracking of set-points is concerned. In [42] MPC structure used four actuator variables and five measured variables. The controller design was based on achieving high level objectives directly with an assumption that direct measurements of performance parameters are available. The model was obtained through system identification. In [43] it was presented that the selection of set-points and thus the cost function had a direct influence on optimization problem and the subsequent performance of the controller. Different outputs were selected and their effect was investigated suggesting that it could be advantageous to use pumping losses and exhaust gas fraction in the cost function while taking the constraint as oxygen to fuel ratio. For systems in which online calculation is possible, MPC has produced good results [44]. But stability apprehensions, lack of

robustness and issues with regards to practical implementation are major research directions [45]. The concerns get multiplied in case of system faults, same have not been addressed in these schemes.

2.4.4 Sliding Mode Control

SM frame-work for control of air management system actuators was proposed in [32, 46–48]. In [32, 46] controller was developed basing on the reduced order system model and validation was performed on full order model. In [46] reduced order model was transformed to regular form and controller was developed to control VGT only while making an assumption that the EGR valve was controlled by some independently synthesized feedback controller. In [32] an alternative method for planning a sliding surface was suggested in which input/output linearization method was employed to synthesize an SMC, the stability of hidden dynamics was also established. In [47] a hybrid robust non-linear control design encompassing a supervisory control, designed on the basis of finite state machine approach and multivariable SMCs for various combustion modes with integral actions in sliding surfaces, was presented for low temperature and conventional combustion modes of a diesel engine. The use of integral actions in SMC reduced the chattering and achieved asymptotic tracking. Supervisory control was employed to select between various lower level controllers. In [48] an adaptive SMC was designed for MIMO systems. To decrease the chattering, discontinuous term of classical SM law was replaced with an adaptive PD term and for minimizing the error effects, a robust term was supplemented in the designed control law. Adaptive laws, robust control term and parameters were obtained through a Lyapunov stability analysis. Generally small additive or multiplicative faults in the process or actuator can be tolerated because of usual robustness properties of these controllers but for larger faults these schemes fail to provide desired objectives. Additionally fault tolerance is not addressed in all these schemes, resulting in the increased chattering in cases of system mal-function.

2.4.5 Miscellaneous

In [49] a hybrid strategy was proposed for the control of common rail diesel engine. Online estimation of the engine model states and parameters were made. Reduced third order model was used for controller development. EGR was controlled by a conventional PI controller and the VGT controller was made adaptive. In [50] the controller was developed basing on the LPV model and a gain scheduled H_∞ technique. It was shown that the modelling naturally lead to a quasi-LPV structure. The proposed scheme gave improved tracking performance as compared to the standard electronic control unit. In [51] a third order LPV model of air management system diesel engine was used for construction of a gain scheduled controller. It was shown that the scheme reduced the calibration effort significantly, while achieving the same performance as the fully calibrated engine controller.

2.4.6 FTC Schemes

SM structure being robust against matched uncertainties has also been employed for designing FTC schemes for diesel engine air management system actuators [52–56]. All authors proposed passive FTC schemes and used intake-manifold pressure and exhaust-manifold pressure as output parameters. Absence of FDI structure made fault detection and estimation impossible. In [52, 56] adaptive integral SMC approach was employed for construction of control law with reduced order model of the system. The technique allowed dynamic regulation of controller gains to guarantee them higher than the uncertainty bounds. The proposed controller was tested on the reduced order system model. In [53] a disturbance observer centered SMC technique was suggested. Matched and unmatched disturbances are simultaneously estimated and compensated by a disturbance observer. The proposed controller was tested on a reduced order system model. In [54, 55] an FTC scheme for air path was proposed under the concept of HOSMC. It was assumed that the faults were bounded and bounds were known. The controller

gains were ensured to remain at higher level than the known fault bounds. Three state system model was employed for controller construction and validation.

In [57] a strategy for FTC of air path of diesel engine subjected to the leakages in intake manifold defined by Takagi-Sugeno's model was presented. Leakage was identified on the basis of an adaptive observer. Turbo charger dynamics were ignored and the FTC law was realized as an adaptive state feedback controller.

2.5 Research Gap Analysis

Fault tolerance has not been addressed in the control techniques described in Section 2.4.1-2.4.5. Some work has been done regarding FTC schemes for air path actuators as described in Section 2.4.6. The shortcomings in these techniques include:-

1. In most SM based techniques, faults were handled passively by ensuring that controllers were robust. Control gains were kept at a higher level than the known fault bounds, thus, as the magnitude of the fault was increased, higher chattering was observed except in case of [53] and [57].

2. Absence of FDI strategy to detect the occurrence of the fault, diagnose its type and estimate the fault magnitude so as to compensate it's effects.

3. Validation of controller has been performed on the reduced order engine model except in case of [57].

4. Requirement of *apriori* knowledge about fault bounds or some constraint on faults were essentially required in most cases.

5. In [57], only intake manifold leakage was addressed.

It is therefore desired to propose a scheme that have the capability to detect, diagnose and estimate the faults and compensate the fault effects without introducing increased chattering, so as to ensure satisfactory system performance even if some

fault affects the system. Moreover, FTC scheme must address the issues related to FDI-FTC integration and controller re-configuration.

2.6 Chapter Summary

Increased demand of reliability and availability asks for an improved supervision of all sub-systems with an emphasis on a careful designing of safety critical components to ensure fault tolerance in the system. Safety and dependability are usually attained through a blend of fault detection, fault evasion, fault diagnosis, fault elimination, fault tolerance, automatic monitoring and protection. The reliability may be enhanced through over-sizing, protection and maintenance for mechanical, hydraulic, electrical components and by redundancy. Because not all faults and failures can be circumvented entirely, hence, high integrity systems must possess the capability to tolerate faults. This implies that, faults are handled in a manner that they do not fail a system. In power-train this is related to vital actuators and sensors of the engine and transmissions. The discrepancies in existing diesel engine air management system control algorithms have been discussed in Section 2.5. In next Chapter some of the basic concepts of SMC techniques will be reviewed so as to provide a platform for working out FTC schemes for diesel engine air management actuators.

Chapter 3

SMC - Review of Concepts

This chapter presents some of the basic concepts of SM control theory. The motivation for SMC is presented. The SM design problems with regards to robustness and performance along with some of the existing solutions are discussed. Necessary concepts are explained, with an aim to understand the concept of proposed FTC schemes for diesel engine air path actuators. On the basis of this background, FTC schemes will be introduced in succeeding Chapters.

3.1   Motivation

The depiction of any plant or process by a mathematical model is always imprecise, a disparity always exists between actual plant and it's model. This may be due to inadequate system's knowledge referred to as parametric uncertainties or owing to simplifications made while system's modelling, known as un-modelled dynamics. These uncertainties may affect the dynamics of the plant through the input or output channel. It is hence desired that, feedback control system designed on the basis of imperfect plant model must be robust against uncertainties so as to preserve stability and performance. SMC is a simple and effective technique used to develop controllers for uncertain systems. A control law is developed that changes value on the basis of a predefined switching rule such that the states are

driven so as to constrain in a manifold, known as sliding surface or sliding manifold. System's dynamical performance when it is kept inside the sliding manifold is defined as sliding mode. It is accomplished by choosing a set of switching surfaces and designing a discontinuous control law. SM technique makes a problem easier to control by converting it from n-dimensional tracking to first order stabilization. Once the SM is established the controlled plant is invariant to uncertainties whose bounds are known, same are inherent in the control channel termed as matched uncertainties. Stable behavior and reliable performance are then retained. This attribute makes SMC a robust technique for control development.

3.2 Basic Concepts

SMC technique is established on the observation that controlling first order systems (systems defined by first order differential equations), may they be non-linear or uncertain, is easier as compared to control the ith-order systems (systems defined by i^{th}-order differential equations). Design of SMC is accomplished in two steps:- Selecting a set of sliding surfaces that denote desired objectives. Designing a discontinuous controller that ensures the attractiveness of sliding manifold and also assures the convergence to the sliding surfaces. When the dynamics of the system are restricted to the sliding surfaces, it is known as a sliding motion. Thereon, the system dynamics are dependent on the characteristics of the designed sliding surfaces.

Consider a system affected by some matched uncertainty, affine in input, as:-

$$
\begin{aligned}
\dot{x}_1 &= x_2, \\
\dot{x}_2 &= x_3, \\
&\vdots \\
&\vdots \\
\dot{x}_n &= f(x,t) + g(x,t)(u + F(x,t)), \\
y &= x_1,
\end{aligned}
\tag{3.1}
$$

where $x \in \mathbb{R}^n$ is the state vector, $u \in \mathbb{R}$ is the input, $y \in \mathbb{R}$ is the plant output and $F(x,t)$ represents the bounded matched uncertainty.

It has been supposed that $f(x)$ and $g(x)$ are known and smooth, defined on an open set in $\mathbb{R}^n$. The control objective is to guarantee that the output of the system y follows a given time varying reference signal y_d.

3.2.1 Sliding Surface Design

The sliding surface is taken as a fictitious output of the system, when kept at zero by application of some control effort, the control aim is achieved. When the system is restricted to the sliding manifold, the dynamics of the system are dictated by the characteristics of the sliding surface and not by system equations. Hence, sliding surface is carefully selected to attain the desired characteristics during sliding. Like, for tracking problem the sliding surface can be chosen as a differential equation in terms of tracking error. Similarly, for stabilization problem the sliding surface is selected as a linear combination of states of the system. The sliding manifold is chosen such that it's relative degree is one with regards to the control input i.e., the controller should appear in the first derivative of the sliding variable.

$$S \quad = \quad S(x,t),$$

where $S(x,t)$ is differentiable. For SM to establish, it is desired that $S(x,t) = 0$. Consider a linear sliding surface for some tracking problem:-

$$S \quad = \quad e^{n-1} + \cdots + \lambda_2 \ddot{e} + \lambda_1 \dot{e} + \lambda_0 e,$$

where $e = y - y_d$. The $\lambda_i s$ are chosen to ensure the conversion of any arbitrary polynomial (3.2) to Hurwitz. By virtue of Hurwitz polynomial, the tracking error

will vanish, if the sliding surface is made zero.

$$e^{n-1} + \sum_{i=0}^{n-2} \lambda_i e^i = 0. \tag{3.2}$$

The first derivative of the sliding variable comes out to be:-

$$\dot{S} = f(x,t) - y_d^n(t) + \sum_{i=0}^{n-2} c_i e^{i+1}(x,t) + g(x,t)(u + F(x,t)). \tag{3.3}$$

The nth order tracking problem is now transformed into the first order stabilization problem. To attain this stabilization objective, control law is designed in next step.

3.2.2 Control Law Design

In this Sub-section, control law will be designed for the system (3.3). It is desired from the controller to push the system trajectories towards the sliding surface and then to keep them contained in the sliding manifold regardless of existence of uncertainties. It is accomplished by enforcing reachability constraints on the controller thus making the sliding surface attractive. Lyapunov's direct method offers a stability analysis tool to propose a controller that makes the sliding surface attractive. The law states that, the dynamic system is stable, if a positive definite function V is worked out, whose derivative along the system trajectories is negative. The complete control structure is:-

$$u = u_{eq} + \bar{u},$$

the u_{eq} stands for equivalent control, it is designed by keeping $S = \dot{S} = 0$ and ignoring uncertain terms. The u_{eq} denotes the average sense of the applied control for $t > t_r$, where t_r stands for reaching time. This selection of u_{eq} will cancel out

all the known terms:-

$$u_{eq} = g(x,t)^{-1}\{-f(x,t) + y_d^n(t) - \sum_{i=0}^{n-2} c_i e^{i+1}(x,t)\}.$$

The left over system is:-

$$\dot{S} = g(x,t)\bar{u} + g(x,t)F(x,t). \tag{3.4}$$

Taking $g(x)F(x,t) = \bar{F}(x,t)$, where $\bar{F}(x,t)$ is supposed to be bounded as:-

$$| \bar{F}(x,t) | \leq \Omega | S(x) |^{\frac{1}{2}},$$
$$\Omega > 0.$$

Taking a positive definite Lyapunov function for regulating the sliding variable:-

$$V = | S |.$$

Taking derivative of Lyapunov function

$$\dot{V} = \text{sign}(S)\dot{S}.$$

Involving SM dynamics

$$\dot{V} = \text{sign}(S)\{g(x,t)\bar{u} + \bar{F}(x,t)\},$$
$$\dot{V} \leq \text{sign}(S)\{g(x,t)\bar{u} + \Omega | S(x) |^{\frac{1}{2}}\}.$$

Taking $\bar{u} = g(x,t)^{-1}\{-k | S(x) |^{\frac{1}{2}} \text{sign}(S)\}$, we have:-

$$\dot{V} \leq \text{sign}(S) | S(x) |^{\frac{1}{2}} \{-k \, \text{sign}(S) + \Omega\}.$$

Selecting $k > \Omega$, $\dot{V}$ becomes negative, hence stability of the closed loop system is confirmed. This selection of $\bar{u}$ makes the sliding surface attractive.

When the system states have reached and confined to the sliding surface, the tracking error will disappear asymptotically according to equation (3.2). During SM the error dynamics will rest on the coefficients $(\lambda_i s)$ of the equation (3.2) and not on the control. The controller task is only to force the system states in the direction of the sliding manifold. The response can be segregated in to two portions as shown in Figure 3.1:-
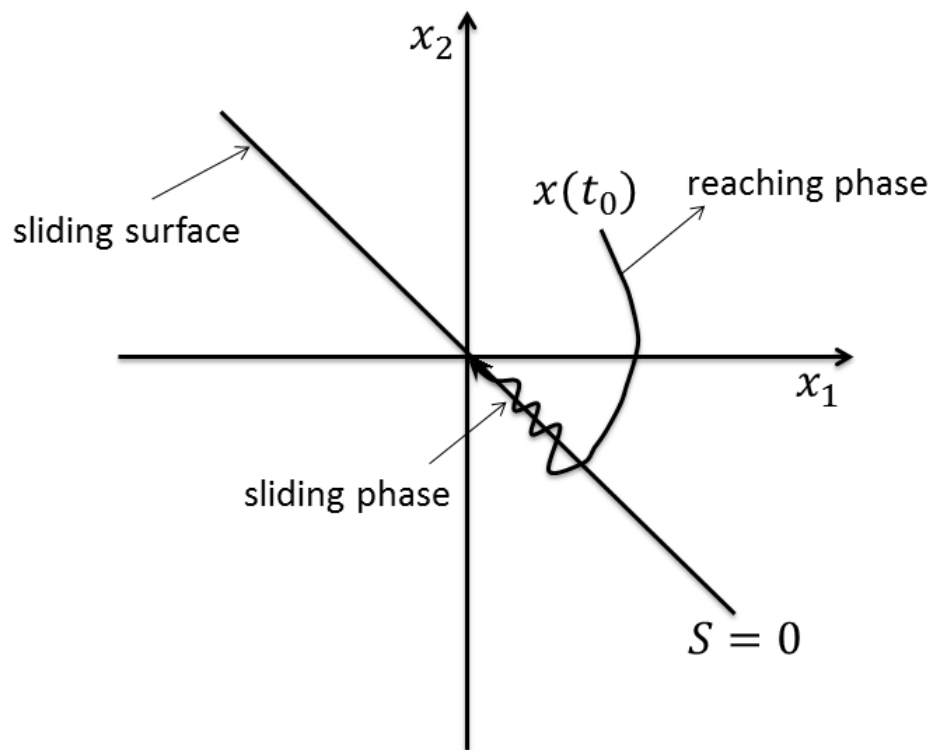
FIGURE 3.1: Sliding mode - system response

1. **Reaching Phase**:- The period of time, $0 < t < t_r$, in which the system trajectories are not contained within the sliding manifold rather approaching it, is known as the reaching phase. This time must be kept to the minimum as system possesses no robustness to matched uncertainties during reaching phase.

2. **Sliding Phase**:- The period of time, $t > t_r$, in which the system trajectories are kept within the sliding manifold, is known as the sliding phase.

The sliding surface has to be accessible in finite time, the advantages of siding motion cannot be recognized by asymptotic convergence of the sliding variable towards the zero. The difficulty is amplified in case of a MIMO system, where chain of sliding surfaces involve hierarchical control and it has been assumed that the trajectory in fact lies in the intersection of all the preceding sliding surfaces. In the case of asymptotic convergence, this idea may not be true.

3.2.3   Robustness Property and Order Reduction

Matched uncertainties affect the system from the input channel. These uncertainties have been totally rejected on the establishment of SM, therefore, the closed loop system is robust against such uncertainties. However, during reaching phase, when SM is not established, these uncertainties may affect the system. Thus the controller should be planned in a way such that the reaching phase is kept as small as possible.

When the SM is established, the dimensions of system are reduced by one, i.e., the system state trajectories now belong to a vector space whose dimension is one less than the dimension of the original system which is also independent of the control. Thus, hereon sliding surface dictates the system performance, while the controller guarantees that the reachability constraints are not violated. Thus, SMC not only ensures robustness, but during sliding phase, the state trajectories belong to a space whose dimensions are fewer as compared to the original system state space. In case of MIMO systems, the reduction in the order of the differential equation describing the system, is by an integer equal to the number of inputs.

3.3   Shortcomings of SMC Technique

Few shortcomings of SMC technique are as follows:-

1. For ideal sliding, controller needs to switch at infinite frequency, so that the trajectories remain confined to the sliding surface. The resulting motion

along sliding surface has to be smooth. In real plants, switching can only be practical at a finite frequency, producing trajectory oscillations in a sliding surface neighborhood. These oscillations are known as chattering. The reasons of chattering are:-

(a) The existence of parasitic dynamics in series with the plant instigates high frequency oscillations that exist in the vicinity of the sliding manifold. These parasitic dynamics denote the fast actuator and sensor dynamics which are mostly ignored in the open loop model used for control design. The interactions among the parasitic dynamics and SMC gives rise to a non decaying oscillatory component of finite amplitude and frequency.

(b) The infinite switching frequency of actuators is never possible practically. Actuators are prone to delays, that forces the system dynamics to oscillate about the sliding manifold.

(c) Any fault in the controlled system may induce a permanent error between actual and desired trajectory in the sliding surface, which is taken as uncertainty. Choosing gain sufficiently high will enforce SM, but at the cost of increased oscillations about the sliding manifold.

2. It is assumed that uncertainty bounds are known. The SM gains are selected accordingly to remain higher than uncertainty bounds. If the uncertainty bounds are not known or cannot be determined, the sliding condition may not be fulfilled.

3. SMC demands the availability of full state vector for the control to be synthesized and applied effectively. But full states may not always be available.

4. In the reaching phase, the system possesses no insensitivity to uncertainties, which may affect the trajectory and produce undesirable results.

3.4 How to Overcome the Shortcomings

Numerous approaches have been proposed and applied to remove the shortcomings of SMC technique. Some of them will be discussed briefly in this Section:-

3.4.1 Chattering Reduction
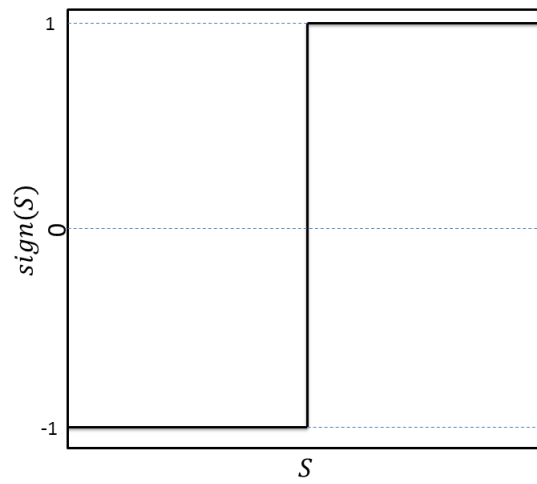
FIGURE 3.2: Signum function

3.4.1.1 Boundary Layer Design

A continuous function that is smooth is introduced to approximate the discontinuous signum function (Figure 3.2) in a region around the sliding surface known as boundary layer [58, 59]. The strategy has two drawbacks. First, the reduction in chattering is attained at the expense of control accuracy. To increase the smoothness in control signals, the thickness of the boundary layer must be kept larger, but this gives greater errors in control precision. Second, when the measurement noise is high, the boundary layer design turn out to be useless in chattering reduction. Few of the possible linear approximations for signum function are briefly explained below, first two approximations are not differentiable, however last three are continuous functions:-

1. Saturation function is a high gain function (Figure 3.3), can be mathematically represented as:-

$$\text{sat}(S, \delta) \;=\; \left\{ \begin{array}{ll} \text{sign}(S), & \mid S \mid > \delta \\ \frac{S}{\delta}, & \mid S \mid \leq \delta \end{array} \right\},$$

where $\delta > 0$ and 2δ is the boundary layer thickness.
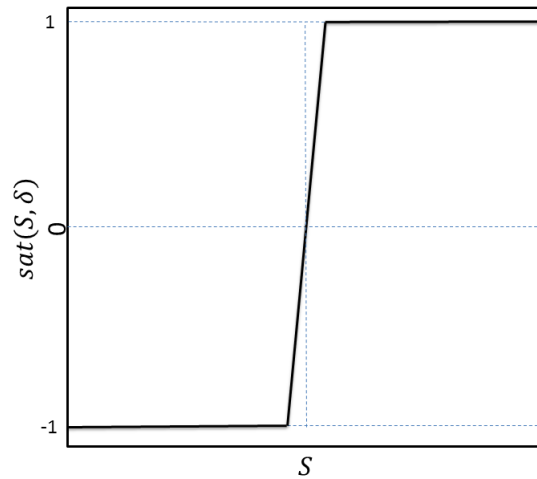
FIGURE 3.3: Saturation function

2. Power law interpolation is another approximation (Figure 3.4), can be mathematically represented as:-

$$v(S, \delta) \;=\; \left\{ \begin{array}{ll} \text{sign}(S), & \mid S \mid > \delta \\ (\frac{\delta}{|S|})^{q-1}\text{sign}(S), & \mid S \mid \leq \delta \\ 0 & S = 0 \end{array} \right\},$$

where $q \in [0, 1)$.
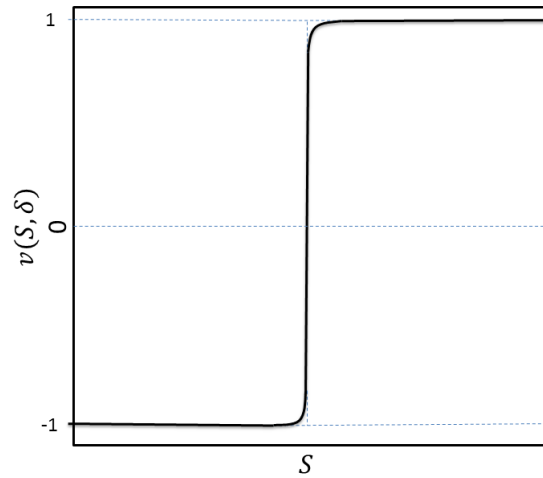
FIGURE 3.4: Power law interpolation

3. Signum like function is the most widely used approximation, it can be pictured as $\delta \to 0$, the function v becomes signum function (Figure 3.5). Mathematically it can be represented as:-

$$v\left(S, \delta\right) \quad = \quad \frac{S}{\mid S \mid + \delta}.$$
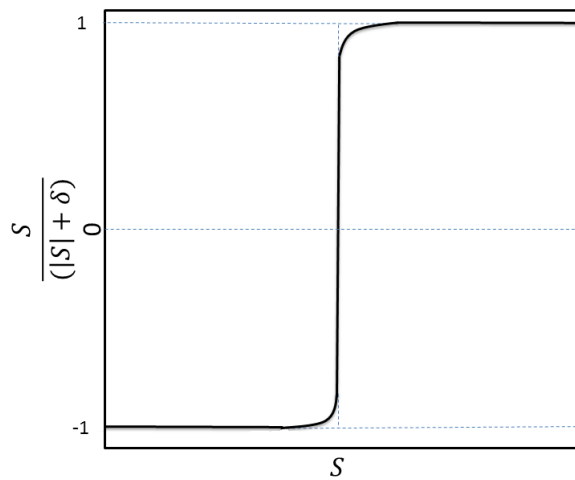
FIGURE 3.5: Signum like function

4. Arctan function is a decent differentiable approximation of the signum function (Figure 3.6):-

$$v\left(S, \delta\right) \quad = \quad k \tan^{-1}(\frac{S}{\delta}),$$

the value of δ should be kept small.
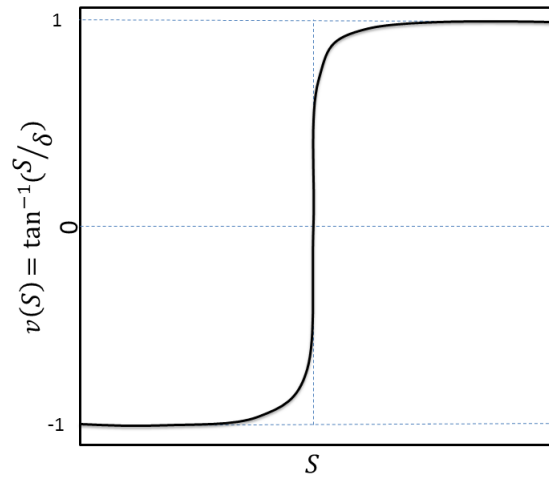
FIGURE 3.6: Arctan function

5. Hyperbolic tan function is another differentiable approximation of the signum function (Figure 3.7):-

$$v\left(S, \delta\right) \;\; = \;\; \tanh(\frac{S}{\delta}),$$

where $\delta < 1$ defines the curve slope.
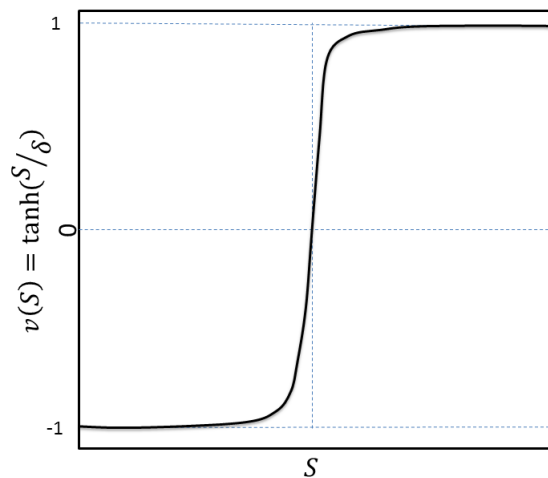
FIGURE 3.7: Hyperbolic tan function

All these approximations are done at the cost of ideal sliding, hence, total invariance property against the matched uncertainty will be lost.

3.4.1.2   Low Pass Filtering the Control Signal

An integrator is introduced before the system to be controlled. An SMC is then synthesized for this extended system. The designed control signal has chattering, but the actual signal applied to the system after integrator is smooth, as the integrator filters out the high frequency chattering by acting as a low pass filter. The chattering suppression is attained by low pass filtering without any deterioration in control precision. Another benefit of this design is that in the presence of noise, chattering increases, however the integrator is capable of filtering out the chattering. Hence, the approach has a better immunity against noise as compared to the conventional boundary layer approach [60, 61].

3.4.1.3   State Observer Based Method

The main reason of employing a state observer in chattering suppression is to disregard un-modelled dynamics from the main control loop. However, this strategy is based on the main assumption that designing of an asymptotic observer is possible and in the existence of noise, observation error can go to zero asymptotically [62]. The performance turns out to be a function of the observer gain that disturbs the tracking error. It is shown that a rise in observer order is counterproductive in minimizing the tracking error [63].

3.4.1.4   State/Output Dependent Gain Method

The amplitude of chattering depends proportionally on the SMC gain. It is therefore useful if a chattering suppression technique could adapt the SM gain without losing the SM condition. In this technique, gain is varied on the basis of system's state/output dependent bounds without spoiling the trajectory tracking convergence rate [64, 65].

3.4.1.5   Uncertainty/Fault Estimation

In SMC design uncertainty/fault is dominated by assuming it to be bounded and choosing sufficiently high controller gain. A disturbance/fault estimater is designed to nullify the fault effects, thus allowing reduction in SMC gain [66].

3.4.1.6   Use of HOSMC

In HOSM based techniques most famous are the second order SM techniques. Alongside removing certain fundamental shortcomings of the classical SMC techniques, they also provide enhanced tracking precision when in sliding motion. The concept of HOSM is the generalization of classical SM, as the former has been realized by generalizing the constraint on the relative degree of the sliding surface. HOSM is realized by basing the design on higher order derivatives of the sliding surface, in contrast to the first derivative as in classical SM. Apart from retaining the major benefits of classical SM, it provides the additional improvements in terms of improved accuracy with regards to switching delay. Various HOSM algorithms exist in literature [64, 67–69].

3.4.2   Estimation of Uncertainty Bounds

The key feature of SMC is, during sliding phase the system remains insensitive to parametric uncertainties and disturbances. However in such design, the assumption that the uncertainties are bounded and their bounds are perfectly known is involved. Sometimes bounds on the uncertainties may not be easily obtainable due to complexities involved in the structure of uncertainties. This results in larger magnitude of control gain and eventually higher control effort. Various approaches have been proposed, like [70, 71], in which the bounds are found adaptively. Adaptation laws proposed in these techniques provide upper bounds on the uncertainties, the use of which guarantees asymptotic stability of uncertain dynamical systems.

3.4.3 State Observation

Many a time controller implementation requires full state vector availability. Full states are mostly not available, making the implementation of these laws impractical. Even if the states are available, the sensor costs may be high thus making the usage of estimators or observers compulsory. One more issue with the real plants is regarding their mathematical models that are not accurate. For these plants, classical Luenberger observer does not produce results with desired accuracy, thus further aggravating the complication of state estimation.

The concept of SMC has been adapted and used for state estimation by designing an observer, for both linear and non-linear systems. Same design principles have been employed as used for SMC. Discontinuous output injectors have been used, the trajectories of the observer are forced to evolve in a finite time on an appropriate sliding surface. Sliding manifold is mostly taken as difference among the observer and the system output. The sliding motion consequently gives the estimated system states. Various SM observers exist in literature, like [72–74]. The necessity to get an estimate of the states and uncertainties together in an integrated way is accomplished by designing an extended state observer [75]. It can estimate the states and uncertainties acting on the system allowing disturbance rejection or compensation.

3.4.4 Reaching Phase Elimination

The motion of systems governed by SMC technique consists of two phases, the reaching phase and the sliding phase. During reaching phase, once the system state is moving in the direction of the sliding surface, the system possesses no insensitivity to the uncertainties and noise. Thus, it is desired to reduce the time of this phase or even completely eliminate it. The issue has been addressed in literature to totally eliminate the reaching phase [76–78]. These techniques re-frame the sliding surface equations so that the system's initial state rests on the modified sliding domain. Since the control action is designed in a way that

system states are confined to the sliding domain, resultantly the reaching phase is eliminated. Additional steps may be required to ensure the convergence of modified sliding surface to the original.

3.5 Integral SMC

As explained previously the system possesses no insensitivity and robustness against uncertainties and noise while in reaching phase. Once the SM is established system becomes robust against these disturbances. Integral SM [78, 79] on the other hand enforces SM right from the initial time instant throughout the entire system response. Unlike standard SM approach their is no reduction in system's order, the order of the system remains equal to the dimensions of original plant. Consider a dynamical system represented by state space equation:-

$$\dot{x} = f(x) + g(x)u, \tag{3.5}$$

where $x \in \mathbb{R}^n$ is a state vector, $u \in \mathbb{R}^m$ is a control vector. If their are no uncertainties in system (3.5), then a closed loop control law $u = u_o(x)$ can stabilize the system in desired way. Such ideal closed loop system can be given as:-

$$\dot{x}_o = f(x_o) + g(x_o)u_o.$$

However in practical systems, uncertainty affects cannot be ignored, hence the real trajectory of the system is given as:-

$$\dot{x} = f(x) + g(x)\{u + F\},$$

where $g(x)F = \bar{F}$ represents the uncertainty fulfilling matching conditions. It is assumed to be bounded with known upper bound. The control structure is taken as:-

$$u = u_o + \bar{u},$$

where $u_o \in \mathbb{R}^m$ is the continuous control, i.e., an ideal control which gives desired output for a nominal plant with no uncertainties or faults, $\bar{u} \in \mathbb{R}^m$ is the discontinuous control that handles the uncertainties.

Consider now the sliding surface:-

$$S \;=\; S_o(x) + z,$$

where S, $S_o(x)$ and $z \in \mathbb{R}^m$. S_o is representing the sliding surface based on the conventional SM design. The dynamics of sliding surface are:-

$$
\begin{aligned}
\dot{S} \;&=\; \frac{\partial S_o}{\partial x}[f(x) + g(x)\{u + F\}] + \dot{z}, \\
&=\; \frac{\partial S_o}{\partial x}[f(x) + g(x)u_o + g(x)\bar{u} + g(x)F] + \dot{z}.
\end{aligned}
$$

The u_o can be synthesized by any control approach like PID, LQR etc. $\dot{z}$ is taken as:-

$$\dot{z} \;=\; -\frac{\partial S_o}{\partial x}\{f(x) + g(x)u_o\}.$$

This selection of $\dot{z}$ and initial condition $z(0)$ will guarantee that reaching phase is eliminated and SM is imposed right from the start time in the absence of uncertainty. The left out system is:-

$$\dot{S}_i \;=\; \frac{\partial S_o}{\partial x}g(x)\bar{u} + \frac{\partial S_o}{\partial x}\bar{F}.$$

The discontinuous control $\bar{u}$ is defined so as to enforce sliding motion along the selected manifold:-

$$\bar{u} \;=\; -M\mathrm{sign}\,(S).$$

The gain M is selected such that SM is enforced on the manifold $S = 0$. Some examples of the ISM technique explaining complete design process are available

at [79].

3.6 Higher Order Sliding Mode

The notion of HOSMs is the extension of classical SM, as the former has been realized by generalizing the constraint on the relative degree of the sliding surface i.e., unlike classical SM where relative degree of one with regards to the control input is must, HOSM relaxes this requirement. The driving idea in HOSM is to base the design on higher order derivatives of the sliding surface unlike the first derivative as the case with classical SM. Apart from retaining the major benefits of classical SM, it gives the added improvement in terms of improved accuracy with regards to switching delay, by enforcing higher order derivatives of sliding surface to zero.

3.6.1 Sliding Motion and Sliding Set

Consider a dynamical system represented by state space equation:-

$$\dot{x} \;=\; f(x) + g(x)\,u, \tag{3.6}$$

where $x \in \mathbb{R}^{\mathrm{n}}$ is a state vector, $u \in \mathbb{R}$ is control. $f(x)$ and $g(x)$ are smooth vector functions of proper dimensions. The control u is obtained by a feedback discontinuous control law $u = U(x,t)$. Defining a sliding surface $S \in \mathbb{R}$ as:-

$$S \;=\; S(x,t), \tag{3.7}$$

such that the control task is achieved by making it zero. If the system (3.6) has a globally defined relative degree r with respect to the sliding variable S (3.7), then

the dynamics of the sliding surface can be represented as:-

$$
\begin{aligned}
S^r &= L_f^r S(x) + L_g L_f^{r-1} S(x) u, \\
&= \Phi(x,t) + \Upsilon(x,t) u, \tag{3.8}
\end{aligned}
$$

where L_g, L_f are Lie derivatives, it has been assumed that $L_g L_f^{r-1} S(x) \neq 0$ holds globally and in the first $(r-1)$ time derivatives of the sliding variable S the discontinuity does not appear, i.e., $S, \dot{S}, \cdots S^{r-1}$, exist and are single valued. The resulting $n-r$ order zero dynamics can be represented as [80]:-

$$
\dot{\eta} = Z(\bar{S}, \eta),
$$

where η fulfills the condition $L_g \eta_i(x) = 0$ for $i = 1, \cdots (n-r)$ and $\bar{S} = [S, \dot{S}, \cdots S^{r-1}] = [S, L_f S, \cdots, L_f^{r-1} S]$. The internal dynamics are assumed stable.
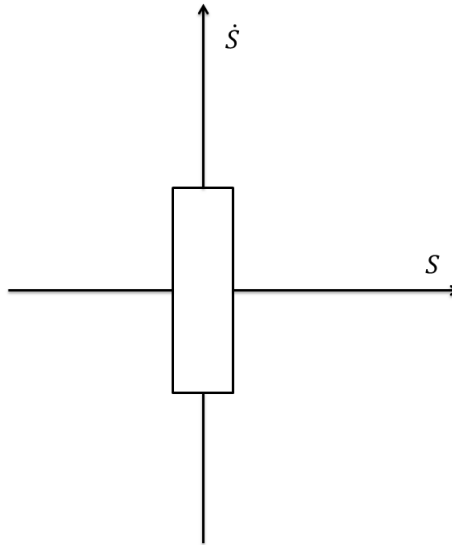
FIGURE 3.8: Classical SMC

The objective now is to workout a controller u that can stabilize the non-linearities and uncertainties of the system (3.8). For the constraint (3.7), the rth order sliding set (S_r) is denoted by r equalities $S = \dot{S} = \cdots = S^{r-1} = 0$ that makes an r-dimensional condition on system states. If the only constraint enforced on the sliding motion is $S = 0$, then the order of the sliding set S is one, which is same as the case of standard SMC (Figure 3.8). The sliding order gives an

idea about the degree of smoothness of the sliding variable in the neighborhood of the SM i.e., incase of second order SM, a finite time converging algorithm with discontinuous controller u can stabilize S and $\dot{S}$ to zero in finite time. Both S and $\dot{S}$ will be smooth but $\ddot{S}$ will be discontinuous, as shown in Figure 3.9. The system converges into 2-dimensional sliding set $S = \dot{S} = 0$. The first order sliding, features finite time convergence while HOSMs may be asymptotic as well as finite time converging.

3.6.2   Real Sliding

For ideal sliding, the constraint are to be retained ideally. however, when the limitations are given consideration and the constraint is retained only approximately, it ends up in real sliding. In r_{th} order SMC, by infinite switching frequency of the discontinuous controller, theoretically the system trajectories are retained inside the r_{th} order sliding set. However, in real sense, infinite switching frequency is never realizable. Hence, any ideal sliding motion should be understood as a limiting motion when switching delays disappear i.e., the switching frequency tends to infinity. Let ϵ be a measure of these switching delays. Then the SM may be defined by a sliding precision asymptotic as $\epsilon \to 0$.

Definition.([68]) Let $\gamma(\epsilon)$ be a real valued function such that $\gamma(\epsilon) \to 0$ as $\epsilon \to 0$. A real sliding algorithm, on the constraint $S = 0$, is said to be of order $r(r > 0)$ with respect to $\gamma(\epsilon)$ if for any compact set of initial conditions and for any time interval $[t_1, t_2]$ there exists a constant C, such that the steady state process for $t \in [t_1, t_2]$ satisfies:-

$$\mid S \mid \ \leq \ C \mid \gamma(\epsilon) \mid^r .$$

In order to achieve r_{th} order of real sliding with discrete switching it is essential to acquire at least the r_{th} order in ideal sliding. Thus, the real sliding order does not

surpass the corresponding SM order. First order real sliding motion is attained by practical application of standard SMC. The second order real sliding motion is attained by discrete application of the second order sliding algorithms. In fact any random order of real sliding can be realized by discretization of the same order sliding algorithms.

3.6.3 Second Order Sliding Control Algorithms

The advantages of SMC can only be exploited if the system trajectories are constrained within the sliding manifold. Asymptotically stable HOSM algorithms are easily found in literature [81, 82]. Second order SM techniques are the most famous among the HOSM algorithms. In order to review some finite time reaching second order SM algorithms consider a system:-

$$\dot{x} = \mathcal{F}\left(x(t), t, u(t)\right),$$

where $x(t) \in \mathbb{R}^n$, $u \in \mathbb{R}$, t is an independent variable and $\mathcal{F}$ is a sufficiently smooth vector function. SM dynamics are represented as:-

$$\dot{S} = f(x, t) + g(x, t)u,$$

here the classical SM control methods can be used to stabilize the system dynamics. Nevertheless second order SMC can be employed for smoothing out the input signal as we are using the derivative of control as an input. The dynamics of the system with new control input then become:-

$$\dot{S} = f(x, t) + g(x, t)u,$$
$$\dot{u} = v,$$

this can be written as:-

$$
\begin{aligned}
\ddot{S} &= \frac{\partial}{\partial t}f(x,t) + \frac{\partial}{\partial x}f(x,t)\mathcal{F}(x,t,u) + \\
&\quad \left[\frac{\partial}{\partial t}g(x,t) + \frac{\partial}{\partial x}g(x,t)\mathcal{F}(x,t,u)\right]u + g(x,t)v, \\
\dot{u} &= v,
\end{aligned}
$$

taking

$$
\begin{aligned}
\frac{\partial}{\partial t}f(x,t) + \frac{\partial}{\partial x}f(x,t)\mathcal{F}(x,t,u) + & \\
\left[\frac{\partial}{\partial t}g(x,t) + \frac{\partial}{\partial x}g(x,t)\mathcal{F}(x,t,u)\right]u &= \Phi(x,t,u), \\
g(x,t) &= \Upsilon(x,t,u),
\end{aligned}
$$

we can write:-

$$
\ddot{S} = \Phi(x,t,u) + \Upsilon(x,t,u)v, \tag{3.9}
$$

$$
\dot{u} = v. \tag{3.10}
$$

It is assumed that the system dynamics (3.9-3.10) satisfy the following bounding conditions:-

$$
\begin{aligned}
0 < \Gamma_m &\leq \Upsilon(x,t,u) \leq \Gamma_M, \\
|S| &\leq S_0, \\
\Phi(x,t,u) &\leq \Phi,
\end{aligned}
$$

where Γ_m, Γ_M, S_0, Φ are some appropriate positive constants. Some finite time converging second order sliding algorithms for stabilization of the systems of type (3.9-3.10) are now discussed. Examples of various HOSM techniques explaining complete design process are available at [69, 83, 84].
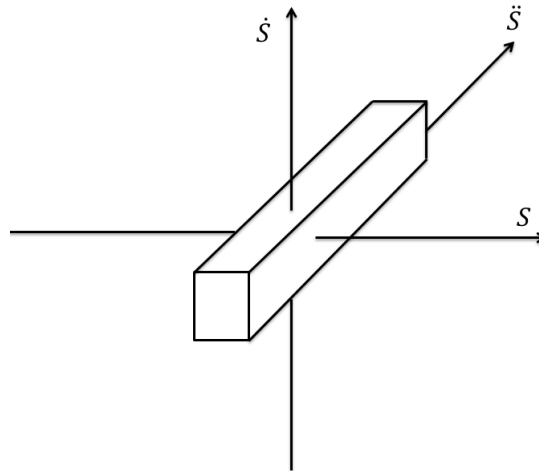
FIGURE 3.9: 2nd order SMC

3.6.3.1   Twisting Algorithm

Twisting algorithm [68] is described by a twisting action of the phase portrait around the origin (as shown in Figure 3.10). The finite time convergence to the origin is for the reason of switching among two dissimilar control amplitudes as the system trajectory approaches closer to the origin. The sliding variable's derivative sign is requisite for decision making. The controller is represented as:-
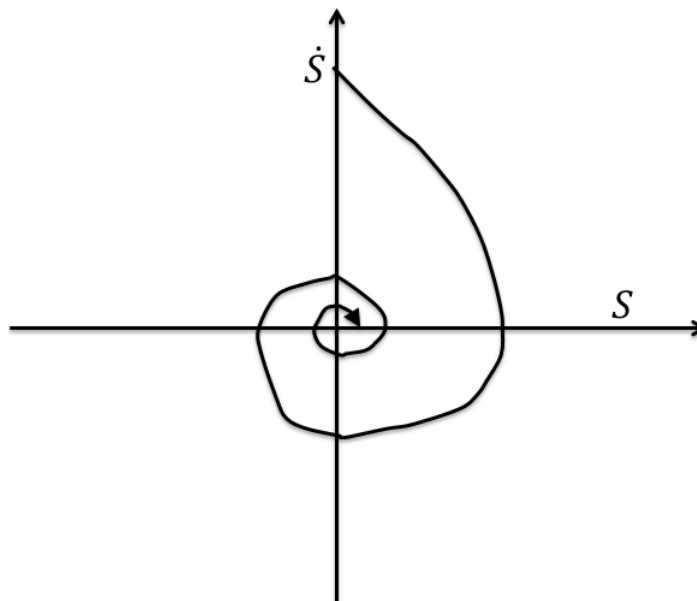
FIGURE 3.10: Twisting algorithm

$$v(t) = \begin{cases} -u, & \mid u \mid > u_0 \\ -V_M \operatorname{sign}(S), & S\dot{S} > 0, \mid u \mid \leq u_0 \\ -V_m \operatorname{sign}(S), & S\dot{S} \leq 0, \mid u \mid \leq u_0 \end{cases},$$

the necessary conditions for the finite time convergence to the sliding manifold are:-

$$\begin{aligned} V_M &> max\left(\frac{4\Gamma_M}{S_0}, \frac{\Phi}{\Gamma_m}\right), \\ V_m &> \frac{\Phi}{\Gamma_m}, \\ \Gamma_m V_M - \Phi &> \Gamma_M V_m + \Phi. \end{aligned}$$

3.6.3.2 Suboptimal Algorithm

Suboptimal algorithm [67] is the optimized twisting algorithm (as shown in Figure 3.11). The controller is represented as:-
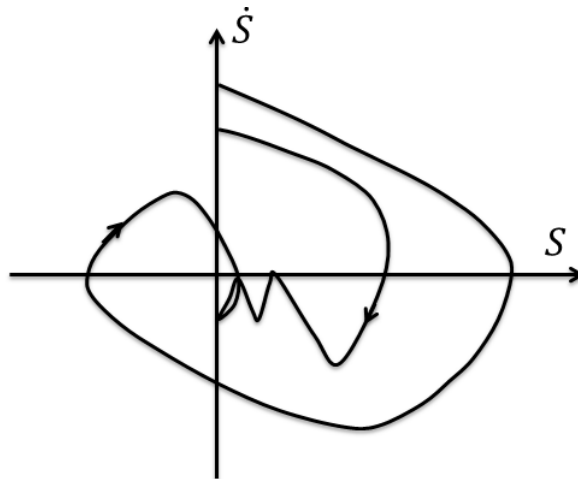
FIGURE 3.11: Suboptimal algorithm

$$v(t) = -\alpha(t)V_M \operatorname{sign}[S(t) - .5S(t_M)],$$

$$\alpha(t) = \left\{ \begin{array}{ll} \alpha^*, & [S(t) - .5S(t_M)]\,[S(t_M) - S(t)] > 0 \\ 1, & [S(t) - .5S(t_M)]\,[S(t_M) - S(t)] \le 0 \end{array} \right\},$$

where t_M is such that $S(t_M) = 0$ and $S(t_M)$ denotes the last stationary value of the $S(t)$ function. The necessary conditions for finite time convergence to the sliding manifold are:-

$$\alpha^* \in (0,1] \cap \left(0, \frac{3\Gamma_m}{\Gamma_M} \right),$$

$$V_M > max \left(\frac{\Phi}{\alpha^*\Gamma_m}, \frac{4\Phi}{3\Gamma_m - \alpha^*\Gamma_M} \right).$$

3.6.3.3 Algorithm with Prescribed Law of Convergence

Algorithm with prescribed law of convergence of S [85], the sliding variable moves towards the origin in accordance with a pre-specified guiding function $\mathcal{L}(S)$ (as shown in Figure 3.12). The controller is represented as:-
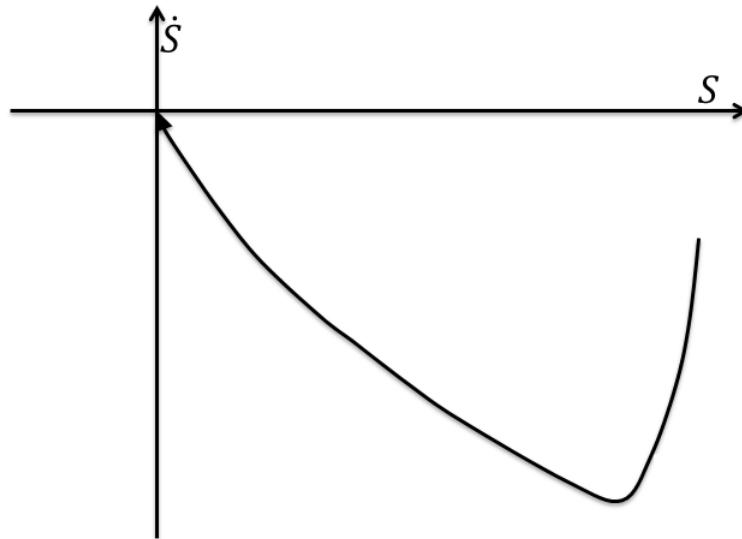
FIGURE 3.12: Algorithm with prescribed law of convergence

$$v(t) \quad = \quad \left\{ \begin{array}{ll} -u, & \mid u \mid > u_0 \\ -V \operatorname{sign}\left(\dot{S} - \mathcal{L}(S)\right), & \mid u \mid \leq u_0 \end{array} \right\},$$

where $V > 0$, the function $\mathcal{L}(S)$ is continuous everywhere except $S = 0$ and it is supposed that all the solutions of the equation $\dot{S} = \mathcal{L}(S)$ disappear in finite time.

3.6.3.4 Drift Algorithm

Drift algorithm [86], it is somewhat diverse as compared to the other second order SM techniques. The sign of sliding variable S remains unchanged till it approaches a certain neighborhood of the origin. This helps removing overshoot for S (as shown in Figure 3.13). A very important aspect of drift algorithm is, it only gives desired results if the switching delay is non-zero and sliding is non-ideal. Thus, the drift algorithm has only a real sliding interpretation. The controller is represented as:-
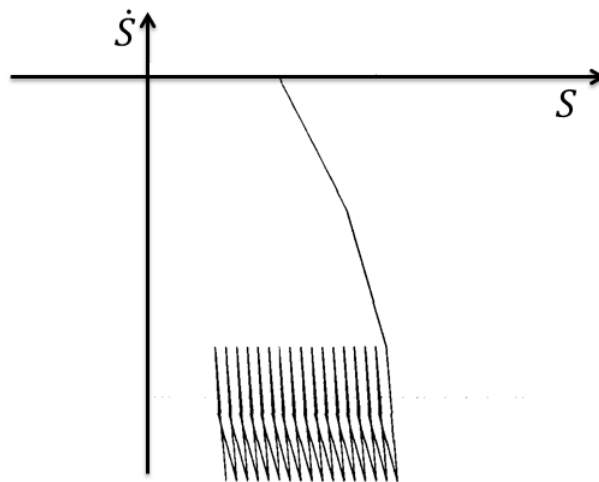
FIGURE 3.13: Drift algorithm

$$v(t) = \begin{cases} -u, & \mid u \mid > u_0 \\ -V_M \operatorname{sign}\left(\dot{S}\right), & S\dot{S} > 0, \mid u \mid \leq u_0 \\ -V_m \operatorname{sign}\left(\dot{S}\right), & S\dot{S} \leq 0, \mid u \mid \leq u_0 \end{cases}.$$

3.6.3.5 Super Twisting Algorithm

STA [68] has been intended for systems that have relative degree one with respect to the sliding variable S and hence the sliding variable dynamics can be represented as:-

$$\dot{S} = f(x,t) + g(x,t)u,$$

with bounding conditions:-

$$\begin{aligned} \Phi(x,t) &\leq \Phi, \\ 0 < \Gamma_m &\leq \Upsilon(x,t,) \leq \Gamma_M, \\ \mid S \mid &\leq S_0, \end{aligned}$$

where Γ_m, Γ_M, S_0, Φ are some appropriate positive constants. The STA when applied to a system (3.9-3.10) converges in finite time. It describes a controller, $u(t)$, that is smooth and can be written as a sum of two terms. Both terms are function of sliding variable. The first one of them is discontinuous function's integral, while the second term is a continuous function. The trajectories of STA are characterized by twisting movement round the origin on the phase portrait of sliding variable (as shown in Figure 3.14). The STA is described by the control law:-
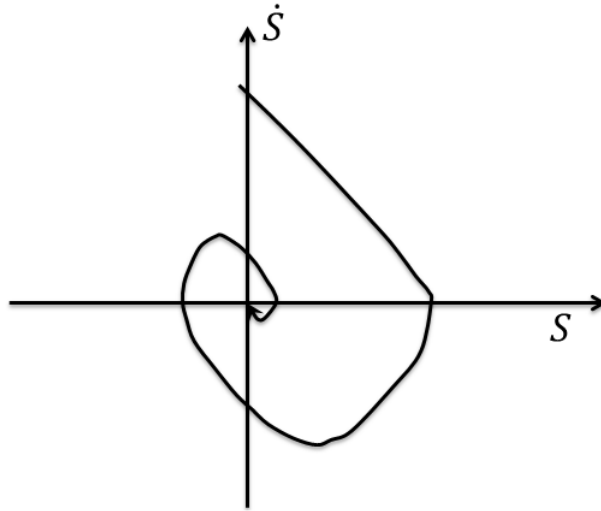
FIGURE 3.14: Super twisting algorithm

$$u(t) = u_1(t) + u_2(t),$$

where

$$u_1(t) = \left\{ \begin{array}{ll} -u, & \mid u \mid > 1 \\ -W \operatorname{sign}(S), & \mid u \mid \leq 1 \end{array} \right\},$$

$$u_2(t) = \left\{ \begin{array}{ll} -\lambda \mid S_0 \mid^\rho \operatorname{sign}(S), & \mid S \mid > S_0 \\ -\lambda \mid S \mid^\rho \operatorname{sign}(S), & \mid S \mid \leq S_0 \end{array} \right\},$$

the corresponding essential conditions for finite time convergence are:-

$$W > \frac{\Phi}{\Gamma_m} > 0,$$

$$\lambda^2 \geq \frac{4\Phi\Gamma_M(W + \Phi)}{\Gamma_m^3(W - \Phi)},$$

$$0 < \rho \leq .5.$$

For $\rho = 1$, the algorithm converges to the origin exponentially. For systems where $S_0 = \infty$ and there is no bound on the control, the algorithm can be simplified as:-

$$
\begin{aligned}
u(t) &= -\lambda \mid S \mid^{\rho} \operatorname{sign}(S) + z, \\
\dot{z} &= -W \operatorname{sign}(S).
\end{aligned}
$$

Some variants of this algorithm will be discussed in succeeding Chapters.

3.7 Chapter Summary

SMC is a robust non-linear control technique, which makes it a very strong candidate to design control algorithms for systems affected by matched uncertainties. On the establishment of SM, the parameter variations and disturbances, which have known bounds, do not affect the plant dynamics, provided they satisfy the matching conditions. The plant simultaneously follows a reduced order system, thereafter the dynamical behavior of the system is governed by the choice of a sliding surface. An n-dimensional tracking problem is transformed to a lower order stabilization problem, which makes handling of the problem less complicated.

Some of the basic concepts of SMC techniques have been reviewed in this Chapter. Few shortcomings and proposed directions to compensate their effects have also been discussed. On the basis of these concepts and directions FTC schemes for diesel engine air management actuators will be formulated in succeeding Chapters.

Chapter 4

Diesel Engine Modelling

4.1 Introduction

Mathematical modelling is a skill of expressing the difficult problems related to application area with tractable mathematical interpretations. The numerical and theoretical analyses of these models then offer solutions, vision, and necessary assistance which is beneficial for the initiating application. It helps to describe the system's functioning. A mathematical model is derived to study the effects of various involved mechanisms, to make estimates about behavior and to propose control systems so as to achieve desired results from the actual system. Mathematical models may be of various forms, like statistical models, differential equations including ODEs and PDEs etc. Models can also be classified on the basis of other criterions like linear versus non-linear, explicit versus implicit, static versus dynamic, deterministic versus probabilistic, discrete versus continuous etc. The quality of a scientific field heavily relies on how well the developed mathematical model emulates the real physical system. The mathematical models contain four major elements i.e., governing equations, constitutive equations, constraints and kinematic equations.

To develop control systems or FTC schemes for a diesel engine it is essential to have a precise mathematical model that agrees with the physical diesel engine.

A lot of models describing the dynamics of diesel engine exist in literature like [87–90]. The model used in this research has been suggested in [90]. It is a fully validated industrial scale MVM of a turbocharged diesel engine that is equipped with the EGR and VGT actuators (Figure 4.1 and 4.2). The model is specially intended to be suitable for applications like analysis of the system, simulations, and construction of model based control schemes. It describes:-

1. Gas flow dynamics.

2. Manifold pressure dynamics.

3. EGR system.

4. Turbocharger.

5. Actuator dynamics.

It has eight states and three control inputs. The adjustment and validation of the model has been done by taking stationary and dynamic measurements on engine test bench. To estimate the model parameters, weighted least squares optimization technique has been used. It is demonstrated that the mean relative errors are less than 5.8 percent in all measured variables. The model captured the system properties like non-minimum phase behaviors, sign reversals, overshoots as well as couplings between the channels that are necessary for control design. The simulink implementation of model is provided for academic work and research on control of diesel engine and is available for download at [91]. The purpose of the application is to offer an industrial scale fully validated diesel engine model to researchers and engineers, which can be utilized for development, simulation and validation of new control algorithms [90].

4.2 System Operation

The air path of an engine is shown in Figure 1.1. It comprises of:-
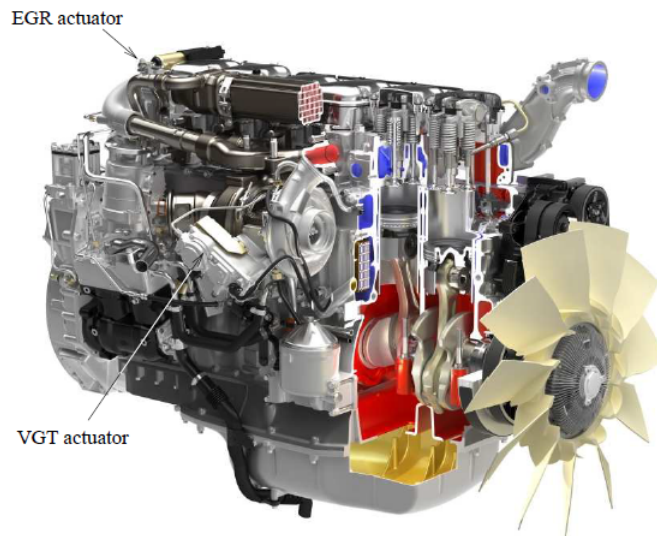
FIGURE 4.1: Six cylinder turbocharged diesel engine - Scania [92]

1. Intake manifold.

2. EGR actuator.

3. VGT actuator.

4. Turbo charger.

5. Cylinders.

6. Exhaust manifold.

7. Inter-cooling units.

8. Sensing units.

The operation of air management system is explained as under:-

4.2.1 EGR Operation

1. The EGR system is responsible for reducing the overall combustion chamber temperature and oxygen concentration.
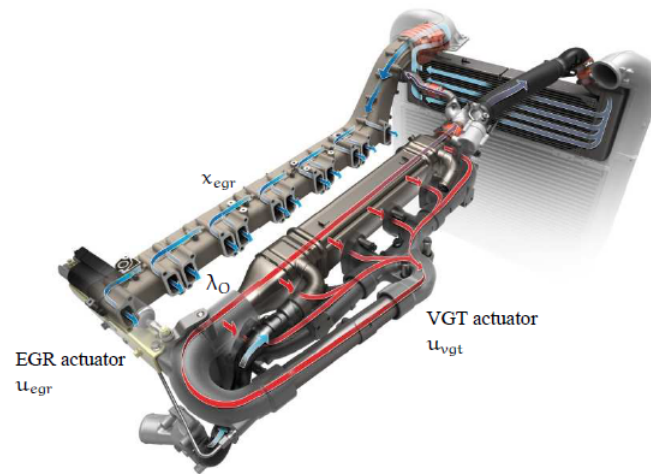
FIGURE 4.2: EGR and VGT actuators located in exhaust channel [92]

2. This is guaranteed by redirecting some quantity of exhaust gas into the intake manifold, after lowering its temperature by passing through inter-cooling unit.

3. The exhaust gas fraction and compressed air coming from the compressor forms a mixture and this mixture enters the cylinders during intake strokes.

4. This operation is controlled by EGR actuator.

4.2.2   VGT Operation

1. After combustion of mixture inside the combustion chambers, exhaust gases are thrown into the engine exhaust.

2. Some percentage of these exhaust gases is redirected to the intake manifold, as explained above, thus becoming a part of the EGR system.

3. Remaining portion of exhaust gases gives drive to a VGT through VGT actuator.

4. VGT energizes compressor, which in return produces compressed air and directs it to the intake manifold.

5. The compressed air blends with the EGR fraction, after passing through the air to air inter-cooling unit, in intake manifold.

The air system actuators provide an important avenue to achieve the stringent low level emission standards EURO V and VI, mainly related to oxides of nitrogen (NO_x) and Particulate Matter (PM) [43]. It has been recognized that NO_x emissions can be decreased by enhancing the cooled exhaust gas concentration inside the intake manifold, as it substitutes some amount of fresh air thus decreasing oxygen concentration and giving lower peak combustion temperature. The PM can be decreased by enhancing the oxygen to fuel ratio, as increase in concentration of oxygen guarantees oxidation of PM [93]. This PM-NO_x trade-off generates a complication very difficult to overcome. It is hence needed to plan a coordinated control approach for the EGR and VGT actuators to fulfill these conflicting requirements [35]. Orthodox mapping and calibration centered techniques, using conventional controllers to follow map based set-points have trouble producing the desired performance regarding emissions at steady state or transient state conditions, especially in case of actuator faults.

4.3 Diesel Cycle

For having a better understanding of physical processes involved in combustion of fuel, it is necessary to have knowledge of diesel cycle. It is a combustion process in which fuel is burnt by heat produced through the compression of air inside the combustion chamber. The ideal diesel cycle undergoes the four different processes, as shown in Figure 4.3. Fuel is sprayed into the cylinder at p_2 when the compression is complete. The heat supplied by the fuel is assumed to be at constant pressure from p_2 to p_3 and rejected at constant volume from p_4 to p_1. The details are as under:-
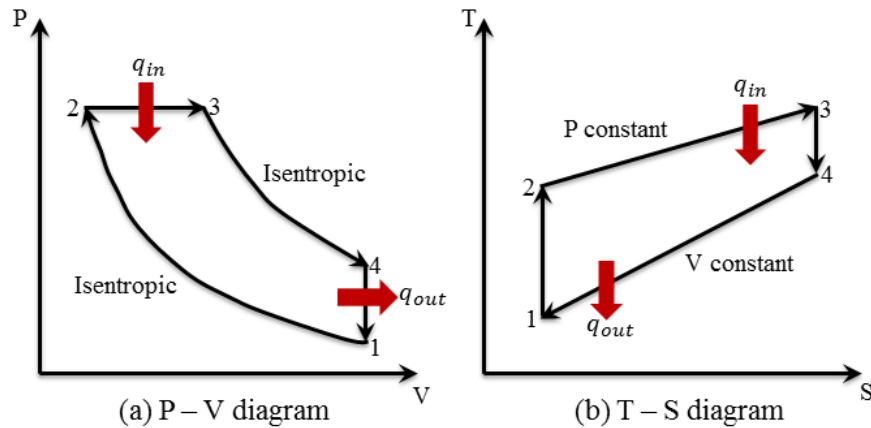
FIGURE 4.3: Diesel cycle

1. Process 1 to 2 in the plot is isentropic compression of the fluid. Energy is transmitted in to the system as work, without any heat loss. This is achieved through the piston compressing the air.

2. Process 2 to 3 in the plot is reversible heating at constant pressure. Energy enters the system as heat. This is done by fuel combustion.

3. Process 3 to 4 in the plot is isentropic expansion. Energy is transmitted out of the system as work without any heat loss. This is done by the working fluid expanding and pushing a piston.

4. Process 4 to 1 in the plot is reversible cooling at constant volume. Some of energy is transmitted out of the system as heat. This is done by venting the air.

The net gain is calculated by working out the difference among the heat entering and leaving the system. The net work produced is also signified as an area enclosed by the cycle on the P-V diagram. The energies, both input and output, and the efficiency can be calculated using the temperatures and specific heats:-

$$
\begin{aligned}
q_{in} &= C_p(T_3 - T_2), \\
q_{out} &= C_v(T_1 - T_4), \\
\eta &= \frac{q_{in} + q_{out}}{q_{in}}.
\end{aligned}
$$

4.4 Mathematical Modelling of a Diesel Engine

The model consists of eight states related to pressures in intake and exhaust manifolds, mass fraction of oxygen in intake and exhaust manifolds, turbocharger speed and remaining three states to describe the dynamics of two actuators i.e., EGR and VGT, that are the control inputs. Figure 4.4 displays the block diagram of a diesel engine, showing various engine sub-systems, states, control inputs and output/performance parameters. The states, control inputs and various involved parameters are described in Table 4.1-4.4. The states of pressures in intake and exhaust manifolds and turbo speed (p_{im}, p_{em}, and ω_t) define the key system dynamics and the significant system attributes, like nonminimum phase behaviors, overshoots and sign reversals. The states of oxygen mass fractions in intake and exhaust manifolds (X_{Oim} and X_{Oem}) have been used to model the dynamics in λ_o. The actuator states ($\tilde{u}_{egr1}$, $\tilde{u}_{egr2}$ and $\tilde{u}_{vgt}$) define the dynamics of actuators, where the dynamics of EGR actuator are modelled as two states ($\tilde{u}_{egr1}$ and $\tilde{u}_{egr2}$), as a second order system, to accurately define the overshoot in the actuator. Model extensions have also been investigated in [90] where the temperature states have been included, it has however been proven that the addition of temperature states do not affect the dynamic behavior. Additionally, the drop in pressure across the inter-cooler is not modelled as it do not affect the dynamic behavior significantly. Still, it affects the stationary values, however incorporation of these details do not improve the overall model. The model is parameterized using the engine speed n_e. The resulting model is given as:-

$$\dot{x} = f\left(x, u, n_e(u_\delta)\right),$$

here speed of engine n_e is taken as the model input. The EGR actuator is shut when it's position is at $u_{egr} = 0$ percent and it is open when $u_{egr} = 100$ percent. Similarly, the VGT actuator is shut when it's position is at $u_{vgt} = 0$ percent and it is open when $u_{vgt} = 100$ percent.
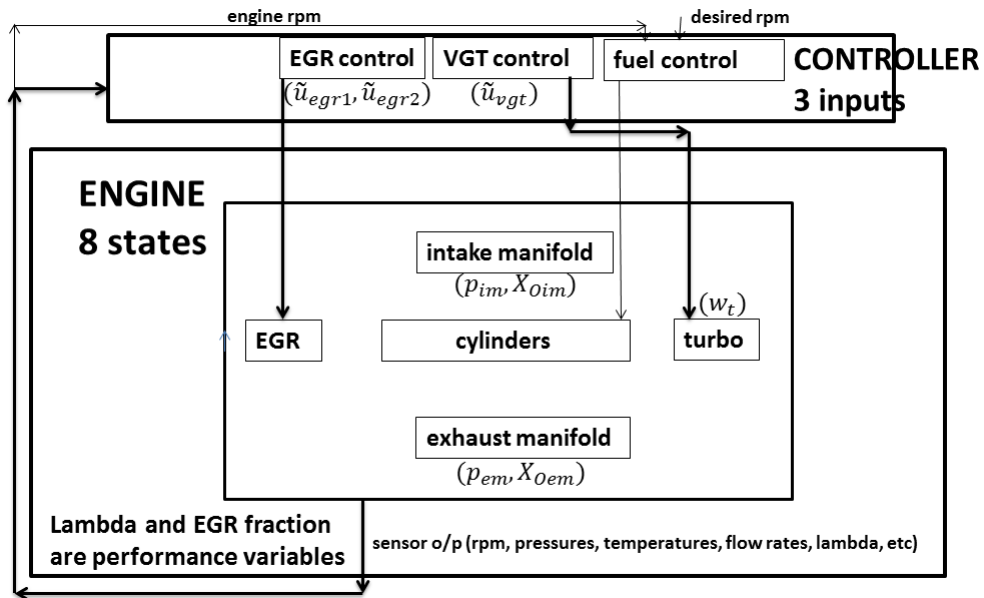
FIGURE 4.4: Engine block diagram

It is easy to reconstruct the model parameters and to use the same tuning techniques to tune the model for diverse range of turbocharged diesel engines that are equipped with EGR and VGT actuators. The use of empirical formulas has increased the flexibility of the model with regards to it's applications. For details on the subject, reader is referred to [90].

4.4.1 Assumptions

To construct a model, that is simple and that displays the key system dynamics, especially the mass flow effects, following assumptions are made:-

1. Standard isothermal processes are assumed for modelling the intake and exhaust manifolds.

2. It has been assumed that gases are ideal. Two sets of thermodynamic properties are followed in this regard:-

    (a) Gas constant of air is taken as R_a and specific heat capacity ratio is taken as γ_a.

(b) Gas constant of exhaust gas is taken as R_e and the specific heat capacity ratio is taken as γ_e.

3. It has been assumed that the gas constant or the specific heat capacity are not effected by the exhaust gas fraction in the intake manifold.

4. Heat transfer in to the intake manifold or from the intake manifold is zero.

5. Back flow of gases is zero in cases of EGR valve, cylinders, compressor and turbine.

6. The oxygen to fuel ratio is taken as greater than one.

7. Ideal conditions are assumed for inter-cooler and EGR cooler.

4.4.2 Stationary and Dynamic Measurements for Model Validation and Tuning

To validate the system's model and tune it's various parameters, stationary and dynamic readings have been taken on an engine test bench. Various variables that are used for making these measurements are shown in Table 4.5 for stationary measurements and Table 4.6 for dynamic measurements. The engine has been run over a large operating range and desired information has been carefully chosen covering different operating conditions i.e., speeds, loads, VGT and EGR actuator positions. To get dynamic data, step inputs are used in VGT actuator control signal, EGR actuator control signal and fuel injection control signal. The stationary measurements have been used for tuning of static model parameters. Same are then validated using dynamic measurements. The dynamic measurements are used to tune dynamic actuator models, manifold models, turbocharger model and torque model, these measurements are also employed for validation of vital system attributes and time constants (Table 4.7). For details on the subject, reader is referred to [90]. Static model parameters are estimated by applying the least square optimization technique and stationary measurement data. The dynamic

model parameters are estimated in two phases. In first, parameters of the actuators are estimated by manual adjusting, until the simulations of actuator models follow their corresponding dynamic responses. In second, the time constant of the engine torque, the volume of the manifolds and the inertia of the turbocharger are estimated by adjusting them manually till full model simulations follow the dynamic responses. Since systematic approach is used, it is easy to reconstruct the model parameters and to use the same tuning techniques on diverse range of turbocharged diesel engines that are equipped with EGR and VGT actuators [90].

4.4.3   Manifold Dynamics

Both manifolds i.e., the intake and the exhaust are modelled as dynamical systems having two states each for pressures and mass fractions of oxygen. The typical model for conservation of mass, gas law for ideal gases and the fact that the temperature of the manifold fluctuates slowly, gives the manifold pressure differential equations as:-

$$\frac{d}{dt}p_{im} = \frac{R_a T_{im}}{V_{im}}\left(W_{comp} + W_{egr} - W_{ei}\right), \tag{4.1}$$

$$\frac{d}{dt}p_{em} = \frac{R_e T_{em}}{V_{em}}\left(W_{eo} - W_t - W_{egr}\right). \tag{4.2}$$

The intake manifold temperature is taken as constant. Descriptions of involved parameters are given in Tables 4.3 and 4.4. Values of various constants and tuning parameters are available at [91].

Table 4.1: States.

States	Variable
Intake manifold pressure	p_{im}
Exhaust manifold pressures	p_{em}
Oxygen concentration intake manifold	X_{Oim}
Oxygen concentration exhaust manifold	X_{Oem}
Turbine speed	w_t
EGR actuator state 1	$\tilde{u}_{egr1}$
EGR actuator state 2	$\tilde{u}_{egr2}$
VGT actuator state	$\tilde{u}_{vgt}$

TABLE 4.2: Control inputs.

Control inputs	Variable
EGR actuator	u_{egr}
VGT actuator	u_{vgt}
Fuel injection	u_δ

TABLE 4.3: Nomenclature of parameters.

Description	Variable	Unit
Area	A	m^2
Actuator dynamics	$\tilde{u}$	$\%$
Blade speed ratio	BSR	$-$
Compression ratio	r_c	$-$
Control	u	$\%$
Diesel injection signal	u_δ	$mg/cycle$
Efficiency	η	$-$
Exhaust gas recirculation fraction	x_{egr}	$-$
Flow rate	W	kg/s
Gas constant	R	J/kgK
Heating value of fuel	q_{HV}	J/kg
Inertia	J	kgm^2
Mass fraction	X	$-$
Number of cylinders	n_{cyl}	$-$
Oxygen - fuel ratio	λ_o	$-$
Power	P	W
Pressure	p	Pa
Pressure ratio	Π	$-$
Radius	R	m
Rotational speed	w	rad/s
Rotational speed	n	rpm
Specific heat capacity - constant pressure	C_p	J/kgK
Specific heat capacity - constant volume	C_v	J/kgK
Specific heat capacity - ratio	γ	$-$
Stoichiometric oxygen - fuel ratio	$(O/F)_s$	$-$
Temperature	T	K
Time	t	sec
Time constants	τ	sec
Torque	M	Nm
Volume	V	m^3

The exhaust gas fraction is calculated as:-

$$x_{egr} \quad = \quad \frac{W_{egr}}{W_{comp} + W_{egr}}. \tag{4.3}$$

TABLE 4.4: Subscripts.

Description	Variable
Air	a
Ambient	amb
Compressor	$comp$
Displaced, Delay	d
Engine	e
Exhaust	e
Exhaust gas recirculation	egr
Engine cylinder in	ei
Exhaust manifold	em
Engine cylinder out	eo
Friction	$fric$
Fuel	f
Fuel injection	δ
Gross indicated	ig
Intake manifold	im
Mechanical	m
Optimal	opt
Oxygen	O
Pumping	p
Turbine	t
Variable geometry turbocharger	vgt
Volumetric	vol

The exhaust gas fraction contains oxygen that may effect in cylinder oxygen to fuel ratio. This is highlighted by modelling the concentrations of oxygen in intake manifold and exhaust manifold as:-

$$X_{Oim} = \frac{m_{Oim}}{m_{totim}}, \tag{4.4}$$

$$X_{Oem} = \frac{m_{Oem}}{m_{totem}}, \tag{4.5}$$

differentiating (4.4-4.5) and using mass conservation gives:-

$$\frac{d}{dt}X_{Oim} = \frac{R_a T_{im}}{p_{im}V_{im}}\left((X_{Oem} - X_{Oim})W_{egr}\right.$$
$$\left. + (X_{Ocomp} - X_{Oim})W_{comp}\right), \tag{4.6}$$

$$\frac{d}{dt}X_{Oem} = \frac{R_e T_{em}}{p_{em}V_{em}}(X_{Oe} - X_{Oem})W_{eo}, \tag{4.7}$$

TABLE 4.5: Parameters used for stationary measurements.

Description	Variable	Unit
Ambient pressure	p_{amb}	Pa
Ambient temperature	T_{amb}	K
Compressor mass flow	W_{comp}	kg/s
EGR control signal	u_{egr}	$\%$
EGR fraction	x_{egr}	-
Engine torque	M_e	Nm
Engine rotational speed	n_e	rpm
Exhaust manifold temperature	T_{em}	K
Exhaust manifold pressure	p_{em}	Pa
Injected fuel	u_δ	$mg/cycle$
Intake manifold pressure	p_{im}	Pa
Intake manifold temperature	T_{im}	K
Pressure after compressor	p_{comp}	Pa
Temperature after compressor	T_{comp}	K
Temperature after turbine	T_t	K
Turbine rotational speed	n_t	rpm
VGT control signal	u_{vgt}	$\%$

TABLE 4.6: Parameters used for dynamic measurements.

Description	Variable	Unit
Compressor mass flow	W_{comp}	kg/s
EGR control signal	u_{egr}	$\%$
EGR position	$\tilde{u}_{egr}$	$\%$
Engine torque	M_e	Nm
Engine rotational speed	n_e	rpm
Exhaust manifold pressure	p_{em}	Pa
Injected fuel	u_δ	$mg/cycle$
Intake manifold pressure	p_{im}	Pa
Turbine rotational speed	n_t	rpm
VGT control signal	u_{vgt}	$\%$
VGT position	$\tilde{u}_{vgt}$	$\%$

here $X_{Ocomp} = 23.14\%$ is constant. Tuning parameters are V_{im} and V_{em}. The tuning parameters are determined as described in [90].

4.4.4 Cylinder Dynamics

Cylinders consist of three sub-models i.e., mass flow model, exhaust temperature model and engine torque model.

TABLE 4.7: The data consists of steps in VGT actuator position, EGR actuator position and fuel control input, it is used for dynamic tuning and validation of parameters. The columns E, I, and J have been employed for tuning of dynamic models, the columns A-D and F-H and J have been employed for validation of vital system attributes and time constants and the columns A-I have been employed for validation of static models.

Data sets	Steps in VGT and EGR position									u_δ
	A	B	C	D	E	F	G	H	I	J
Speed		1200			1500		1900		-	1500
Load	25	40	50	75	50	25	75	100	-	-
Steps	75	35	2	77	77	77	55	1	48	7
Frequency	1	100	100	1	1	1	1	100	100	10

4.4.4.1 Cylinder Flow

Mass flow, W_{ei}, entering the cylinders is modelled by making use of volumetric efficiency η_{vol} as:-

$$W_{ei} = \frac{\eta_{vol} p_{im} n_e V_d}{120 R_a T_{im}},$$
(4.8)

the volumetric efficiency is modelled using an empirical formula [90]:-

$$\eta_{vol} = c_{vol1}\sqrt{p_{im}} + c_{vol2}\sqrt{n_e} + c_{vol3}.$$

The mass flow of fuel entering the cylinders has been controlled by u_δ and is given by:-

$$W_f = \frac{10^{-6}}{120} u_\delta n_e n_{cyl}.$$
(4.9)

The mass flow out of the cylinder is:-

$$W_{eo} = W_f + W_{ei}.$$

The oxygen to fuel ratio is:-

$$\lambda_o = \frac{W_{ei}X_{Oim}}{W_f(O/F)_s}.$$
(4.10)

The oxygen concentration out of the cylinders (unburned) is:-

$$X_{Oe} = \frac{W_{ei}X_{Oim} - W_f(O/F)_s}{W_{eo}}.$$

The tuning parameters, c_{vol1}, c_{vol2} and c_{vol3}, are determined as described in [90].

4.4.4.2 Exhaust Temperature

It consists of two sub-models i.e., temperature at the cylinder out and the loss of heat through the exhaust pipes.

4.4.4.3 Cylinder Out Temperature

The cylinder out temperature T_e is modelled basing on the ideal gas Seliger cycle [90], given as:-

$$T_e = \eta_{sc}\left(\frac{p_{em}}{p_{im}}\right)^{1-1/\gamma_a} r_c^{1-\gamma_a} x_p^{1/\gamma_a-1}\left(q_{in}\left(\frac{1-x_{cv}}{C_{pa}} + \frac{x_{cv}}{C_{va}}\right) + T_1 r_c^{\gamma_a-1}\right),$$

here η_{sc} is representing the compensation factor for non ideal cycles and x_{cv} is the ratio of fuel consumed during constant volume combustion. The remaining fuel $(1 - x_{cv})$ is consumed during constant pressure combustion. The model also includes under mentioned components:-

The pressure ratio between "after combustion" (point 3) and "before combustion" (point 2) in the Seliger cycle:-

$$x_p = \frac{p_3}{p_2} = 1 + \frac{q_{in}x_{cv}}{C_{va}T_1 r_c^{\gamma_a-1}},$$

the specific energy contents of the charge:-

$$q_{in} = \frac{W_f q_{HV}}{W_{ei} + W_f}(1 - x_r),$$

as the inlet valve closes after the intake stroke, the temperature is:-

$$T_1 = x_r T_e + (1 - x_r) T_{im},$$

the residual gas fraction is:-

$$x_r = \frac{\left(\frac{p_{em}}{p_{im}}\right)^{1/\gamma_a} x_p^{-1/\gamma_a}}{r_c x_v},$$

the volume ratio between "after combustion" (point 3) and "before combustion" (point 2) in the Seliger cycle:-

$$x_v = \frac{v_3}{v_2} = 1 + \frac{q_{in}(1 - x_{cv})}{C_{pa}\left(\frac{q_{in}x_{cv}}{C_{va}} + T_1 r_c^{\gamma_a - 1}\right)}.$$

Since, the above mentioned equations are non-linear and rely on each other, the temperature at the cylinder out is worked out numerically using a fixed-point iteration technique, starting by taking initial values of $x_{r,0}$ and $T_{1,0}$ as:-

$$q_{in,k+1} = \frac{W_f q_{HV}}{W_{ei} + W_f}(1 - x_{r,k}),$$

$$x_{p,k+1} = 1 + \frac{q_{in,k+1} x_{cv}}{C_{va} T_{1,k} r_c^{\gamma_a - 1}},$$

$$x_{v,k+1} = 1 + \frac{q_{in,k+1}(1 - x_{cv})}{C_{pa}([q_{in,k+1}x_{cv}/c_{va}] + T_{1,k} r_c^{\gamma_a - 1})},$$

$$x_{r,k+1} = \frac{\Pi_e^{1/\gamma_a} x_{p,k+1}^{-1/\gamma_a}}{r_c x_{v,k+1}},$$

$$T_{e,k+1} = \eta_{sc} \Pi_e^{1 - 1/\gamma_a} r_c^{1 - \gamma_a} x_{p,k+1}^{1/\gamma_a - 1}(q_{in,k+1}(\frac{1 - x_{cv}}{C_{pa}} + \frac{x_{cv}}{C_{va}}) + T_{1,k} r_c^{\gamma_a - 1}),$$

$$T_{1,k+1} = x_{r,k+1} T_{e,k+1} + (1 - x_{r,k+1}) T_{im},$$

the subscript k represents the number of iteration.

4.4.4.4   Heat Losses in the Pipe

To increase accuracy in the estimation of exhaust manifold temperature, the heat losses from the exhaust pipes to the surroundings in between the cylinder and the exhaust manifold have also been considered. This gives exhaust manifold temperature as:-

$$T_{em} \;=\; T_{amb} + (T_e - T_{amb})e^{\frac{h_{tot}\pi d_{pipe}l_{pipe}n_{pipe}}{W_{eo}C_{pe}}}. \tag{4.11}$$

here h_{tot} is the total heat transfer coefficient, d_{pipe} is the diameter of the pipe, l_{pipe} is the length of the pipe and n_{pipe} is the number of pipes. It has been established in [90] that one iteration is enough to estimate exhaust manifold temperature. The tuning parameters are compensation factor for non ideal cycles η_{sc}, ratio of fuel consumed during constant volume combustion x_{cv} and total heat transfer coefficient h_{tot}. The tuning parameters are determined as described in [90].

4.4.4.5   Engine Torque

The torque produced is modelled using three components i.e., gross indicated torque, pumping torque and friction torque, given as:-

$$M_e \;=\; M_{ig} - M_p - M_{fric},$$

where pumping torque and the gross indicated torque, which come from the energy produced by fuel combustion, are given as:-

$$\begin{aligned}
M_p &\;=\; \frac{V_d}{4\pi}(p_{em} - p_{im}), \\
M_{ig} &\;=\; \frac{u_\delta 10^{-6} n_{cyl} q_{HV} \eta_{ig}}{4\pi}, \\
\eta_{ig} &\;=\; \eta_{igch}\left(1 - \frac{1}{r_c^{\gamma_{cyl}-1}}\right).
\end{aligned}$$

It has been assumed that the frictional torque is a quadratic polynomial in engine speed:-

$$
\begin{aligned}
M_{fric} &= \frac{V_d}{4\pi}10^5(c_{fric1}n_{eratio}^2 + c_{fric2}n_{eratio} + c_{fric3}), \\
n_{eratio} &= \frac{n_e}{1000}.
\end{aligned}
$$

The tuning parameters, combustion chamber efficiency η_{igch}, c_{fric1}, c_{fric2} and c_{fric3}, are determined as described in [90].

4.4.5 EGR Valve

It comprises of two sub-models i.e., EGR mass flow and EGR actuator.

4.4.5.1 EGR Mass Flow

The EGR actuator mass flow is modelled using a simplification of a compressible flow through restriction having a variable area. It is assumed that there is no reverse flow so as to get a simpler model. The mass flow through the restriction is given as:-

$$
W_{egr} = \frac{A_{egrmax}f_{egr}(\tilde{u}_{egr})p_{em}\Psi_{egr}}{\sqrt{T_{em}R_e}}, \tag{4.12}
$$

the function Ψ_{egr} is modelled as a parabolic function:-

$$
\Psi_{egr} = 1 - (\frac{1 - \Pi_{egr}}{1 - \Pi_{egropt}} - 1)^2, \tag{4.13}
$$

Π_{egr} over the valve is limited when the flow is choked, various involved functions are as under:-

$$\Pi_{egr} = \left\{ \begin{array}{cc} \Pi_{egropt}, & \frac{p_{im}}{p_{em}} < \Pi_{egropt} \\ \frac{P_{im}}{P_{em}}, & \Pi_{egropt} \leq \frac{p_{im}}{p_{em}} \leq 1 \\ 1, & 1 < \frac{p_{im}}{p_{em}} \end{array} \right\}, \quad (4.14)$$

$$\Pi_{egropt} = \left(\frac{2}{\gamma_{e+1}}\right)^{\gamma_e/\gamma_e - 1}. \quad (4.15)$$

The function $f_{egr}(\tilde{u}_{egr})$ is modelled as a polynomial in terms of EGR actuator $\tilde{u}_{egr}$, where $\tilde{u}_{egr}$ describes the EGR actuator dynamics:-

$$f_{egr}(\tilde{u}_{egr}) = \left\{ \begin{array}{cc} C_{egr1}\tilde{u}_{egr}^2 + C_{egr2}\tilde{u}_{egr} + C_{egr3}, & \tilde{u}_{egr} \leq -\frac{C_{egr2}}{2C_{egr1}} \\ C_{egr3} - \frac{C_{egr2}^2}{4C_{egr1}}, & \tilde{u}_{egr} > -\frac{C_{egr2}}{2C_{egr1}} \end{array} \right\}. \quad (4.16)$$

The tuning parameters, Π_{egropt}, C_{egr1}, C_{egr2} and C_{egr2}, are determined as described in [90].

4.4.5.2 EGR Actuator

In order to encapsulate the properties like an overshoot and time delay, EGR actuator dynamics are modelled as a second order system, this is done by subtracting two first order systems with different time constants and gains:-

$$\frac{d}{dt}\tilde{u}_{egr1} = \frac{1}{\tau_{egr1}}\left(u_{egr}\left(t - \tau_{degr}\right) - \tilde{u}_{egr1}\right), \quad (4.17)$$

$$\frac{d}{dt}\tilde{u}_{egr2} = \frac{1}{\tau_{egr2}}\left(u_{egr}\left(t - \tau_{degr}\right) - \tilde{u}_{egr2}\right), \quad (4.18)$$

$$\tilde{u}_{egr} = k_{egr}\tilde{u}_{egr1} - (k_{egr} - 1)\tilde{u}_{egr2}. \quad (4.19)$$

The tuning parameters, τ_{egr1}, τ_{egr2}, τ_{degr} and k_{egr}, are determined as described in [90].

4.4.6 Turbocharger

It consists of four sub-models i.e., turbo inertia model, turbine model, VGT actuator model and compressor model.

4.4.6.1 Turbo Inertia Model

Newton's second law of motion offers:-

$$\frac{d}{dt}w_t = \frac{P_t\eta_m - P_c}{J_t w_t}. \tag{4.20}$$

The tuning parameters J_t is determined as described in [90].

4.4.6.2 Turbine

It further consists of two sub-models i.e., turbine efficiency model and the turbine mass flow model, it also includes VGT actuator dynamics as a sub-model. In order to increase model accuracy η_{tm} is used:-

$$\Pi_t = \frac{p_{amb}}{p_{em}},$$
$$P_t\eta_m = \eta_{tm}W_t C_{pe}T_{em}(1 - \Pi_t^{1-1/\gamma_e}),$$

where η_{tm} is governed by the BSR as a parabolic function. BSR is the ratio of the turbine blade tip speed and the speed at which gas reaches when expanded isentropically at the given pressure ratio Π_t:-

$$\eta_{tm} = \eta_{tm,max} - c_m(BSR - BSR_{opt})^2,$$
$$BSR = \frac{R_t w_t}{\sqrt{2C_{pe}T_{em}(1 - \Pi_t^{1-1/\gamma_e})}},$$

where c_m is modelled as a as a function of the turbo speed:-

$$c_m = c_{m1}[max(0, w_t - c_{m2})]^{c_{m3}}.$$

The tuning parameters, $\eta_{tm,max}$, BSR_{opt}, c_{m1}, c_{m2} and c_{m3}, are determined as described in [90].

The mass flow through turbine is modelled making use of the corrected mass flow to incorporate density variations as:-

$$W_t = \frac{A_{vgtmax} f_{vgt}(\tilde{u}_{vgt}) p_{em} f_{\Pi_t}(\Pi_t)}{\sqrt{T_{em} R_e}}. \tag{4.21}$$

Measurements confirm that corrected mass flow is dependent on the pressure ratio and the VGT actuator signal. When there is a decrease in pressure ratio, the corrected mass flow increases till the gas touches the sonic condition and the flow is choked. This can be defined by a choking function:-

$$f_{\Pi_t}(\Pi_t) = \sqrt{1 - \Pi_t^{k_t}}. \tag{4.22}$$

Owing to the turbine's geometry, the change in effective area is larger in response to the larger VGT actuator control signal. This can be defined by a part of an ellipse, which gives effective area ratio function as:-

$$f_{vgt}(\tilde{u}_{vgt}) = C_{f1} \sqrt{max\left(0, 1 - \left(\frac{\tilde{u}_{vgt} - C_{vgt2}}{C_{vgt1}}\right)^2\right)} + C_{f2}. \tag{4.23}$$

The tuning parameters, k_t, C_{f1}, C_{f2}, C_{vgt1} and C_{vgt2}, are determined as described in [90].

The VGT actuator dynamics are modelled as a first order system:-

$$\frac{d}{dt}\tilde{u}_{vgt} = \frac{1}{\tau_{vgt}}\left(u_{vgt}(t - \tau_{dvgt}) - \tilde{u}_{vgt}\right). \tag{4.24}$$

The tuning parameters, τ_{vgt} and τ_{dvgt}, are determined as described in [90].

4.4.6.3 Compressor

It consists of two sub-models i.e., compressor efficiency model and mass flow model. The compressor power is:-

$$
\begin{aligned}
P_{comp} &= \frac{W_{comp} C_{pa} T_{amb}}{\eta_{comp}} (\Pi_{comp}^{1-1/\gamma_a} - 1), \\
\Pi_{comp} &= \frac{p_{im}}{p_{amb}}.
\end{aligned}
$$

The efficiency is modelled using ellipses, but with a non-linear transformation on the axis for the pressure ratio. The model can be improved with corrected mass flow so as to involve deviations in the environmental conditions. The ellipses can be defined as:-

$$
\eta_{comp} = \eta_{compmax} - x^T Q_{comp} x,
$$

where the input vector is:-

$$
x = \begin{bmatrix} W_{comp} - W_{compopt} \\ \pi_{comp} - \pi_{compopt} \end{bmatrix},
$$

the non-linear transformation and the symmetric and positive definite matrix Q_{comp} are:-

$$
\begin{aligned}
\pi_{comp} &= (\Pi_{comp} - 1)^{c_\pi}, \\
Q_{comp} &= \begin{bmatrix} a_1 & a_3 \\ a_3 & a_2 \end{bmatrix}.
\end{aligned}
$$

The tuning parameters are $\eta_{compmax}$, $W_{compopt}$, $\pi_{compopt}$, c_π, a_1, a_2 and a_3. These are determined as described in [90].

The mass flow through the compressor is modelled using two dimensionless variables i.e., energy transfer coefficient Ψ_{comp} and volumetric flow coefficient ϕ_{comp}:-

$$
\begin{aligned}
W_{comp} &= \frac{p_{amb}\pi R_{comp}^3 w_t}{R_a T_{amb}} \phi_{comp}, \\
\phi_{comp} &= \sqrt{max(0, \frac{1 - c_{\Psi 1}(\Psi_{comp} - c_{\Psi 2})^2}{c_{\phi 1}}) + c_{\phi 2}}, \\
\Psi_{comp} &= \frac{2C_{pa}T_{amb}(\Pi_{comp}^{1-1/\gamma_a} - 1)}{R_{comp}^2 w_t^2}.
\end{aligned}
$$

Energy transfer coefficient is the ratio of the isentropic kinetic energy of the gas at the given pressure ratio Π_{comp} and the kinetic energy of the compressor blade tip. Volumetric flow coefficient is the ratio of volume flow rate of air into the compressor and the rate at which volume is displaced by the compressor blade.

The parameters $c_{\Psi 1}$ and $c_{\phi 1}$ are modelled as polynomials:-

$$
\begin{aligned}
c_{\Psi 1}(w_t) &= c_{w\Psi 1}w_t^2 + c_{w\Psi 2}w_t + c_{w\Psi 3}, \\
c_{\phi 1}(w_t) &= c_{w\phi 1}w_t^2 + c_{w\phi 2}w_t + c_{w\phi 3}.
\end{aligned}
$$

The tuning parameters are $c_{\Psi 2}$, $c_{\phi 2}$, $c_{w\Psi 1}$, $c_{w\Psi 2}$, $c_{w\Psi 3}$, $c_{w\phi 1}$, $c_{w\phi 2}$ and $c_{w\phi 3}$. These are determined as described in [90].

To ensure simplicity in model, the inter-cooler and the EGR cooler are taken as ideal, hence we get:-

$$
\begin{aligned}
p_{out} &= p_{in}, \\
W_{out} &= W_{in}, \\
T_{out} &= T_{cool},
\end{aligned}
$$

where T_{cool} is the cooling temperature.

4.4.7 Analysis of Mathematical Model of a Diesel Engine

An analysis of mathematical model of a diesel engine equipped with VGT and EGR sub-systems is available at [94]. Just to give an idea about the VGT and EGR control problem, same is briefly discussed here. The main task is to control the performance variables i.e., oxygen to fuel ratio λ_O and EGR fraction x_{egr} by utilizing the two actuators i.e., VGT u_{vgt} and EGR u_{egr}. Giving step inputs over the entire operating range indicates that the channels u_{vgt} to λ_O, u_{egr} to λ_O, and u_{vgt} to x_{egr} have nonminimum phase behaviors and sign reversals. The necessary physical justification of these system properties is that the system contains two dynamic effects that interfere with each other, these are fast pressure dynamics in the manifolds and a slow turbocharger dynamics. It is revealed that engine often works in operating regions where the nonminimum phase behaviors and sign reversals take place for the channels u_{vgt} to λ_O and u_{vgt} to x_{egr} and therefore, it is vital to deliberate these attributes in a control design. The specific circumstances for sign reversal are owing to complex interactions between flows, pressures and temperatures in the complete operating range. Furthermore, an investigation of zeros for linearized MIMO mathematical model of an engine reveals that they are nonminimum phase over the entire operating range. A mapping of the performance variables λ_O and x_{egr} and the relative gain array reveals that the system from u_{egr} and u_{vgt} to λ_O and x_{egr} is strongly coupled in a large operating range. Some additional physical justifications of the system properties for VGT and EGR actuator positions are explained in subsequent paragraph.

Closing the VGT actuator increases the exhaust manifold pressure and consequently increases EGR mass fraction, thus decreasing concentration of intake manifold oxygen and λ_O, initially. However, increased exhaust manifold pressure later increases VGT rpm and hence compressor mass flow. The effect is increased λ_O, this increase is higher than the initial decrease. The growth in λ_O is slower owing to the slower dynamics of VGT rpm, implying that VGT actuator to λ_O has a nonminimum phase behavior. There is also a nonminimum phase behavior in the VGT rpm response. Similarly, closing of the EGR actuator decreases EGR mass

fraction, resulting in instant reduction in p_{im} and escalation in p_{em}. Closing the EGR actuator also reduces the circulation of exhaust gases to the intake manifold, consequently, more exhaust gases give drive to VGT. This moves the VGT to higher rpm and subsequently increases the p_{im} that is greater than the initial reduction. Due to the slower dynamics of the VGT rpm, this effect is slower, hence, EGR actuator to p_{im} has a nonminimum phase behavior. Since total flow into the engine and λ_O are affected by p_{im}, hence there is also a nonminimum phase behavior in λ_O. For details, see [94].

4.5 Reduced State Control Oriented Model

Generally modelling of any physical system ends up in a complex higher order dynamical model. In most cases, the volume of data enclosed in a complex model is much more than the desired, hence it hides simple, insightful behaviors, which may be well understood and used by a model with low order. In the case of designing a control, where the procedure involves complex algorithms, it might be computationally very challenging. Limited computational resources on the other hand certainly benefit from low order models. Hence, it is desirable to represent complex higher order models with simpler models having reduced order. It is however a necessity for reduced model to capture the significant properties of the actual system with high order. Reducing the system model can be accomplished in different ways [95]:-

4.5.1 Single Component Model Reduction

The quality of the reduced order model and the assumptions made are generally assessed by observing the model reduction error, i.e., the signal produced by calculating the difference among the outputs of the original system and the outputs of the reduced model, both energized by the similar input signal, as shown in Figure 4.5.
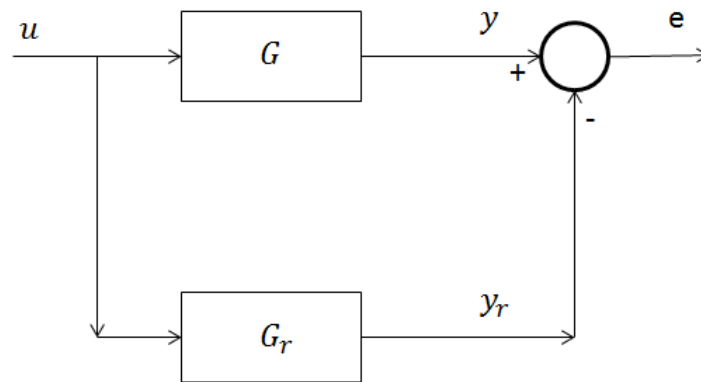
FIGURE 4.5: Single component model reduction

4.5.2 Multi Component Model Reduction

If a system consists of more then one components, interconnected with each other, as shown in Figure 4.6. Model reduction procedure is chosen for each component such that the overall system error is small.
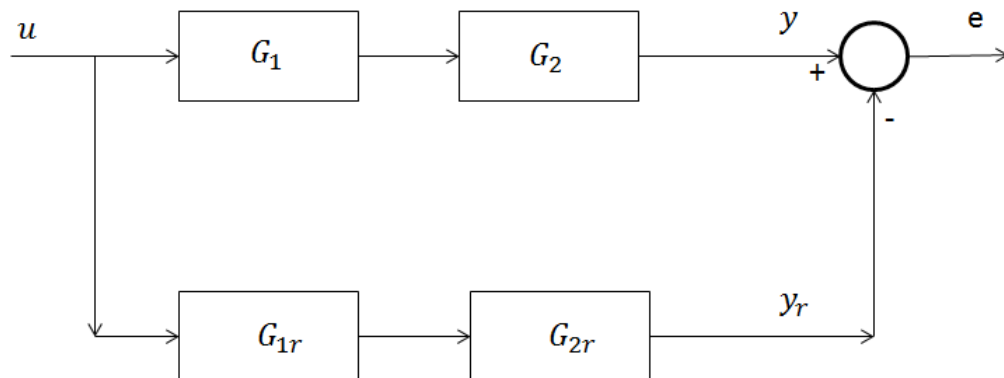
FIGURE 4.6: Multi component model reduction

Various techniques can be used to reduce the system's order. Some of the techniques are explored by the researchers in [95–98].

For ease in control development, reduced state control oriented diesel engine model has been proposed in [87] and used by various researchers e.g., [35, 37]. Same reduced state model will be used for FTC development in this proposed work. Reduced state control oriented model consists of three states $X = (p_{im}, \ p_{em}, \ P_{comp})^T$ and two control inputs $u = (W_{egr}, \ W_t)^T$. It takes into account the important system attributes, that include the turbocharger dynamics and pressure dynamics in the intake manifold and exhaust manifold. An analysis of reduced order diesel engine model is available at [87], the reduced state third order non-linear diesel engine model reflects some of the essential system properties, like nonminimum phase behavior and sign reversal. The generalizations made to get the reduced state control oriented model are appended below.

4.5.3 Assumptions

Following assumptions have been made in [90] to obtain the reduced state control oriented model:-

1. The states X_{Oim} and X_{Oem} have been ignored, in order to reduce the states.

2. The performance variable λ_O depends on X_{Oim} and X_{Oem}, so, it is also ignored as it cannot be chosen as an output.

3. Actuator states have been ignored assuming that actuators dynamics are fast.

4. It is assumed that fuel is available from a separate fuel controller.

5. The variations in temperature of the exhaust manifold, T_{em}, are assumed slow.

6. The efficiencies of various assemblies like turbine and compressor are taken as constants.

7. The dynamics of turbocharger are modelled as a first order system by taking compressor power, P_{comp}, as a state.

8. EGR flow, W_{egr}, and turbine flow, W_t, are taken as reduced state control oriented model's inputs u_1 and u_2.

9. The values of actual actuator positions, u_{egr} and u_{vgt}, are obtained by inverting the actuator position-flow models by neglecting the actuator dynamics, as proposed in [99] and explained in succeeding paragraph.

4.5.4 Reduced Model

The assumptions give the following reduced state control oriented model for control design:-

$$\frac{d}{dt}p_{im} = k_1 \left(W_{comp} + u_1 - k_e p_{im} \right), \tag{4.25}$$

$$\frac{d}{dt}p_{em} = k_2 \left(k_e p_{im} + W_f - u_2 - u_1 \right), \tag{4.26}$$

$$\frac{d}{dt}P_{comp} = -\frac{1}{\tau} \left(P_{comp} - \eta_m P_t \right), \tag{4.27}$$

where

$$k_1 = \frac{R_a T_{im}}{V_{im}},$$

$$k_e = \frac{\eta_{vol} n_e v_d}{120 R_a T_{im}},$$

$$u_1 = W_{egr},$$

$$k_2 = \frac{R_e T_{em}}{V_{em}},$$

$$W_f = \frac{10^{-6}}{120} u_\delta n_e n_{cyl},$$

$$u_2 = W_t,$$

$$P_t = \eta_{tm} u_2 C_{pe} T_{em} \left\{ 1 - \left(\frac{p_{amb}}{p_{em}} \right)^{\mu_e} \right\},$$

$$W_{comp} = \frac{\eta_{comp} P_{comp}}{T_{amb} C_{pa} \left\{ \left(\frac{p_{im}}{p_{amb}} \right)^{\mu_a} - 1 \right\}}.$$

4.6 Non-linear Input Transformation

By ignoring the actuator states and assuming that actuators dynamics are fast, system model equations (4.12-4.16) and (4.21-4.23) have been used to get back the valve positions from flow rates, as under [99]:-

$$f_{egr} = \frac{u_1 \sqrt{T_{em} R_e}}{A_{egrmax} p_{em} max(\Psi_{egr}, .1)}, \tag{4.28}$$

$$v_{egr} = -\frac{C_{egr2}}{2C_{egr1}} - \sqrt{max\left(\left(\frac{C_{egr2}}{2C_{egr1}}\right)^2 - \frac{C_{egr3}}{C_{egr1}} + \frac{f_{egr}}{C_{egr1}}, 0\right)}, \tag{4.29}$$

$$u_{egr} = \begin{cases} u_{egr}^{max}, & v_{egr} \geq u_{egr}^{max} \\ v_{egr}, & u_{egr}^{min} < v_{egr} < u_{egr}^{max} \\ u_{egr}^{min}, & v_{egr} \leq u_{egr}^{min} \end{cases}, \tag{4.30}$$

$$f_{vgt} = \frac{u_2 \sqrt{T_{em} R_e}}{A_{vgtmax} p_{em} max(f_{\Pi_t}, .1)}, \tag{4.31}$$

$$v_{vgt} = C_{vgt2} - C_{vgt1} \sqrt{max\left(1 - \left(\frac{max\,(f_{vgt} - C_{f2}, 0)}{C_{f1}}\right)^2, 0\right)}, \tag{4.32}$$

$$u_{vgt} = \begin{cases} u_{vgt}^{max}, & v_{vgt} \geq u_{vgt}^{max} \\ v_{vgt}, & u_{vgt}^{min} < v_{vgt} < u_{vgt}^{max} \\ u_{vgt}^{min}, & v_{vgt} \leq u_{vgt}^{min} \end{cases}. \tag{4.33}$$

Various involved parameters are defined in Table 4.3, Table 4.4, Sub-sub-section 4.4.5.1, Sub-sub-section 4.4.6.2 and Sub-section 4.5.4.

4.7 Chapter Summary

This Chapter focuses on the modeling of a diesel engine, both full order and reduced order models are discussed. The model stated in this Chapter has established extensive recognition in automotive industry and is used in both academic and industrial applications. A vital aspect of the model is its module based configuration with parameterized functions for addressing the component performance.

This decreases the reliance on maps and their related performance. In next Chapter two passive FTC techniques, basing on the SM framework, will be proposed for diesel engine air management actuators.

Chapter 5

Passive FTC - Diesel Engine Air Path

5.1 Objectives, Significance and Motivation

As explained earlier, physical systems are prone to faults. A conventionally designed controller for some plant or vehicle may perform well for faultless system but results in unacceptable performance and even total instability, in case of malfunctions in actuators and other sub-system components. In order to alleviate this limitation, FTC schemes are being developed which can tolerate component mal-functions while still preserving desired performance.

As mentioned in Section 2.4.6 some work has been done on diesel engines with regards to development of SM based FTC schemes for air system actuators. In most cases fault tolerance is achieved by inducing increased chattering i.e., the controller gains dominate the fault bounds. This may be a good approach for smaller inaccuracies but as the magnitude of fault increases the chattering increases, which makes implementation of such schemes impractical. Secondly, absence of FDI scheme and requirement of *apriori* knowledge about fault bounds were some of the constraints in the proposed schemes. It is hence desired to have a

scheme that detects the fault and compensates its effects without inducing excessive chattering and without the requirement of prior knowledge of fault bound. In this Chapter passive FTC schemes will be discussed that do not require FDI module or online controller alterations. These schemes require controllers to be robust against a class of presumed faults, thus they possess limited fault tolerant capabilities. The limitations of these schemes will be highlighted by computer simulations and these limitations will be compensated by proposing unified FDI and FTC schemes in next Chapter.

5.2   General Assumptions

Under mentioned assumptions have been followed in this Chapter and the subsequent Chapters:-

1. System is fault free except EGR and VGT sub-systems.

2. The faults in EGR and VGT sub-systems are not of extreme nature that may lead to a complete system failure.

3. Faults can be handled by re-positioning of particular faulty actuator (i.e., i^{th} actuator will handle uncertainty/fault in i^{th} channel).

5.3   Proposed FTC Schemes for Diesel Engine Air System

Following passive SM frame work based schemes will be discussed here along with complete approach and results:-

1. Standard super twisting algorithm.

2. Variable gain super twisting algorithm.

5.4 Standard STA for FTC Development

5.4.1 Controller Structure

Design of a controller basing on a classical SM method has been suggested in [32]. The key drawback of this method is the infinite frequency oscillations, chattering, at system's output that can harm the actuators. Parametric uncertainties, actuator faults and modelling errors will further enhance chattering. One of the means that can eradicate chattering is by using HOSMC centered approaches. These approaches extend the rudimentary SM idea by encompassing higher order derivatives of sliding variable. Hence same performance and robustness as of conventional SM is retained but with decrease in chattering [69]. Various HOSMC procedures are found in literature [69, 100]. Some of these approaches need knowledge related to the sliding surface higher order derivatives, which is constraining. Nevertheless, this restriction can be escaped by the use of super twisting approach. With its ease of implementation and capability to eradicate chattering, STA is selected. Super twisting controller consists of two terms. First is the continuous function of sliding variable while the second is obtained by taking the integral of discontinuous action:-

$$\bar{u}_i = -k_{1i} \mid S_i \mid^{\frac{1}{2}} \text{sign}(S_i) + z_i, \tag{5.1}$$

$$\dot{z}_i = -k_{2i} \text{sign}(S_i), \tag{5.2}$$

where i is control input index. k_{1i}, $k_{2i} > 0$ are gains, that allow dealing with the uncertainties.

For stability analysis, consider an affected MIMO system, given as:-

$$\dot{x}(t) = f(x) + \sum_{i=1}^{m} g_i(x)(u_i + F_i(x,t)), \tag{5.3}$$

$$y_i = h_i(x), \tag{5.4}$$

where $x(t) \in \mathbb{R}^n$, $u \in \mathbb{R}^m$ and $y \in \mathbb{R}^m$ and $F_i(x,t)$ represents the bounded uncertainty.

Making an assumption that the vector fields $f(x)$ and $g_i(x)$ are known and smooth and $h_i(x)$ are known smooth functions, that are defined on an open subset in $\mathbb{R}^n$. If a system has a vector relative degree $\{r_1,..,r_m\}$ with regards to $\{y_1,..,y_m\}$ at a point x_o and if $r = r_1 + ... + r_m$ is strictly less than n, it is possible to represent the system in new coordinates (ξ, η) where $\xi \in \mathbb{R}^r$ and $\eta \in R^{n-r}$.

Appropriate sliding surfaces are chosen as per the desired objectives. It has been supposed that the system (5.3) has stable internal dynamics. It is further supposed that the relative degrees of S_i with respect to u_i are one. The dynamics of sliding surfaces $(i = 1....m)$ can be given as:-

$$\dot{S}_i = \frac{\partial S_i}{\partial x_i}[f_i(x,t) + \sum_{k=1}^{m} g_k(x,t)\{u_k + F_k(x,t)\}].$$

In compact form, for $(i = 1....m)$, it can be written as:-

$$\dot{S} = \Psi(S,t) + G(S,t)(U + F), \tag{5.5}$$

where $\Psi(S,t) = \left[\frac{\partial S_1}{\partial x_1}f_1(x,t)....\frac{\partial S_m}{\partial x_m}f_m(x,t)\right]^T$, $G(S,t) = [G_1....G_m]^T$, and $G_i\{U +$

$F\} = \frac{\partial S_i}{\partial x_i} \sum_{k=1}^{m} g_k(x,t)\{u_k + F_k(x,t)\}.$

Assuming that $G(S,t)^{-1}$ exists and taking U as:-

$$U = G(S,t)^{-1}\{-\Psi(S,t) + \bar{U}\}, \tag{5.6}$$

where $G(S,t)^{-1}\{-\Psi(S,t)\}$ will cancel out the known terms, thus, giving desired output for a nominal plant and $\bar{U} = [\bar{u}_1....\bar{u}_m]^T$ will take care of uncertain terms

and actuator faults, The left over system is:-

$$\dot{S}_i \quad = \quad \bar{F}_i(x,t) + \bar{u}_i. \tag{5.7}$$

It is supposed that the uncertainty is bounded as:-

$$| \bar{F}_i(x,t) | \quad \leq \quad \Omega_i \mid S_i(x) \mid^{\frac{1}{2}}, \tag{5.8}$$

$$\Omega_i \quad > \quad 0.$$

5.4.1.1 Lyapunov Stability Analysis

Consider a weak Lyapunov function for analyzing the stability of MIMO controller as:-

$$V \quad = \quad \sum_{i=1}^{m} [k_{2i} \mid S_i \mid + \frac{1}{2} z_i^2].$$

Taking derivative of Lyapunov function

$$\dot{V} \quad = \quad \sum_{i=1}^{m} [k_{2i} \, \text{sign} \, (S_i) \, \dot{S}_i + z_i \dot{z}_i].$$

Involving SM dynamics

$$\dot{V} \quad \leq \quad \sum_{i=1}^{m} [k_{2i} \, \text{sign} \, (S_i) \, \{\Omega_i \mid S_i \mid^{\frac{1}{2}} - k_{1i} \mid S_i \mid^{\frac{1}{2}} \, \text{sign}(S_i) + z_i - z_i\}].$$

We have:-

$$\dot{V} \leq \sum_{i=1}^{m} [k_{2i} \operatorname{sign}(S_i) \{\Omega_i \mid S_i \mid^{\frac{1}{2}} - k_{1i} \mid S_i \mid^{\frac{1}{2}} \operatorname{sign}(S_i)\}].$$

Selecting $k_{1i} > \Omega_i$, $\dot{V}$ becomes negative semidefinite. Nevertheless, using the invariance principle of Krasovskii-LaSalle, for the system (5.7, 5.1, 5.2), $z_i = 0$, all the states of closed loop system will be bounded and asymptotic stability of the closed loop system is ensured.

5.4.2 Reduced State Control Oriented Model for Controller Development

Simplified engine model as proposed in Section 4.5 is used for controller development.

5.4.3 Output Set-Points

Control objective is to maintain λ_o and x_{egr} to their desired set-points. A non-linear diesel engine model as proposed in Section 4.4 is used to obtain desired set-points, the x_{egr} is maximized while ensuring that λ_o has been retained above a certain level, this avoids generation of visible smoke [101] and NO_x. For reduced state control oriented model as discussed in Section 4.5, the measurement of λ_o is not available, hence it cannot be taken as performance parameter. The apparent options of outputs can be W_{egr} and W_{comp}. It is proven in [32] that these outputs will give a relative degree one and two hidden dynamics, if extended by input/output linearization technique, p_{em} is an unstable hidden dynamic. In order

to circumvent this problem, outputs are re-defined as:-

$$y_1 = W_{comp} - W_{comp}^d, \tag{5.9}$$

$$y_2 = p_{em} - p_{em}^d. \tag{5.10}$$

A transformation as proposed in [35] is used to convert the set-points for λ_o and x_{egr} to W_{comp} and p_{em}:-

$$W_{comp}^d = \frac{W_f}{2X_{Ocomp}} \left(\beta + \sqrt{\beta \frac{1}{2} + 4\lambda_o^d (O/F)_s \left(1 - x_{egr}^d\right) X_{Ocomp}} \right),$$

$$W_{egr}^d = \frac{x_{egr}^d}{1 - x_{egr}^d} W_{comp}^d,$$

$$p_{im}^d = \frac{W_{comp}^d + W_{egr}^d}{k_e},$$

$$p_{em}^d = p_{amb} \left(1 - \frac{C_{pa} \left(\left(\frac{P_{im}^d}{P_{amb}} \right)^{\mu_a} - 1 \right) T_{amb} W_{comp}^d}{C_{pe} \eta_{cmt} T_{em} \left(W_{comp}^d + W_f \right)} \right),$$

where

$$\beta = \left(\lambda_o^d (O/F)_s - X_{Ocomp} \right) \left(1 - x_{egr}^d\right) + \left((O/F)_s x_{egr}^d \right),$$

$$\eta_{cmt} = \eta_{comp} \eta_m \eta_t.$$

5.4.4 Input/Output Linearization

With outputs as above, input/output linearization of the model in Section 4.5 gives:-

$$\dot{y}_1 = -\left(\frac{W_{comp}}{\tau} \right) - a \left(W_{comp} - k_e p_{im} \right) - au_1 + bu_2, \tag{5.11}$$

$$\dot{y}_2 = k_2 \left(k_e p_{im} + W_f^d \right) - k_2 u_1 - k_2 u_2, \tag{5.12}$$

where

$$a = \frac{k_1 \mu_a W_{comp} \left(\frac{p_{im}}{p_{amb}}\right)^{\mu_a - 1}}{p_{amb} \left\{ \left(\frac{p_{im}}{p_{amb}}\right)^{\mu_a} - 1 \right\}},$$

$$b = \left[\frac{\left(1 - \frac{p_{amb}}{p_{em}}\right)^{\mu_e}}{\left\{ \left(\frac{p_{im}}{p_{amb}}\right)^{\mu_a} - 1 \right\}} \right] \frac{T_{em}}{\tau T_{amb}} \left[\frac{C_{pe}\eta_{cmt}}{C_{pa}} \right].$$

The relative degree comes out to be two with one hidden dynamic, p_{im}. It is proven in [32, 35] that zero dynamic, p_{im}, is stable. The system possess a singularity at $p_{im} = p_{amb}$, it has however been established in [32, 35] that the space $\psi = \{(p_{im}, p_{em}, P_{comp}) : p_{im} > p_{amb}, p_{em} > p_{amb}, P_{comp} > 0\}$ is invariant for all t.

5.4.5 Control Law

SM design is accomplished in two steps, in first step sliding surface is designed and in second control law is developed in such a way that the system trajectories are forced towards the sliding surface. The affected system can be represented as 5.3 and the bounded unknown faults, representing the over or under flow through the actuators, as 5.8

Defining the sliding surfaces $S_1 = y_1 = W_{comp} - W_{comp}^d$ and $S_2 = y_2 = p_{em} - p_{em}^d$. The aim is to develop a STA based controller that guarantees two sliding requirements $S_i = \dot{S}_i = 0$, for $i = 1, 2$ and ensures $W_{comp} = W_{comp}^d$ and $p_{em} = p_{em}^d$ in the presence of system faults, parametric uncertainties and modelling errors. We can write the dynamics of the sliding variables as:-

$$\dot{S}_1 = -\left(\frac{W_{comp}}{\tau}\right) - a\left(W_{comp} - k_e p_{im}\right) + bu_2 - au_1, \tag{5.13}$$

$$\dot{S}_2 = k_2 \left(k_e p_{im} + W_f^d\right) - k_2 u_1 - k_2 u_2. \tag{5.14}$$

Involving faults that can affect the system, they include actuator getting chocked with soot or tar, leakages in the system resulting in exhaust gas escape, faulty

actuation mechanisms that result in offset in actuator positions, wearing of actuator components due to erosion or corrosion and components getting coated with exhaust PM. In broader terms the fault effects can be segregated into two groups i.e., over-flow and under-flow through actuators. It has been assumed that upper bounds of these faults are known:-

$$
\begin{aligned}
\dot{S}_1 &= -\left(\frac{W_{comp}}{\tau}\right) - a\left(W_{comp} - k_e p_{im}\right) + b u_2 - a u_1 - F_1, \\
\dot{S}_2 &= k_2\left(k_e p_{im} + W_f^d\right) - k_2 u_1 - k_2 u_2 - F_2.
\end{aligned}
$$

The control action is taken as (5.6). This gives u_1 and u_2 as:-

$$
\begin{aligned}
u_1 &= \frac{1}{a+b}\left[-W_{comp}\left(a + \frac{1}{\tau}\right) + (a+b)k_e p_{im} + b W_f^d - \bar{u}_1 - \frac{b}{k_2}\bar{u}_2\right], \\
u_2 &= \frac{1}{a+b}\left[W_{comp}\left(a + \frac{1}{\tau}\right) + a W_f^d + \bar{u}_1 - \frac{a}{k_2}\bar{u}_2\right].
\end{aligned}
$$

The super twisting controller terms $\bar{u}_i$ are selected as (5.1-5.2). The gains k_{1i} for $i = 1, 2$ are selected as $k_{1i} > \Omega_i$.

5.4.6   Results and Discussion

The controller proposed in Section 5.4.5 has been checked on a full order diesel engine model as defined in Section 4.4. A non-linear input transformation [99] as described in Section 4.6 has been used by reversing the EGR and turbine flow models which have actuator positions as the inputs and flow rates as the outputs. These inversions have given the new control inputs u_{egr} and u_{vgt} corresponding u_1 and u_2. The simulations are performed, results are as under:-
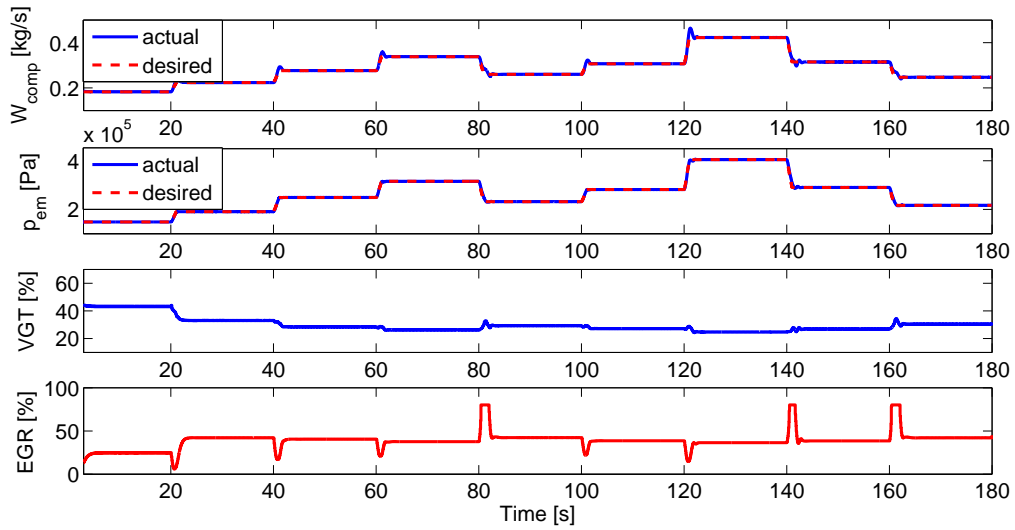
FIGURE 5.1: Results, when system is fault free

Figure 5.1 shows the tracking performance of standard STA based controllers when system is fault free. The set-points to be tracked are W_{comp}^d and p_{em}^d, both are shown in first two plots. The controller inputs u_{egr} and u_{vgt}, shown in last two plots, are made to track W_{comp}^d and p_{em}^d respectively. The controllers remained successful in tracking the desired set-points. Use of STA ensured minimal chattering. Moreover, robustness to matched uncertainties is also ensured being inherent quality of SMC based techniques, same is evident from results explained in subsequent paragraphs.
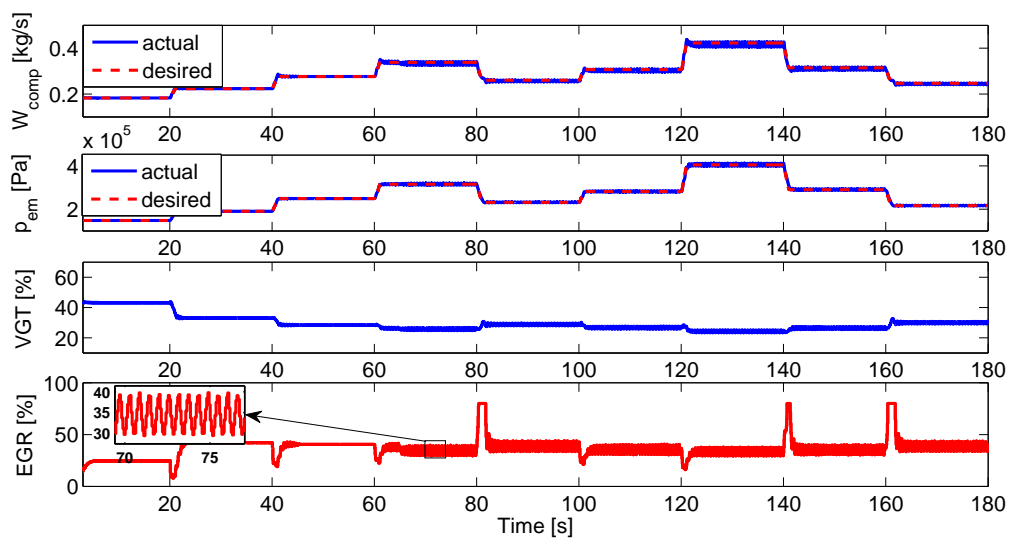
FIGURE 5.2: Results, 10% error has been introduced in EGR flow rate at $t \geq 65$ seconds

Figure 5.2 shows the tracking performance of standard STA based controllers by inducing a 10% error in EGR flow at $t \geq 65$ seconds, that depicts an over-flow case. The set-points to be tracked are exhaust manifold pressure p_{em}^d and compressor flow W_{comp}^d, both are shown in first two plots. The controllers tracked the desired set-points successfully. Though fault has been rejected by the controllers, still it has clearly been seen that chattering increases as the fault effects the system. This is because of the errors in actual and desired values of exhaust manifold pressure and compressor flow. *Apriori* knowledge about fault bound is essentially required, as the controller gains are selected to be higher then the fault bounds. It has also been observed that fault is more pronounced at higher rpm because of the increased flow rates. Fault detection is not possible through standard STA based approach, being passive approach, it can only reject the matched disturbances and not isolate or quantify the fault.

5.5   VGSTA for FTC Development

The standard super twisting controller performed satisfactorily till the time actuator fault has not been introduced in the system. With the introduction of bounded actuator fault chattering increases. It has however been observed that error because of faulty actuator varies with operating range. At higher engine speeds and torque requirements, error and hence chattering is more pronounced. To minimize the chattering in faulty system, the standard STA can be substituted with VGSTA. The technique (VGSTA) has been proposed for SISO systems in [64] and extended for MIMO systems in [65]. The proposed scheme offers robustness against minor system faults by making controller gains variable according to the fault bounds represented as known functions and resultantly decreases the chattering.

5.5.1 Controller Structure

As discussed earlier, in case of standard super twisting controller, actuator chattering increases with the system faults i.e., higher the fault magnitude more will be the actuator chattering. The reason is, at higher engine rpms, manifold pressures are high, increased pressure differences result in increased leakages, thus increasing the errors in the set-point tracking. This motivates the use of variable gains based algorithm such that the controller gains are made to vary as per the fault bounds, that are dependent on the known functions.

The VGSTA algorithm as proposed in [64] has an extra linear term for correction, that helps reducing the difference between actual and desired set point. Gains depend upon state/output dependent bounds. The VGSTA allows compensating a larger class of perturbations in comparison to standard STA. When on-line perturbation bounds are known, the gains of the VGSTA can be calculated and made variable accordingly, refining the algorithm performance. The VGSTA can replace the discontinuous SM based control by a continuous control. It guarantees the exact compensation of Lipchitz continuous uncertainties, that are bounded along with their gradients by known functions almost everywhere. As the design utilizes Lyapunov approach hence estimation of convergence time using a simple formula is possible. The controller structure is as under [65]:-

$$\bar{u}_i \;\; = \;\; -k_{1i}(x,t)\Phi_{1i}(S_i) - \int_0^t k_{2i}(x,t)\Phi_{2i}(S_i)d\tau, \tag{5.15}$$

$$\Phi_{1i}(S_i) \;\; = \;\; \mid S_i \mid^{\frac{1}{2}} \mathrm{sign}\,(S_i) + k_{3i}S_i, \tag{5.16}$$

$$\Phi_{2i}(S_i) \;\; = \;\; \dot{\Phi}_{1i}(S_i)\Phi_{1i}(S_i) \;\; = \tfrac{1}{2}\mathrm{sign}\,(S_i) +$$
$$\tfrac{3}{2}k_{3i} \mid S_i \mid^{\frac{1}{2}} \mathrm{sign}\,(S_i) + k_{3i}^2 S_i, \tag{5.17}$$

where $k_{3i} > 0$ handles the perturbations growing linearly in S_i and $i = 1..m$ represents the number of input channel. The variable gains k_{1i} and k_{2i} leave the sliding surface insensitive to perturbations rising with the bounds, that are represented by known functions. A non-linear system with matched uncertainty/disturbance

is represented as:-

$$\dot{x}(t) \;=\; f(x,t) + g(x,t)(u + F(x,t)),$$

where $x(t) \in \mathbb{R}^n$, $u \in \mathbb{R}^m$. Making an assumption that the vector fields $f(x,t)$ and $g(x,t)$ are known and smooth, that are defined on an open subset in $\mathbb{R}^n$. $F(x,t)$ and its gradient are bounded with known functions everywhere. Hidden dynamics are supposed to be stable, it is further assumed that the relative degrees of sliding surfaces S_i with respect to u_i are one. SM dynamics are given by:-

$$\dot{S}_i \;=\; \frac{\partial S_i}{\partial x_i}[f_i(x,t) + \sum_{k=1}^{m} g_k(x,t)\{u_k + F_k(x,t)\}].$$

In compact form, for $(i = 1....m)$, it can be written as:-

$$\dot{S} \;=\; \Psi(S,t) + G(S,t)(U + F), \tag{5.18}$$

where $\Psi(S,t) = \left[\frac{\partial S_1}{\partial x_1}f_1(x,t)....\frac{\partial S_m}{\partial x_m}f_m(x,t)\right]^T$, $G(S,t) = [G_1....G_m]^T$, and $G_i\{U +$

$F\} = \frac{\partial S_i}{\partial x_i} \sum_{k=1}^{m} g_k(x,t)\{u_k + F_k(x,t)\}$.

Assuming that $G(S,t)^{-1}$ exists and taking U as:-

$$U \;=\; G(S,t)^{-1}\{-\Psi(S,t) + \bar{U}\}, \tag{5.19}$$

where $G(S,t)^{-1}\{-\Psi(S,t)\}$ will cancel out the known terms, thus, giving required output for a nominal plant and $\bar{U} = [\bar{u}_1....\bar{u}_m]^T$ will take care of uncertain terms and actuator faults, The left over system is:-

$$\begin{aligned}
\dot{S}_i \;&=\; \bar{u}_i + (\Psi_i(S_i,t) - \Psi_i(0,t)) + \bar{F}_i(S_i,t), \\
&=\; \bar{u}_i + \Theta_i(S_i,t), \tag{5.20}
\end{aligned}$$

where $\Theta_i(S_i, t) = \Psi_i(S_i, t) - \Psi_i(0, t) + \bar{F}_i(S_i, t)$ is uncertain term, it can be written as $\Theta_i(S_i, t) = (\Theta_i(S_i, t) - \Theta_i(0, t)) + \Theta_i(0, t)$.

Taking $f_{1i}(S_i, t) = \Theta_i(S_i, t) - \Theta_i(0, t)$ and $f_{2i}(t) = \Theta_i(0, t)$, where $f_{1i}(S_i, t) = 0$ when $S_i = 0$. It is supposed that f_{1i} and f_{2i} are bounded, they must fullfil [64]:-

$$| f_{1i}(S_i, t) | \leq \rho_{1i}(x, t) | \Phi_{1i}(S_i) | = \rho_{1i}(x, t)(| S_i |^{\frac{1}{2}} + k_{3i} | S_i |), \quad (5.21)$$

$$| \frac{d}{dt} f_{2i}(S_i, t) | \leq \rho_{2i}(x, t) | \Phi_{2i}(S_i) | = \frac{1}{2}\rho_{2i}(x, t) +$$

$$k_{3i}\rho_{2i}(x, t)(\frac{3}{2} | S_i |^{\frac{1}{2}} + k_{3i} | S_i |), \quad (5.22)$$

where $\rho_{1i} \geq 0$ and $\rho_{2i} \geq 0$ are continuous functions, that are known. As described earlier $f_{1i}(S_i, t) = 0$ when $S_i = 0$, this is not the case for the derivative of the perturbation component $f_{2i}(S_i, t)$, since for $S_i = 0$ it is sufficient that this derivative is bounded by $\frac{1}{2}\rho_{2i}(x, t)$ [64]. System 5.20 driven by controller 5.15 is:-

$$\dot{S}_i = -k_{1i}(x, t)\Phi_{1i}(S_i) + f_{1i}(S_i, t) + z_i,$$

$$\dot{z}_i = -k_{2i}(x, t)\Phi_{2i}(S_i) + \frac{d}{dt}f_{2i}(S_i, t).$$

The finite time convergence of the sliding variables to the origin despite perturbations is guaranteed if the variable gains are chosen as:-

$$k_{1i}(x, t) = \delta_i + \frac{1}{\beta_i}\left[\frac{1}{4\epsilon_i}(2\epsilon_i\rho_{1i} + \rho_{2i})^2 + \epsilon_i\right.$$

$$\left. +2\epsilon_i\rho_{2i} + (2\epsilon_i + \rho_{1i})(\beta_i + 4\epsilon_i^2)\right], \quad (5.23)$$

$$k_{2i}(x, t) = \beta_i + 4\epsilon_i^2 + 2\epsilon_i k_{1i}, \quad (5.24)$$

where δ_i β_i and ϵ_i are arbitrary positive constants. The convergence time (for $m = 2$) is given by $T = \frac{2}{\gamma_{22}}ln\left[\frac{\gamma_{22}}{\gamma_{12}}V^{\frac{1}{2}}(0) + 1\right]$. Here $V = \sum_{i=1}^{m} \varsigma_i^T P_i \varsigma_i$ is the Lyapunov function, $\varsigma_i^T = [| S_i |^{\frac{1}{2}} \text{sign}(S_i) + k_{3i}S_i, z_i]$, $\gamma_{1i} = \frac{\epsilon_i\lambda_{mi}\{P_i\}}{\lambda_{Mi}\{P_i\}}$ and $\gamma_{2i} = \frac{2\epsilon_i k_{3i}}{\lambda_{Mi}\{P_i\}}$. For detailed derivation and description of parameters, reader is referred to [65].

5.5.1.1 Lyapunov Stability Analysis

Consider the following Lyapunov function [65]:-

$$V = \sum_{i=1}^{m} \varsigma_i^T P_i \varsigma_i, \tag{5.25}$$

where for $m = 2$

$$V = V_1 + V_2,$$
$$\varsigma_i^T = [\, |\, S_i\, |^{\frac{1}{2}} \, \text{sign}\, (S_i) + k_{3i} S_i, \; z_i],$$
$$P_i = \begin{bmatrix} p_{1i} & p_{3i} \\ p_{3i} & p_{2i} \end{bmatrix} = \begin{bmatrix} \beta_i + 4\epsilon_i^2 & -2\epsilon_i \\ -2\epsilon_i & 1 \end{bmatrix},$$

with β_i and $\epsilon_i > 0$. Function (5.25) is a time invariant, global, robust and strict Lyapunov function for the system (5.20). It is continuous and differentiable everywhere except at $S_i = 0$.

The inequalities (5.21-5.22) can be written as:-

$$|\, f_{1i}(S_i, t)\, | = \alpha_{1i}(x, t)\, |\, \Phi_{1i}(S_i)\, |,$$
$$|\, \frac{d}{dt} f_{2i}(S_i, t)\, | = \alpha_{2i}(x, t)\, |\, \Phi_{2i}(S_i)\, |,$$

for some

$$|\, \alpha_{1i}(x, t)\, | \leq \rho_{1i}(x, t),$$
$$|\, \alpha_{2i}(x, t)\, | \leq \rho_{2i}(x, t).$$

Using these functions one can show:-

$$
\begin{aligned}
\dot{\varsigma}_i &= \begin{bmatrix} \dot{\Phi}_{1i}(S_i) - \{-k_{1i}(x,t)\Phi_{1i}(S_i) + z_i + f_{1i}(S_i,t)\} \\ -k_{2i}(x,t)\Phi_{2i}(S_i) + \frac{d}{dt}f_{2i}(S_i,t) \end{bmatrix}, \\
&= \dot{\Phi}_{1i}(S_i) \begin{bmatrix} -k_{1i}(x,t) - \alpha_{1i}(x,t) & 1 \\ -k_{2i}(x,t) - \alpha_{2i}(x,t) & 0 \end{bmatrix} \varsigma_i, \\
&= \dot{\Phi}_{1i}(S_i) A_i(x,t) \varsigma_i.
\end{aligned}
$$

The time derivative of V comes out to be:-

$$
\begin{aligned}
\dot{V} &= \sum_{i=1}^{m} \dot{\Phi}_{1i}(S_i) \varsigma_i^T \{A_i^T(x,t)P_i + P_i A_i(x,t)\} \varsigma_i, \\
&= \sum_{i=1}^{m} -\dot{\Phi}_{1i}(S_i) \varsigma_i^T Q_i(x,t) \varsigma_i,
\end{aligned}
$$

where

$$
Q_i = \begin{bmatrix} 2(k_{1i}(x,t) - \alpha_{1i})p_{1i} + 2(k_{2i}(x,t) - \alpha_{2i})p_{3i} & * \\ (k_{1i}(x,t) - \alpha_{1i})p_{3i} + (k_{2i}(x,t) - \alpha_{2i})p_{2i} - p_{1i} & -2p_{3i} \end{bmatrix},
$$

where $*$ is used to indicate symmetric element. Putting in the value of P_i, gains k_{1i} and k_{2i}

$$
\begin{aligned}
Q_i - 2\epsilon_i &= \begin{bmatrix} 2\beta_i k_{1i} + 4\epsilon_i(2\epsilon_i k_{1i} - k_{2i}) - 2(\beta_i + 4\epsilon_i^2)\alpha_{i1} + 4\epsilon_i\alpha_{2i} - 2\epsilon_i & * \\ k_{2i} - 2\epsilon_i k_{1i} - (\beta_i + 4\epsilon_i^2) + 2\epsilon_i\alpha_{1i} - \alpha_{2i} & 2\epsilon_i \end{bmatrix}, \\
&= \begin{bmatrix} 2\beta_i k_{1i} - (\beta_i + 4\epsilon_i^2)(4\epsilon_i + 2\alpha_{i1}) + 4\epsilon_i\alpha_{2i} - 2\epsilon_i & * \\ 2\epsilon_i\alpha_{1i} - \alpha_{2i} & 2\epsilon_i \end{bmatrix}.
\end{aligned}
$$

This gives:-

$$\dot{V} = \sum_{i=1}^{m} -\dot{\Phi}_{1i}(S_i)\varsigma_i^T Q_i(x,t)\varsigma_i \le \sum_{i=1}^{m} -2\epsilon_i\dot{\Phi}_{1i}(S_i)\varsigma_i^T\varsigma_i,$$

$$= \sum_{i=1}^{m} -2\epsilon_i\left(\frac{1}{2\mid S_i\mid^{\frac{1}{2}}} + k_{3i}\right)\varsigma_i^T\varsigma_i.$$

Since $\lambda_{mi}\{P_i\}\|\varsigma_i\|_2^2 \le \varsigma_i^T P_i\varsigma_i \le \lambda_{Mi}\{P_i\}\|\varsigma_i\|_2^2$, where $\|\varsigma_i\|_2^2 = \varsigma_{1i}^2 + \varsigma_{2i}^2 =\mid S_i\mid +2k_{3i}\mid S_i\mid^{\frac{3}{2}} + k_{3i}^2 S_i^2 + z_i^2$ is Euclidean norm, and

$$\mid \varsigma_{1i}\mid \le \|\varsigma_i\|_2 \le \frac{V_i^{1/2}}{\lambda_{mi}^{1/2}\{P_i\}}.$$

Hence it is concluded that

$$\dot{V} \le \sum_{i=1}^{m}\left(-\gamma_{1i}V_i^{1/2} - \gamma_{2i}V_i\right), \tag{5.26}$$

where $\gamma_{1i} = \frac{\epsilon_i\lambda_{mi}\{P_i\}}{\lambda_{Mi}\{P_i\}}$ and $\gamma_{2i} = \frac{2\epsilon_i k_{3i}}{\lambda_{Mi}\{P_i\}}$. Suppose the controller (5.15) gains are selected such that for any non-negative quantities γ_{ij}, $i,j = 1,2$ the following inequalities are fulfilled:-

$$\gamma_{21} > \gamma_{22},$$
$$\gamma_{11} > \gamma_{12},$$

then for m=2 case, (5.26) can be transformed into [65]:-

$$\dot{V} \le -\gamma_{22}V - \gamma_{12}V^{1/2}. \tag{5.27}$$

Since the solution of the differential equation (5.27)

$$\dot{v} \ \leq \ -\gamma_{22}v - \gamma_{12}v^{1/2}, \ \ v(0) = v_0 \geq 0,$$

is given as:-

$$v(t) \ = \ \exp\left(-\gamma_{22}t\right)\left[v_0^{1/2} + \frac{\gamma_{12}}{\gamma_{22}}\left(1 - \exp\left(\frac{\gamma_{22}}{2}t\right)\right)\right]^2.$$

Hence the system $(S_i(t), \ z_i(t))$ converges to zero in finite time. This concludes the stability analysis.

5.5.2 Reduced State Control Oriented Model for Controller Development

Reduced order engine model as proposed in Section 4.5 is used for controller development.

5.5.3 Output Set-Points

Output set-points are selected as W_{comp} and p_{em}. The set-points for λ_o and x_{egr} can be worked out and transformed into the set-points for W_{comp} and p_{em} using the procedure as described in Section 5.4.3.

5.5.4 Input/Output Linearization

With outputs as above, input/output linearization of model in Section 4.5 gives the system as described in Section 5.4.4.

5.5.5 Control Law

Defining the sliding surfaces $S_1 = y_1 = W_{comp} - W_{comp}^d$ and $S_2 = y_2 = p_{em} - p_{em}^d$. The aim is to synthesize a VGSTA based controller that can meet two sliding requirements $S_i = \dot{S}_i = 0$, for $i = 1, 2$ and guarantees $W_{comp} = W_{comp}^d$ and $p_{em} = p_{em}^d$ in the existence of actuators faults, parametric uncertainties and modelling errors. The dynamics of the sliding variables after considering perturbations and faults Θ_i comes out to be:-

$$\dot{S}_1 = -\left(\frac{W_{comp}}{\tau}\right) - a\left(W_{comp} - k_e p_{im}\right) + bu_2 - au_1 - \Theta_1, \qquad (5.28)$$

$$\dot{S}_2 = k_2\left(k_e p_{im} + W_f^d\right) - k_2 u_1 - k_2 u_2 - \Theta_2, \qquad (5.29)$$

where $\Theta_1 = f_{11} + f_{21}$ and $\Theta_2 = f_{12} + f_{22}$. The control action is proposed as (5.19). To calculate control, ignoring perturbations/faults in sliding variable dynamics:-

$$\dot{S}_1 = -\left(\frac{W_{comp}}{\tau}\right) - a\left(W_c - k_e p_{im}\right) + bu_2 - au_1,$$

$$\dot{S}_2 = k_2\left(k_e p_{im} + W_f^d\right) - k_2 u_1 - k_2 u_2.$$

The controls come out to be:-

$$u_1 = \frac{1}{a+b}\left[-W_{comp}\left(a + \frac{1}{\tau}\right) + (a+b)k_e p_{im} + bW_f^d - \bar{u}_1 - \frac{b}{k_2}\bar{u}_2\right], (5.30)$$

$$u_2 = \frac{1}{a+b}\left[W_{comp}\left(a + \frac{1}{\tau}\right) + aW_f^d + \bar{u}_1 - \frac{a}{k_2}\bar{u}_2\right]. \qquad (5.31)$$

The $\bar{u}_i$s are selected as proposed in Section 5.5.1. To get perturbation/fault bounds when $S_i = 0$, $f_{1i} = 0$, hence $\rho_{1i} = 0$, this gives $\rho_{11} = 0$ and $\rho_{12} = 0$. f_{2i} and it's derivatives can be represented as:-

$$f_{21} = \Delta_1 u_1 \leq \tilde{\Delta}_1 W_{egr},$$

where $\tilde{\Delta}_1$ denotes the percentage of under or over flow through EGR actuator upper bound. It is supposed to be known.

$$\frac{d}{dt}f_{21} \quad = \quad \tilde{\Delta}_1 \dot{W}_{egr}.$$

Similarly

$$f_{22} \quad = \quad \Delta_2 u_2 \quad \leq \tilde{\Delta}_2 W_t,$$

where $\tilde{\Delta}_2$ denotes the percentage of under or over flow through VGT actuator upper bound. It is supposed to be known.

$$\frac{d}{dt}f_{22} \quad = \quad \tilde{\Delta}_2 \dot{W}_t.$$

Using (5.22), the continuous functions ρ_{21} and ρ_{22} are:-

$$\rho_{21} \quad = \quad 2\tilde{\Delta}_1 \mid \dot{W}_{egr} \mid,$$
$$\rho_{22} \quad = \quad 2\tilde{\Delta}_2 \mid \dot{W}_t \mid.$$

k_{1i} and k_{2i} are calculated as proposed in (5.23-5.24).

5.5.6   Results and Discussion

The proposed controller has been checked on a full order diesel engine model as described in Section 4.4. A non-linear input transformation [99] is employed by reversing the EGR and VGT flow model having position of actuators as the inputs and gas flow as the outputs. These inversions have given the new control inputs u_{egr} and u_{vgt} corresponding to u_1 and u_2, as explained in Section 4.6. The results of VGSTA based controller are compared with standard STA based controller [4] having controller structure (5.30-5.31) and $\bar{u}_i s$ as (5.32-5.33), it has been supposed that uncertainties $F_i(x,t)$ are bounded as $\mid F_i(x,t) \mid \leq \zeta_i \mid S_i(x) \mid^{\frac{1}{2}}$, where $\zeta_i > 0$.

Fixed gains of standard STA based controller have been chosen as $k_{1i} > \zeta_i$.

$$\bar{u}_i = -k_{1i} \mid S_i \mid^{\frac{1}{2}} \text{sign}\,(S_i) + z_i, \tag{5.32}$$

$$\dot{z}_i = -k_{2i}\,\text{sign}\,(S_i). \tag{5.33}$$
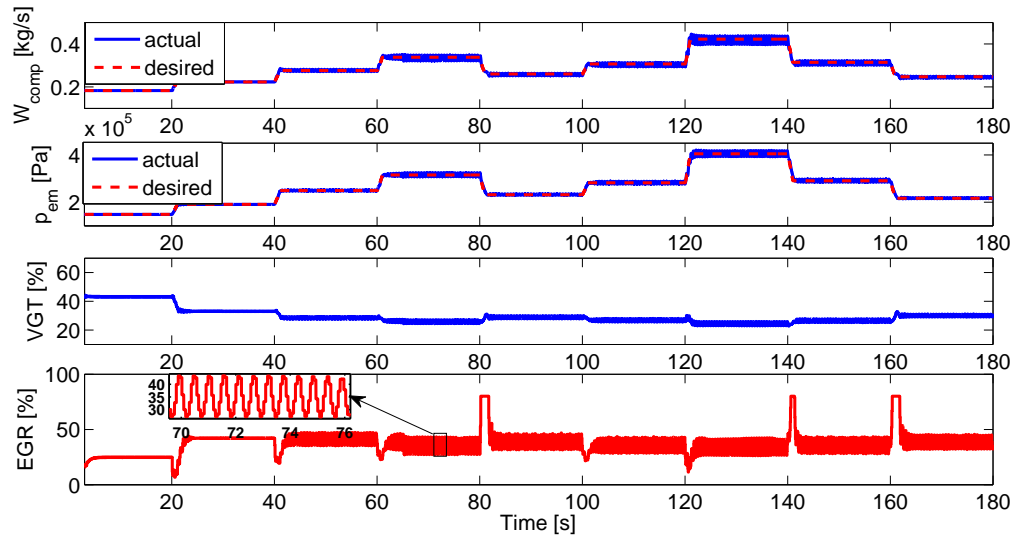
FIGURE 5.3: Results of standard STA, 10% error has been introduced in EGR flow rate at $t \geq 65$ seconds
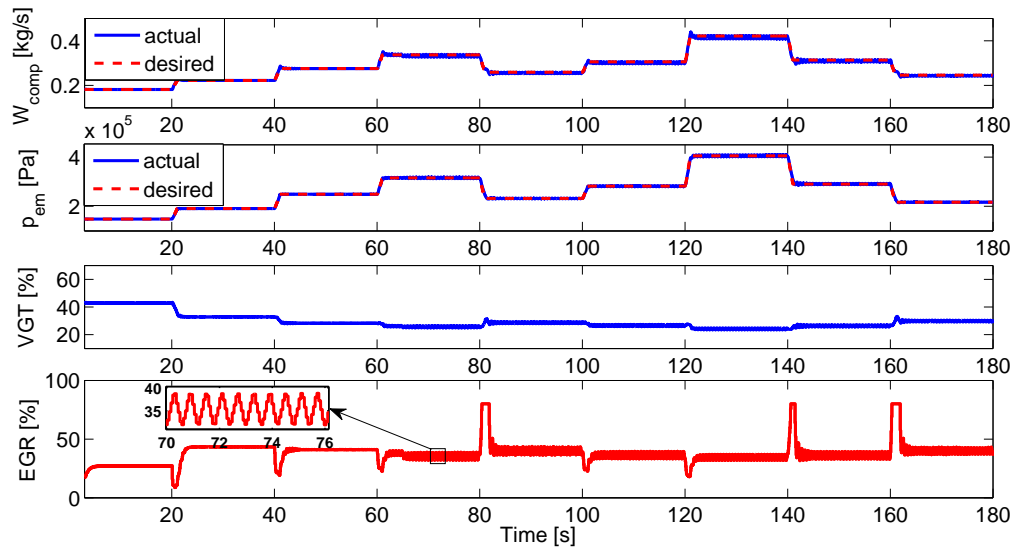
FIGURE 5.4: Results of VGSTA, 10% error has been introduced in EGR flow rate at $t \geq 65$ seconds

The simulation results are shown by inducing a 10% error in EGR flow rate at $t \geq 65$ seconds, that depicts an over-flow case. The set-points to be tracked are

exhaust manifold pressure p_{em}^d and compressor flow W_{comp}^d, both are shown in first two plots of Figures 5.3 and 5.4. As evident from Figures, the controllers tracked the desired set-points successfully with minimal chattering, as both algorithms are based on HOSM concept. As the bounded fault is introduced in the system, actuator chattering increases, this is because of the errors in actual and desired set-points of exhaust manifold pressure and compressor flow. However, chattering is much less in case of VGSTA based controllers as compared to the STA based controllers. The gains in case of VGSTA based controllers are made to vary as per the fault bounds dependent on the known functions, thus resulting in reduced control effort as compared to the STA based controllers and eventually less chattering. Few pros and cons of this scheme are:- Though fault has been rejected by the controllers still chattering exists. *Apriori* knowledge about fault bound is essentially required for selection of controller gains. Fault detection algorithm has not been implemented. Fault diagnosis has not been carried out. Magnitude of fault has not been estimated. The faults have been handled passively. Hence, the algorithm is only suitable for minor faults.

5.6 Chapter Summary

In feedback control systems, minor additive or multiplicative faults in the method or actuator can be compensated by making robust controllers. This property is hence a passive control loop fault tolerance. Permanent additive faults like actuator mal-functions will however directly affect the tracking of reference signals. For large variations in actuator, process or sensor behavior, the dynamic control performance turn out to be too sluggish or improperly damped and in extreme cases, unstable. Then, a very robust controller or an active FTC system is needed to ensure the desired operation. In order to remove the drawbacks of passive FTC techniques, that have been discussed in this Chapter, unified FDI and FTC schemes will be proposed in next Chapter.

Chapter 6

Unified FDI and FTC - Diesel Engine Air Path

6.1 Objectives, Significance and Motivation

Occurrence of faults in automatically controlled systems i.e., actuator, process or sensor faults will generally effect the operating behavior. With passive feedback control, generally small multiplicative or additive faults in the method or actuator can be tolerated because of inherent robustness properties of the controller but for larger faults these passive schemes fail to provide desired objectives. Same have been explored in previous Chapter where it was established that SM frame work based passive FTC schemes may be good approaches for a system with smaller inaccuracies but as the magnitude of fault increases the chattering increases, which makes implementation of such schemes impractical. Secondly, requirement of *apriori* knowledge about fault bound is one of the major constraints in the passive schemes. It is therefore desired to have a structure that detects the fault and compensate its effects without inducing excessive chattering and without the requirement of prior knowledge of fault bound. In this Chapter unified FDI and FTC schemes will be discussed. General assumptions as mentioned in Section 5.2 will be followed. In these approaches FDI module will be used in support

of FTC technique, so as to synthesize a self-repairing controller. Since the FDI module may not always provide timely fault information, an integrated diagnosis and control strategy will be considered.

6.2 Proposed FTC Schemes for Diesel Engine Air System

Following unified FDI-FTC schemes will be discussed here along with complete approach and results:-

1. Certainty equivalence super twisting algorithm.

2. Integral sliding mode extended with an adaptive part.

6.3 CESTA for FTC Development

The VGSTA based controller performs satisfactorily and has given improved results in comparison to the standard STA based controller. It has however been observed that chattering still exists and further increases with the increase in fault magnitude. To eliminate this unwanted chattering caused by the system faults, FDI module that can detect and estimate the faults, has to be introduced in the system. To achieve these objectives, STA will be extended with an adaptation law using the certainty equivalence principle. The CESTA algorithm has been proposed for SISO systems in [66], same will be extended for MIMO systems and applied for development of unified FDI and FTC scheme for diesel engine air path actuators. The algorithm will detect, diagnose and estimate the occurrence of faults with no requirement of any prior information about the faults or fault bounds and compensates fault effects by re-organizing the control effort, thus, reducing the chattering.

6.3.1 Controller Structure

The concept is to make a combination of SM and adaptive control methodologies. Adaptive control part will help in fault detection and estimation. Same will be compensated by the overall control structure. Conventionally designed SM algorithms do not differentiate among structured and unstructured uncertainties. The mutual influence of both is dominated by keeping the controller gains higher than the uncertainty bounds. This may be a good approach if uncertainties are smaller, but gives increased chattering as the magnitude of uncertainty increases, same is evident from the results of previous Chapter. The CESTA approach on the other hand takes into consideration the structural information about the uncertainties and resultantly decreases the gains of the SM based part of the controller. It is achieved by segregating the total uncertainties into structured and unstructured parts. An adaptive algorithm basing on the certainty equivalence principle is added into the controller using Lyapunov approach. This adaptive part estimates the structured faults/uncertainties and cancels them out, thus in some cases removing the chattering altogether. Consider a MIMO system, represented as:-

$$\dot{x}(t) = f(x) + \sum_{i=1}^{m} g_i(x)(u_i + F_i(x,t)), \qquad (6.1)$$

$$y_i = h_i(x), \qquad (6.2)$$

where $F_i(x,t)$ represents the uncertain term. $x(t) \in \mathbb{R}^n$, $u \in \mathbb{R}^m$ and $y \in \mathbb{R}^m$. Subscript i is used to represent the number of input channel.

The uncertain term $F_i(x,t)$ can be written as a sum of structured and unstructured parts:-

$$F_i(x,t) = f_{si}(x) + f_{ui}(x,t).$$

Writing the structured uncertainty as a product of an unknown constant parameter $\triangle_i$ and a known base function $\Psi_i(x)$ as:-

$$f_{si}(x) \;=\; \triangle_i \Psi_i(x).$$

Making an assumption that the vector fields $f(x)$ and $g_i(x)$ are known and smooth and $h_i(x)$ are known smooth functions, that are defined on an open set in $\mathbb{R}^n$. If the system has a vector relative degree $\{r_1, .., r_m\}$ with respect to $\{y_1, .., y_m\}$ at a point x_o and if $r = r_1 + .. + r_m$ is strictly less than n, it is possible to represent the system in new coordinates (ξ, η) where $\xi \in \mathbb{R}^r$ and $\eta \in \mathbb{R}^{n-r}$.

Appropriate sliding surfaces $S_i = S_i(x)$ have been selected as per the desired objectives. Internal dynamics of the system (6.1) are assumed to be stable. It is further assumed that the relative degrees of S_i with respect to u_i are one. The dynamics of sliding surfaces $(i = 1..m)$ can be written as:-

$$\dot{S}_i \;=\; \frac{\partial S_i}{\partial x_i}[f_i(x) + \sum_{k=1}^{m} g_k(x)\{u_k + F_k(x,t)\}],$$

$$= \;\frac{\partial S_i}{\partial x_i}f_i(x) + \frac{\partial S_i}{\partial x_i}\sum_{k=1}^{m} g_k(x)\{u_k + F_k(x,t)\}. \tag{6.3}$$

For $(i = 1....m)$ in compact form, we can write:-

$$\dot{S} \;=\; N(x) + G(x)(U + F), \tag{6.4}$$

where $N(x) = \left[\frac{\partial S_1}{\partial x_1}f_1(x)....\frac{\partial S_m}{\partial x_m}f_m(x)\right]^T$, $G(x) = [G_1(x)....G_m(x)]^T$, and $G_i(x)\{U +$

$F\} = \frac{\partial S_i}{\partial x_i}\sum_{k=1}^{m} g_k(x)\{u_k + F_k(x,t)\}.$

Making assumption that $G^{-1}(x)$ exists and taking U as:-

$$U \;=\; G^{-1}(x)\{-N(x)+\bar{U}\}, \tag{6.5}$$

where $G^{-1}(x)\{-N(x)\}$ will handle the known terms and $\bar{U} = [\bar{u}_1....\bar{u}_m]^T$ will handle uncertain terms/actuator faults, with an assumption that actuator faults can be handled by re-positioning of particular faulty actuator (i.e., i^{th} actuator will handle fault in i^{th} channel). This selection of U will decouple the system, the left over system consists of only matched uncertainties, that can be handled as under:-

$$\dot{S}_i \;=\; F_i + \bar{u}_i, \tag{6.6}$$

$$\dot{S}_i \;=\; \triangle_i \Psi_i(x) + f_{ui}(x,t) + \bar{u}_i. \tag{6.7}$$

It is assumed that the unstructured uncertainties are bounded as:-

$$\mid f_{ui}(x,t) \mid \;\leq\; \Omega_i \mid S_i(x) \mid^{\frac{1}{2}}, \tag{6.8}$$

$$\Omega_i \;>\; 0.$$

CESTA resorts to a conventional super twisting controller as a nominal controller. The controller structure is [66]:-

$$\bar{u}_i \;=\; -k_{1i} \mid S_i \mid^{\frac{1}{2}} \mathrm{sign}\,(S_i) + z_i - \hat{\triangle}_i \Psi_i(x), \tag{6.9}$$

$$\dot{z}_i \;=\; -k_{2i}\,\mathrm{sign}\,(S_i)\,, \tag{6.10}$$

where controller gains k_{1i}, $k_{2i} > 0$ allow to deal with the unstructured uncertainties. $\hat{\triangle}_i$ is the estimate of unknown parameter $\triangle_i$ and z_i is a controller state.

6.3.1.1   Lyapunov Stability Analysis 1

Taking Lyapunov function for analyzing stability of MIMO controller as:-

$$V = \sum_{i=1}^{m} \left[k_{2i} \mid S_i \mid + \frac{1}{2} z_i^2 + \frac{1}{2\gamma_i} \tilde{\triangle}_i^2 \right], \qquad (6.11)$$

where $\gamma_i > 0$ and $\tilde{\triangle}_i = \hat{\triangle}_i - \triangle_i$. Taking derivative of Lyapunov function (6.11):-

$$\dot{V} = \sum_{i=1}^{m} \left[k_{2i} \operatorname{sign}(S_i) \dot{S}_i + z_i \dot{z}_i + \frac{1}{\gamma_i} \tilde{\triangle}_i \dot{\hat{\triangle}}_i \right]. \qquad (6.12)$$

Involving system (6.7-6.10) in (6.12), we get:-

$$\dot{V} = \sum_{i=1}^{m} \left[k_{2i} \operatorname{sign}(S_i) \{ f_{ui}(x,t) - k_{1i} \mid S_i \mid^{\frac{1}{2}} \right.$$

$$\left. \operatorname{sign}(S_i) - (\hat{\triangle}_i - \triangle_i) \Psi_i(x) \} + \frac{1}{\gamma_i} \tilde{\triangle}_i \dot{\hat{\triangle}}_i \right],$$

$$\dot{V} = \sum_{i=1}^{m} \left[k_{2i} \operatorname{sign}(S_i) \{ \Omega_i \mid S_i \mid^{\frac{1}{2}} - k_{1i} \mid S_i \mid^{\frac{1}{2}} \right.$$

$$\left. \operatorname{sign}(S_i) \} + \tilde{\triangle}_i \left\{ -k_{2i} \operatorname{sign}(S_i) \Psi_i(x) + \frac{1}{\gamma_i} \dot{\hat{\triangle}}_i \right\} \right].$$

If we know the $\hat{\triangle}_i's$ exactly, then the error $\tilde{\triangle}_i = 0$ and $\dot{V}$ reduces to:-

$$\dot{V} \leq \sum_{i=1}^{m} [k_{2i} \operatorname{sign}(S_i) \{ \Omega_i \mid S_i \mid^{\frac{1}{2}} - k_{1i} \mid S_i \mid^{\frac{1}{2}} \operatorname{sign}(S_i) \}].$$

Choosing $k_{1i} > \Omega_i$, $\dot{V}$ comes out to be negative semi definite. Making use of Krasovskii LaSalle's invariance principle, as $\dot{V} = 0$ implies $S_i = 0$. Considering equations (6.7) to (6.10), the only available solution is $z_i = 0$. Hence, asymptotic stability of the closed loop system is confirmed.

$\hat{\triangle}'_i s$ are however not known, hence taking adaptation laws as:-

$$\dot{\hat{\triangle}}_i = \gamma_i k_{2i} \operatorname{sign}(S_i) \Psi_i(x). \tag{6.13}$$

The value of adaptation parameter $\hat{\triangle}_i$ will remain close to zero in cases where their is no structured uncertainty or fault in the system. As soon as some fault affects the system, the value of adaptation parameter increases according to the magnitude of the fault. Nonzero value of adaptation parameter indicates the presence of the fault. Appropriate threshold is chosen to clarify the existence of the fault. The left over system is:-

$$\dot{V} \leq \sum_{i=1}^{m} [k_{2i} \operatorname{sign}(S_i) \{ \Omega_i \mid S_i \mid^{\frac{1}{2}} -k_{1i} \mid S_i \mid^{\frac{1}{2}} \operatorname{sign}(S_i) \}].$$

Select $k_{1i} > \Omega_i$. $\dot{V}$ comes out to be negative semi definite, however, with non-zero z_i and $\hat{\triangle}_i$ and assumption that internal dynamics are stable, we can say that system will converge to $S_i = 0$. Thus, all states of the closed loop system will be bounded. The complete controller structure comes out to be:-

$$\begin{aligned}
\bar{u}_i &= -k_{1i} \mid S_i \mid^{\frac{1}{2}} \operatorname{sign}(S_i) + z_i - \hat{\triangle}_i \Psi_i(x), \\
\dot{z}_i &= -k_{2i} \operatorname{sign}(S_i), \\
\dot{\hat{\triangle}}_i &= \gamma_i k_{2i} \operatorname{sign}(S_i) \Psi_i(x).
\end{aligned} \tag{6.14}$$

6.3.1.2 Lyapunov Stability Analysis 2

In Sub-sub-section 6.3.1.1 time derivative of Lyapunov function is negative semi-definite when worked out along the trajectories of system (6.7). Consequently some additional techniques are essentially required to conclude the asymptotic stability of the system states. To resolve the issue, the positive definite Lyapunov function as proposed in [102] has been adapted for MIMO systems:-

$$
V = \sum_{i=1}^{m} \left[\frac{2}{3} k_{1i} \mid S_i \mid^{\frac{3}{2}} - S_i z_i + \frac{2}{3 k_{1i}^2} \mid z_i \mid^3 + \frac{1}{2\gamma_i} \tilde{\triangle}_i^2 \right], \qquad (6.15)
$$

where $\gamma_i > 0$ and $\tilde{\triangle}_i = \hat{\triangle}_i - \triangle_i$. Taking derivative of Lyapunov function (6.15):-

$$
\dot{V} = \sum_{i=1}^{m} \left[\dot{S}_i \left\{ k_{1i} \mid S_i \mid^{\frac{1}{2}} \operatorname{sign}(S_i) - z_i \right\} + \dot{z}_i \left\{ \frac{2}{k_{1i}^2} \mid z_i \mid^2 \operatorname{sign}(z_i) - S_i \right\} \right.
$$
$$
\left. + \frac{1}{\gamma_i} \tilde{\triangle}_i \dot{\hat{\triangle}}_i \right].
$$

Involving (6.7), (6.9) and (6.10):-

$$
\dot{V} = \sum_{i=1}^{m} \left[- \mid S_i \mid \left(k_{1i}^2 - k_{2i} \right) + 2 k_{1i} \mid S_i \mid^{\frac{1}{2}} \operatorname{sign}(S_i) z_i - \mid z_i \mid^2 + \tilde{\triangle}_i \right.
$$
$$
\left\{ \frac{1}{\gamma_i} \dot{\hat{\triangle}}_i - \Psi_i(x) \left(k_{1i} \mid S_i \mid^{\frac{1}{2}} \operatorname{sign}(S_i) - z_i \right) \right\} - \frac{2 k_{2i}}{k_{1i}^2} \mid z_i \mid^2 \operatorname{sign}(S_i z_i)
$$
$$
\left. + f_{ui}(x,t) \left(k_{1i} \mid S_i \mid^{\frac{1}{2}} \operatorname{sign}(S_i) - z_i \right) \right].
$$

Assuming that their are no uncertainties in the system i.e., $\tilde{\triangle}_i = 0$ and $f_{ui}(x,t) = 0$, we have:-

$$
\dot{V}_0 = \sum_{i=1}^{m} \left[-\mid S_i \mid \left(k_{1i}^2 - k_{2i} \right) + 2k_{1i} \mid S_i \mid^{\frac{1}{2}} \operatorname{sign}(S_i) z_i \right.
$$

$$
\left. - \mid z_i \mid^2 - \frac{2k_{2i}}{k_{1i}^2} \mid z_i \mid^2 \operatorname{sign}(S_i z_i) \right],
$$

$$
= \sum_{i=1}^{m} \left[-\mid S_i \mid \left(k_{1i}^2 - k_{2i} \right) + 2k_{1i} \mid S_i \mid^{\frac{1}{2}} \operatorname{sign}(S_i) z_i \right.
$$

$$
\left. - \mid z_i \mid^2 \left(1 + \frac{2k_{2i}}{k_{1i}^2} \operatorname{sign}(S_i z_i) \right) \right].
$$

Making assumptions:-

$$
\delta_{1i} = k_{1i}^2 - k_{2i}, \tag{6.16}
$$

$$
\delta_{2i} = 2k_{1i}, \tag{6.17}
$$

$$
\delta_{3i} = 1 - \frac{2k_{2i}}{k_{1i}^2}, \tag{6.18}
$$

$$
\delta_{4i} = 1 + \frac{2k_{2i}}{k_{1i}^2}. \tag{6.19}
$$

We get:-

$$
\dot{V}_0 \leq \sum_{i=1}^{m} \begin{bmatrix} -\delta_{1i} \mid S_i \mid + \delta_{2i} \mid S_i \mid^{\frac{1}{2}} \mid z_i \mid - \delta_{3i} \mid z_i \mid^2 & S_i z_i \geq 0 \\ -\delta_{1i} \mid S_i \mid - \delta_{2i} \mid S_i \mid^{\frac{1}{2}} \mid z_i \mid - \delta_{4i} \mid z_i \mid^2 & S_i z_i < 0 \end{bmatrix}. \tag{6.20}
$$

We can write (6.20) as:-

$$
\dot{V}_0 \leq \sum_{i=1}^{m} \begin{bmatrix} -\varsigma_i^T A_{1i} \varsigma_i & S_i z_i \geq 0 \\ -\varsigma_i^T A_{2i} \varsigma_i & S_i z_i < 0 \end{bmatrix},
$$

where

$$A_{1i} = \begin{bmatrix} \delta_{1i} & \frac{-\delta_{2i}}{2} \\ \frac{-\delta_{2i}}{2} & \delta_{3i} \end{bmatrix},$$

$$A_{2i} = \begin{bmatrix} \delta_{1i} & \frac{-\delta_{2i}}{2} \\ \frac{-\delta_{2i}}{2} & \delta_{4i} \end{bmatrix},$$

$$\varsigma_i^T = \begin{bmatrix} | S_i |^{\frac{1}{2}} \operatorname{sign}(S_i) & z_i \end{bmatrix}.$$

Selecting $k_{1i}^2 > 2k_{2i}$ matrices A_{1i} and A_{2i} become positive definite which shows negative definiteness of $\dot{V}_0$.

Now consider the case of non-zero uncertainties i.e., $\tilde{\triangle}_i \neq 0$ and $f_{ui}(x,t) \neq 0$,

$$\dot{V} = \dot{V}_0 + \sum_{i=1}^{m} \left[\tilde{\triangle}_i \left\{ \frac{1}{\gamma_i} \dot{\hat{\triangle}}_i - \Psi_i(x) \left(k_{1i} | S_i |^{\frac{1}{2}} \operatorname{sign}(S_i) - z_i \right) \right\} \right.$$
$$\left. + f_{ui}(x,t) \left(k_{1i} | S_i |^{\frac{1}{2}} \operatorname{sign}(S_i) - z_i \right) \right].$$

Taking

$$\dot{\hat{\triangle}}_i = \gamma_i \Psi_i(x) \left(k_{1i} | S_i |^{\frac{1}{2}} \operatorname{sign}(S_i) - z_i \right),$$

we are left with:-

$$\dot{V} \leq \dot{V}_0 + \sum_{i=1}^{m} \left[| f_{ui}(x,t) | \left(| k_{1i} | S_i |^{\frac{1}{2}} \operatorname{sign}(S_i) - z_i | \right) \right],$$

$$\leq \dot{V}_0 + \sum_{i=1}^{m} \left[\Gamma_i \| \varsigma_i \| | f_{ui}(x,t) | \right], \tag{6.21}$$

where $\Gamma_i = \sqrt{k_{1i}^2 + 1}$.

For $S_i z_i \geq 0$ the equation (6.21) can be written as:-

$$\dot{V} \leq \sum_{i=1}^{m} \left[-\varsigma_i^T A_{1i} \varsigma_i + \Gamma_i \|\varsigma_i\| \mid f_{ui}(x,t) \mid \right],$$

$$\leq \sum_{i=1}^{m} \left[-\lambda_i \|\varsigma_i\|^2 + \Gamma_i \|\varsigma_i\| \mid f_{ui}(x,t) \mid \right],$$

where $\lambda_i = \lambda_{im}\{A_{1i}\}$ represents the eigenvalue (minimum) of A_{1i}. $\dot{V}$ is negative whenever fulfills:-

$$\|\varsigma_i\| > \frac{\Gamma_i}{\lambda_i} \mid f_{ui}(x,t) \mid . \tag{6.22}$$

For $S_i z_i < 0$ the conditions for $\dot{V} < 0$ are [102]:-

$$\frac{\delta_{1i}}{k_{1i}} \mid S_i \mid^{\frac{1}{2}} + \frac{\delta_{3i}}{k_{1i}} \mid z_i \mid > \mid f_{ui}(x,t) \mid, \tag{6.23}$$

$$\delta_{2i} \mid S_i \mid^{\frac{1}{2}} + \delta_{4i} \mid z_i \mid > \mid f_{ui}(x,t) \mid, \tag{6.24}$$

where the constants δ_{1i}, δ_{2i}, δ_{3i} and δ_{4i} are chosen as in (6.16-6.19). For meeting inequalities (6.22-6.24) the absolute values of the state variables S_i and z_i have to be greater then certain values, so as to dominate the uncertainty $f_{ui}(x,t)$. As long as the inequalities (6.22-6.24) are fulfilled, $\dot{V} < 0$ and thus S_i and z_i converge to the origin. Each time these conditions are not met, $\dot{V}$ may turn into positive and S_i and z_i may then grow till inequalities (6.22-6.24) are satisfied again and resultantly $\dot{V}$ is negative. Hence, Lyapunov function V along with the state and estimation error variables remain bounded for all time.

If unstructured uncertainties are bounded as (6.8), than (6.22-6.24) can be reformulated as:-

$$
\begin{aligned}
\frac{\lambda_i}{\Gamma_i} &> \Omega_i, \\
\frac{\delta_{1i}}{k_{1i}} &> \Omega_i, \\
\delta_{2i} &> \Omega_i.
\end{aligned}
$$

The complete controller structure comes out to be:-

$$
\begin{aligned}
\bar{u}_i &= -k_{1i} \mid S_i \mid^{\frac{1}{2}} \operatorname{sign}(S_i) + z_i - \hat{\triangle}_i \Psi_i(x), \\
\dot{z}_i &= -k_{2i} \operatorname{sign}(S_i), \\
\dot{\hat{\triangle}}_i &= \gamma_i \Psi_i(x) \left(k_{1i} \mid S_i \mid^{\frac{1}{2}} \operatorname{sign}(S_i) - z_i \right).
\end{aligned}
$$

6.3.2 Reduced State Control Oriented Model for Controller Development

Reduced order engine model as proposed in Section 4.5 is used for controller development.

6.3.3 Output Set-Points

Output set-points are selected as W_{comp} and p_{em}. The set-points of λ_o and x_{egr} can be worked out and transformed into the set-points for W_{comp} and p_{em} using the procedure as described in Section 5.4.3.

6.3.4 Input/Output Linearization

With outputs as above, input/output linearization of model in Section 4.5 gives the system as described in Section 5.4.4.
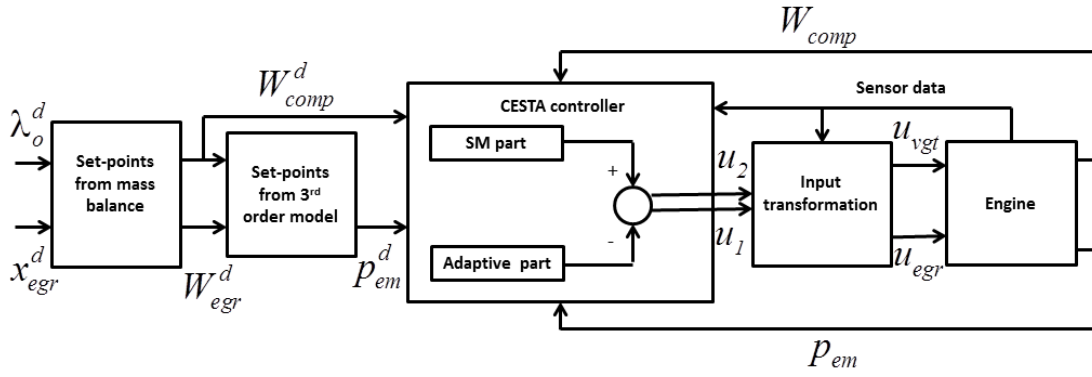
FIGURE 6.1: Block diagram - CESTA based controller

6.3.5   Control Law

Defining the sliding surfaces $S_1 = W_{comp} - W^d_{comp}$ and $S_2 = p_{em} - p^d_{em}$. The aim is to propose a CESTA based controller which ensures two sliding conditions $S_i = \dot{S}_i = 0$, for $i = 1, 2$ and guarantees $W_{comp} = W^d_{comp}$ and $p_{em} = p^d_{em}$ in the existence of actuators faults, parametric uncertainties and modelling errors. The overall control structure is shown in Figure 6.1. The dynamics of the sliding variables comes out to be:-

$$\dot{S}_1 = -\left(\frac{W_{comp}}{\tau}\right) - a\left(W_{comp} - k_e p_{im}\right) + bu_2 - au_1 - \Theta_1 - f_{u1}, \quad (6.25)$$

$$\dot{S}_2 = k_2\left(k_e p_{im} + W^d_f\right) - k_2 u_1 - k_2 u_2 - \Theta_2 - f_{u2}, \quad (6.26)$$

here $\Theta'_i s$ denote structured faults. The faults are, actuator getting chocked with soot or tar, leakages in the system resulting in exhaust gas escape, faulty actuation mechanisms that result in offset in actuator positions, wearing of actuator components due to erosion or corrosion and components getting coated with exhaust PM. In broader terms the fault effects can be segregated into two groups, overflow and under-flow through actuators. Structured faults can be represented in terms of flow rates as:-

$$\Theta_1 = \triangle_1 \Psi_1(x) = \triangle_1 W_{egr}, \quad (6.27)$$

$$\Theta_2 = \triangle_2 \Psi_2(x) = \triangle_2 W_t, \quad (6.28)$$

where Θ_1 denotes the under or over flow through EGR actuator, Θ_2 denotes the under or over flow through VGT actuator, $\Psi_1(x) = W_{egr}$, $\Psi_2(x) = W_t$. The terms $\triangle_1$ and $\triangle_2$ are percentage faults in EGR and VGT flow rates respectively, both are not known and unbounded. The $\triangle_i s$ will be estimated by adaptation law (6.13). *Apriori* knowledge about fault occurrence or fault bound is not needed. Algorithm itself detects the fault and estimates it's magnitude and type and compensates it's effects. Unstructured uncertainties are denoted as f_{u1} and f_{u2}. It is supposed that unstructured uncertainties are bounded as:-

$$
\begin{aligned}
\mid f_{u1}(x,t) \mid &\leq \Omega_1 \mid S_1(x) \mid^{\frac{1}{2}}, \\
\Omega_1 &> 0,
\end{aligned}
\tag{6.29}
$$

$$
\begin{aligned}
\mid f_{u2}(x,t) \mid &\leq \Omega_2 \mid S_2(x) \mid^{\frac{1}{2}}, \\
\Omega_2 &> 0.
\end{aligned}
\tag{6.30}
$$

The control action is proposed as (6.5). To calculate $u_i s$ ignoring perturbations/-faults in sliding variable dynamics:-

$$
\begin{aligned}
\dot{S}_1 &= -\left(\frac{W_{comp}}{\tau}\right) - a\left(W_{comp} - k_e p_{im}\right) + bu_2 - au_1, \\
\dot{S}_2 &= k_2\left(k_e p_{im} + W_f^d\right) - k_2 u_1 - k_2 u_2.
\end{aligned}
$$

We get:-

$$
u_1 = \frac{1}{a+b}\left[-W_{comp}\left(a + \frac{1}{\tau}\right) + (a+b)k_e p_{im} + bW_f^d - \bar{u}_1 - \frac{b}{k_2}\bar{u}_2\right], \tag{6.31}
$$

$$
u_2 = \frac{1}{a+b}\left[W_{comp}\left(a + \frac{1}{\tau}\right) + aW_f^d + \bar{u}_1 - \frac{a}{k_2}\bar{u}_2\right]. \tag{6.32}
$$

The $\bar{u}_i s$ are selected as proposed in Sub-section 6.3.1 and Sub-sub-section 6.3.1.1. Gains are selected ensuring $k_{1i} > \Omega_i$.

The controller structure and adaptation law as proposed in Sub-sub-section 6.3.1.2 will give more or less the same results.

6.3.6 Results and Discussion

The proposed FTC algorithm has been checked on full order model of a diesel engine as described in Section 4.4. An input transformation [99] is employed by reversing the EGR flow model and VGT flow model having position of actuators as the inputs and gas flow as the outputs. These inversions have given the new control inputs u_{egr} and u_{vgt} corresponding to u_1 and u_2, as explained in Section 4.6. The results of CESTA based controllers are compared with standard STA based controllers [4] having structure (6.5) and (6.33-6.34). The $u_i s$ are taken as (6.31-6.32), it is supposed that uncertainties $F_i(x,t)$ of the system (6.1-6.2) are bounded as $\mid F_i(x,t) \mid \leq \zeta_i \mid S_i(x) \mid^{\frac{1}{2}}$, where $\zeta_i > 0$. Fixed gains of standard STA based controller are chosen accordingly as $k_{1i} > \zeta_i$.

$$\bar{u}_i = -k_{1i} \mid S_i \mid^{\frac{1}{2}} \mathrm{sign}\,(S_i) + z_i, \tag{6.33}$$

$$\dot{z}_i = -k_{2i}\,\mathrm{sign}\,(S_i). \tag{6.34}$$
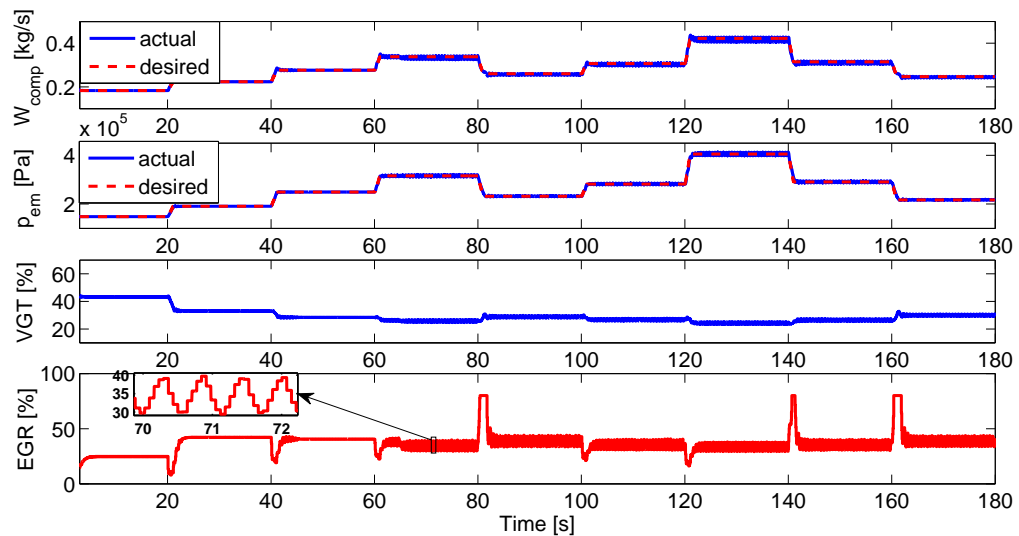
FIGURE 6.2: Results of standard STA, 10% error has been introduced in EGR flow rate at $t \geq 65$ seconds
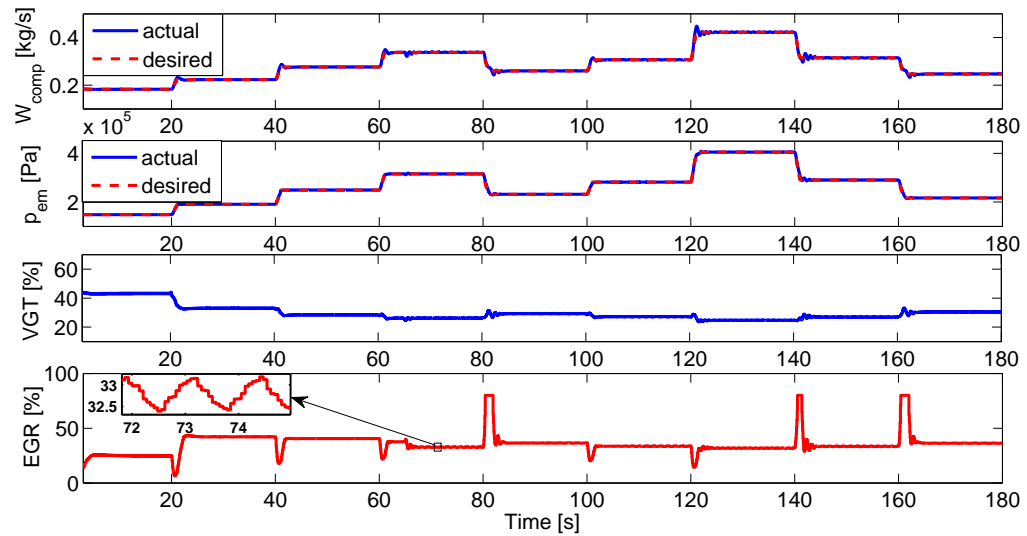
FIGURE 6.3: Results of CESTA, 10% error has been introduced in EGR flow rate at $t \geq 65$ seconds

The simulation results are shown by inducing a 10% error in EGR flow rate at $t \geq 65$ seconds, that depicts an over-flow case. Figure 6.2 and 6.3 illustrate the tracking performance of standard STA and CESTA based controllers respectively. The controller inputs u_{egr} and u_{vgt} are made to track W_{comp}^d and p_{em}^d respectively. In both cases, the controllers tracked the desired set-points successfully, however, in case of standard STA it has been observed that as the bounded fault is introduced in the system chattering increases. On the other hand CESTA based controller rejects the induced fault without creating excessive chattering, this is because, the presence of FDI module made fault detection, diagnoses and estimation possible, without any requirement of *apriori* knowledge. The effects of fault are minimized by re-positioning the actuators. The unstructured uncertainties are dealt with the fixed controller gains.
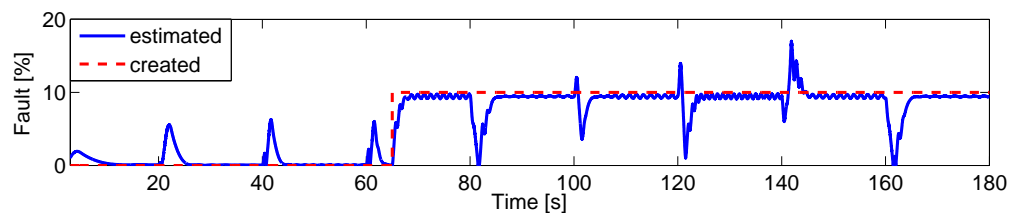
FIGURE 6.4: Results of CESTA, 10% error has been introduced in EGR flow rate at $t \geq 65$ seconds

Figure 6.4, with the same over-flow fault of 10% in EGR system, illustrate the estimated fault. "+ive" or "-ive" sign with $\hat{\triangle}_1$ provides the information regarding fault type i.e., over-flow or under-flow. Jumps in the result after every T seconds are visible. Changes in rpm or torque requirement affect the injected fuel quantity. This change desires for the new air and exhaust gas fractions. Controller re-positions EGR and VGT actuators to fulfill new requirements. The algorithm estimates this deficit or excess of exhaust gas fraction or air and take it as a fault. Same is depicted as spikes in the plot. This phenomenon has been observed even in no fault case. A small error between actual and estimated fault is the result of assumptions made while reducing the system's order for ease in controller development. It has been handled by controller gains.
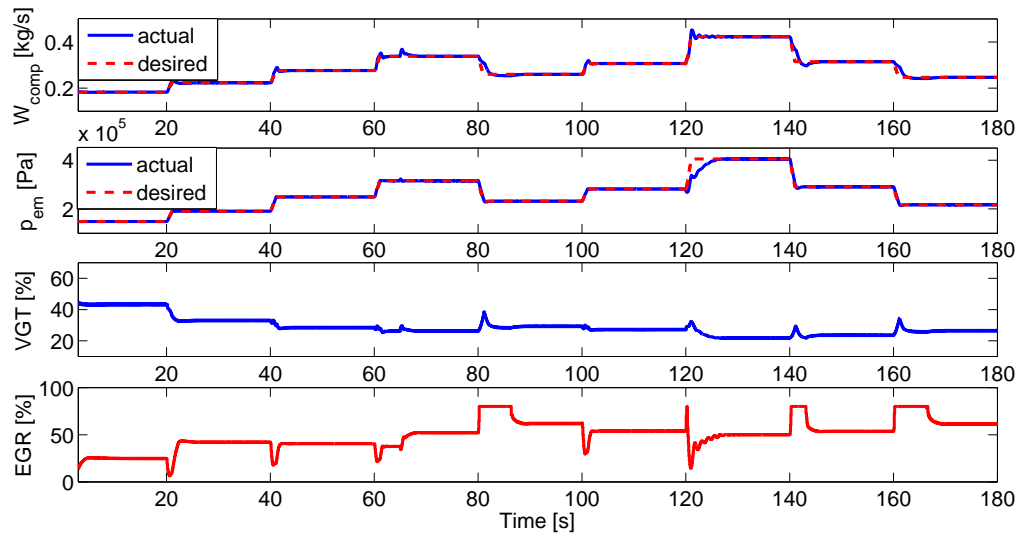
FIGURE 6.5: Results of CESTA, 20% error has been introduced in EGR flow rate at $t \geq 65$ seconds and 10% error in VGT flow rate at $t \geq 120$ seconds
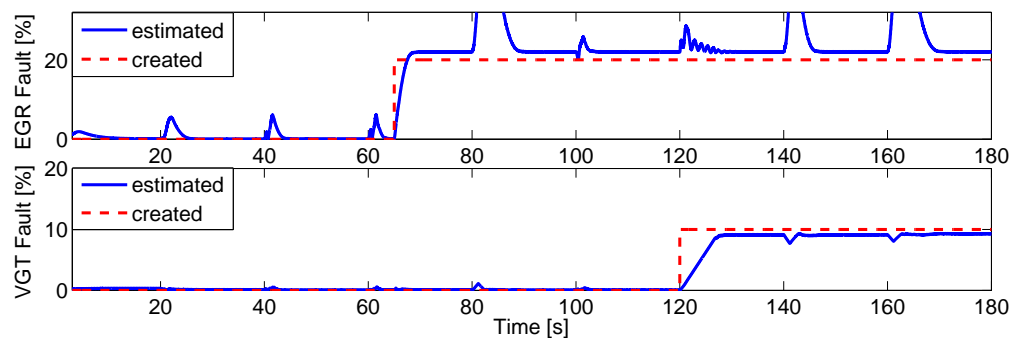
FIGURE 6.6: Results of CESTA, 20% error has been introduced in EGR flow rate at $t \geq 65$ seconds and 10% error in VGT flow rate at $t \geq 120$ seconds

Figure 6.5 and 6.6 illustrate the tracking results of CESTA based controller, when 20% under-flow fault has been induced in EGR flow rate at $t \geq 65$ seconds and 10% over-flow fault has been induced in VGT flow rate at $t \geq 120$ seconds. The occurrence of fault has been detected, its magnitude has been estimated. The fault effects are compensated, consequently, reducing the unwanted chattering. Re-positioning of actuators is evident from Figure 6.7. The controller will carry on with the compensation of the fault effects until actuators physical extremes, i.e., 0% or 100%, have been attained. Same is shown in Figure 6.8, the overflow of 0.065 kg/s has been induced in EGR flow at $t \geq 25$ seconds. For $25 \leq t \leq 60$ seconds and desired rpm, the requirement of EGR flow can be met by re-positioning the actuator. However, for $60 \leq t \leq 140$ seconds the actuator re-positions to nullify the effects of the fault, but it could not close lower than 0% position. Hence, could not track W_{comp}^d. However, effects of the faults are reduced by the controller. As the rpm of engine rises ($t \geq 140$ seconds), EGR actuator tracks the W_{comp} set-point successfully. Cases where complete actuator fails, will not be handled by this algorithm.
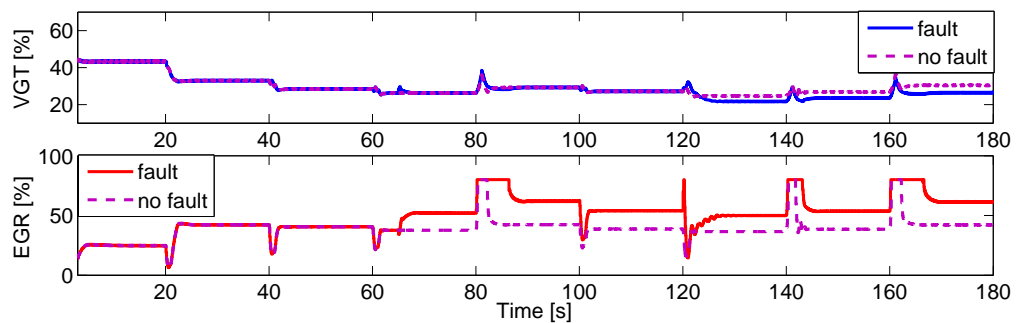
FIGURE 6.7: Results of CESTA, 20% error has been introduced in EGR flow rate at $t \geq 65$ seconds and 10% error in VGT flow rate at $t \geq 120$ seconds
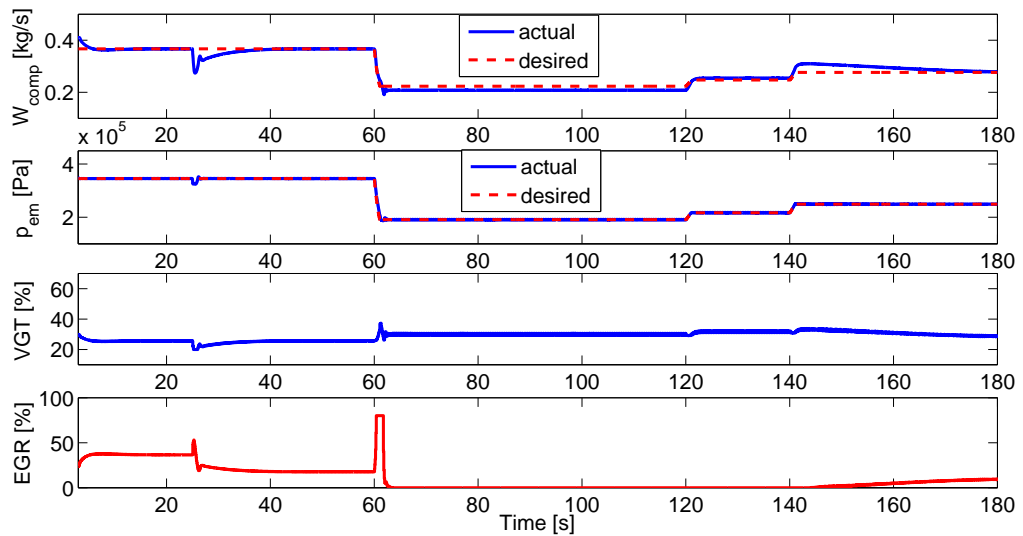
FIGURE 6.8: Results of CESTA, over-flow fault of 0.065 kg/s has been introduced in EGR flow rate at $t \geq 25$ seconds

6.4 ISM Extended with an Adaptive Part for FTC Development

In previous Section we have seen that unified FDI and FTC scheme based on CESTA has successfully removed the unwanted chattering caused by the actuator faults. The improvement in results is obvious as compared to standard STA and VGSTA based controllers. However, for the duration of reaching phase, before the establishment of sliding motion, system does not possess insensitivity to uncertainties [78]. The concept of ISM, on the other hand, concentrates on the robustness of the motion in the whole state space. Unified FDI and FTC scheme based on the concept of ISM will be explored in this Section. This will permit reduction of SM controller gains even in presence of actuator faults while preserving robustness all the way through an entire response of the system, beginning from the initial time instance. The algorithm will detect, diagnose and estimate the occurrence of faults with no requirement of any prior information about the faults or fault bounds and compensate fault effects by re-organizing the control effort, thus, reducing the chattering.

6.4.1 Controller Structure

To propose a controller that can ensure stable closed loop performance in the existence of uncertainties, SMC is considered to be one of the most effective techniques. However, the controller parameters are generally selected basing on the extreme case assumptions on the uncertainties. This results in higher controller gains and consequently chattering at the system's output that can harm the actuators [103]. The chattering grows with system faults. The chattering can be reduced by removing or reducing the uncertainties. This can be attained by using the information regarding the structure of the uncertainties. Conventional SM based techniques do not separate the uncertainties into structured and unstructured parts. Both classes of uncertainties are ruled out by choosing higher controller gains. The authors of [66] exploited the structure of uncertainties by the merger of adaptive control and STA. However, in reaching phase, the system owns no insensitivity to uncertainties [78]. The notion of ISM, on the other hand, ensures the robustness of the motion in the whole state space. This allows the reduction of controller gains even though the robustness is maintained during the complete system response starting from the initial time instance. Consider a MIMO non-linear system affected by some fault in input channel, represented as matched uncertainty:-

$$
\begin{aligned}
\dot{x}(t) &= f(x) + \sum_{i=1}^{m} g_i(x)(u_i + F_i(x,t)), \\
y_i &= h_i(x),
\end{aligned}
\tag{6.35}
$$

where $x(t) \in \mathbb{R}^n$, $u \in \mathbb{R}^m$ and $y \in \mathbb{R}^m$. The subscript i represents the input channel. Making an assumption that the vector fields $f(x)$ and $g_i(x)$ are known and smooth and $h_i(x)$ are known smooth functions, that are defined on an open subset in $\mathbb{R}^n$. The uncertain term $F_i(x,t)$ can be written as a sum of structured and unstructured parts:-

$$
F_i(x,t) = \vartheta_{si}(x) + \vartheta_{ui}(x,t).
\tag{6.36}
$$

Writing the structured uncertainty as a product of an unknown constant parameter $\triangle_i$ and a base function $\Xi_i(x)$, which is known:-

$$\vartheta_{si}(x) \;=\; \triangle_i \Xi_i(x).$$

Internal dynamics of the system (6.35) are assumed stable. Consider now the sliding surfaces:-

$$S_i \;=\; S_{oi}(x) + z_i,$$

where S_i, $S_{oi}(x)$ and $z_i \in \mathbb{R}^m$. S_{oi} is representing the sliding surface based on the conventional SM design. It has been assumed that the relative degrees of S_i with respect to u_i are one. The dynamics of sliding surfaces $(i = 1, \ldots, m)$ are:-

$$\dot{S}_i \;=\; \frac{\partial S_{oi}}{\partial x_i}[f_i(x) + \sum_{k=1}^{m} g_k(x)\{u_k + F_k(x,t)\}] + \dot{z}_i,$$

$$\dot{S}_i \;=\; \frac{\partial S_{oi}}{\partial x_i} f_i(x) + \frac{\partial S_{oi}}{\partial x_i} \sum_{k=1}^{m} g_k(x)\{u_k + F_k(x,t)\} + \dot{z}_i. \tag{6.37}$$

For $(i = 1 \ldots m)$ in compact form, we can write:-

$$\dot{S} \;=\; N(x) + G(x)(U + F) + \dot{Z}, \tag{6.38}$$

where $N(x) = \left[\frac{\partial S_{o1}}{\partial x_1} f_1(x) \ldots \frac{\partial S_{om}}{\partial x_m} f_m(x) \right]^T$, $G(x) = [G_1(x) \ldots G_m(x)]^T$, $\dot{Z} = [\dot{z}_1 \ldots \dot{z}_m]^T$

and $G_i(x)\{U + F\} = \frac{\partial S_{oi}}{\partial x_i} \sum_{k=1}^{m} g_k(x)\{u_k + F_k(x,t)\}.$

Ignoring uncertainties, $\dot{Z}$ (6.38), making assumption that $G^{-1}(x)$ exists and taking U as:-

$$U \;=\; G^{-1}(x)\{-N(x) + \bar{U}\}, \tag{6.39}$$

where $G^{-1}(x)\{-N(x)\}$ will handle the known terms and $\bar{U} = [\bar{u}_1....\bar{u}_m]^T$ will handle uncertain terms/actuator faults, with an assumption that actuator faults can be handled by re-positioning of particular faulty actuator (i.e., i^{th} actuator will handle fault in i^{th} channel).

This selection of U will decouple the system. By ignoring $\bar{U}$ in (6.39) the control U gives desired output for a nominal plant with no uncertainties or faults. Taking $\dot{Z}$ as:-

$$\dot{Z} \;=\; -N(x) - G(x)U. \tag{6.40}$$

The selection of $\dot{z}_i$ and initial condition $z_i(0) = -S_{oi}(0)$ will guarantee that reaching phase is eliminated and SM is imposed right from the start time in the absence of uncertainties. The left out system is:-

$$\dot{S}_i \;=\; F_i + \bar{u}_i, \tag{6.41}$$
$$\dot{S}_i \;=\; \triangle_i \Xi_i(x) + \vartheta_{ui}(x,t) + \bar{u}_i. \tag{6.42}$$

The unstructured uncertainty is supposed to be bounded as:-

$$\mid \vartheta_{ui}(x,t) \mid \;\leq\; \Omega_i \mid S_i(x) \mid^{\frac{1}{2}}, \tag{6.43}$$
$$\Omega_i \;>\; 0.$$

The controller $\bar{u}_i$ is taken as :-

$$\bar{u}_i \;=\; -M_i \mid S_i \mid^{\frac{1}{2}} \operatorname{sign}(S_i) - \hat{\triangle}_i \Xi_i(x), \tag{6.44}$$

where controller gains $M_i > 0$ allow to deal with the unstructured uncertainties and $\hat{\triangle}_i$ is the estimate of unknown parameters $\triangle_i$. It only remains to define the dynamics for $\hat{\triangle}_i$ for which the error $\triangle_i - \hat{\triangle}_i = 0$.

6.4.1.1 Lyapunov Stability Analysis

Consider the Lyapunov function:-

$$V = \sum_{i=1}^{m} \left[\mid S_i \mid + \frac{1}{2\gamma_i} \tilde{\triangle}_i^2 \right], \tag{6.45}$$

where $\gamma_i > 0$ and $\tilde{\triangle}_i = \hat{\triangle}_i - \triangle_i$. Taking time derivative of the Lyapunov function (6.45):-

$$\dot{V} = \sum_{i=1}^{m} \left[\text{sign}\,(S_i)\, \dot{S}_i + \frac{1}{\gamma_i} \tilde{\triangle}_i \dot{\hat{\triangle}}_i \right]. \tag{6.46}$$

Using (6.42-6.44) in (6.46):-

$$\dot{V} = \sum_{i=1}^{m} \left[\text{sign}\,(S_i) \{ \vartheta_{ui}(x,t) - M_i \mid S_i \mid^{\frac{1}{2}} \text{sign}\,(S_i) \right.$$

$$\left. - (\hat{\triangle}_i - \triangle_i) \Xi_i(x) \} + \frac{1}{\gamma_i} \tilde{\triangle}_i \dot{\hat{\triangle}}_i \right],$$

$$\dot{V} = \sum_{i=1}^{m} \left[\text{sign}\,(S_i) \{ \Omega_i \mid S_i \mid^{\frac{1}{2}} - M_i \mid S_i \mid^{\frac{1}{2}} \text{sign}\,(S_i) \} \right.$$

$$\left. + \tilde{\triangle}_i \left\{ -\text{sign}\,(S_i)\, \Xi_i(x) + \frac{1}{\gamma_i} \dot{\hat{\triangle}}_i \right\} \right].$$

If $\hat{\triangle}_i s$ are known, then $\tilde{\triangle}_i = 0$ and $\dot{V}$ becomes:-

$$\dot{V} \leq \sum_{i=1}^{m} [\mid S_i \mid^{\frac{1}{2}} \text{sign} (S_i) \{\Omega_i - M_i \text{sign} (S_i)\}].$$

Now selecting $M_i > \Omega_i$, $\dot{V}$ becomes negative. Hence, asymptotic stability of the closed loop system is established.

$\hat{\triangle}_i s$ are however not known, taking the adaptation law as:-

$$\dot{\hat{\triangle}}_i = \gamma_i \, \text{sign} (S_i) \, \Xi_i(x). \tag{6.47}$$

The value of adaptation parameter $\hat{\triangle}_i$ will remain close to zero in cases where their is no structured uncertainty or fault in the system. As soon as some fault affects the system, the value of adaptation parameter increases according to the fault magnitude, thus detecting the fault. Appropriate threshold is chosen to clarify the existence of the fault. The left over system is:-

$$\dot{V} \leq \sum_{i=1}^{m} [\mid S_i \mid^{\frac{1}{2}} \text{sign} (S_i) \{\Omega_i - M_i \text{sign} (S_i)\}].$$

Selecting $M_i > \Omega_i$, $\dot{V}$ becomes negative. The system (6.42 and 6.47) will converge to $S_i = 0$, with non-vanishing $\hat{\triangle}_i$. As, the internal dynamics with respect to the sliding surface are assumed stable, thus, all states of the closed loop system will be bounded. This concludes the stability analysis.

Remark 1: The Lyapunov function based adaptation law (6.47) may give the exact estimate of the fault and it does not demand any constraints on the structured uncertainty.

Remark 2: If the uncertainty can be separated into structured and unstructured parts (6.36), the controller gain can be reduced significantly.

6.4.2 Reduced State Control Oriented Model for Controller Development

Reduced order system model as highlighted in Section 4.5 is used for controller development.

6.4.3 Output Set-Points

Output set-points are selected as W_{comp} and p_{em}. The set-points of λ_o and x_{egr} can be worked out and transformed into the set-points for W_{comp} and p_{em} using the procedure as described in Section 5.4.3.

6.4.4 Input/Output Linearization

With outputs as above, input/output linearization of model in Section 4.5 gives the system as described in Section 5.4.4.
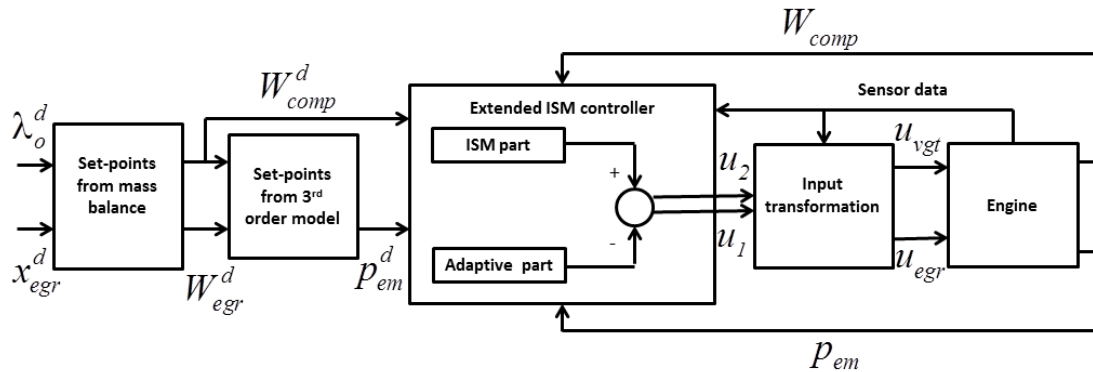
FIGURE 6.9: Block diagram - ISM extended with adaptive part, based controller

6.4.5 Control Law

Selecting the sliding surfaces $S_{o1} = y_1 = W_{comp} - W_{comp}^d$ and $S_{o2} = y_2 = p_{em} - p_{em}^d$. The aim is to synthesize an ISM based controller extended with an adaptive term, which meets two sliding requirements $S_i = \dot{S}_i = 0$, for $i = 1, 2$ and guarantees

$W_{comp} = W_{comp}^d$ and $p_{em} = p_{em}^d$ in the existence of actuators faults, parametric uncertainties and modelling errors. The overall control structure is shown in Figure 6.9. The dynamics of the sliding variables come out to be:-

$$\dot{S}_1 = -\left(\frac{W_{comp}}{\tau}\right) - a\left(W_{comp} - k_e p_{im}\right) + bu_2 - au_1 - \Theta_1 - \vartheta_{u1} + \dot{z}_1, \quad (6.48)$$

$$\dot{S}_2 = k_2\left(k_e p_{im} + W_f^d\right) - k_2 u_1 - k_2 u_2 - \Theta_2 - \vartheta_{u2} + \dot{z}_2, \quad (6.49)$$

here $\Theta_i, \quad i = 1, 2$ denote structured faults. The faults are, actuator getting chocked with soot or tar, leakages in the system resulting in exhaust gas escape, faulty actuation mechanisms that result in offset in actuator positions, wearing of actuator components due to erosion or corrosion and components getting coated with exhaust PM. In broader terms the fault effects can be segregated into two groups, over-flow and under-flow through actuators. Structured faults can be represented in terms of flow rates as:-

$$\Theta_1 = \triangle_1 \Xi_1(x) = \triangle_1 W_{egr}, \quad (6.50)$$

$$\Theta_2 = \triangle_2 \Xi_2(x) = \triangle_2 W_t, \quad (6.51)$$

where Θ_1 denotes the under or over flow through EGR actuator, Θ_2 denotes the under or over flow through VGT actuator, $\Xi_1(x) = W_{egr}$, $\Xi_2(x) = W_t$. The terms $\triangle_1$ and $\triangle_2$ are percentage faults in EGR and VGT flow rates respectively, both are not known and unbounded. The $\triangle_i, \quad i = 1, 2$ will be estimated by adaptation law (6.47). *Apriori* knowledge about fault occurrence or fault bound is not needed. Algorithm itself detects the fault, estimates it's magnitude and type and compensates it's effects. Unstructured uncertainties are denoted as ϑ_{u1} and ϑ_{u2}. It is supposed that unstructured uncertainties are bounded (6.43):-

$$| \vartheta_{u1}(x, t) | \leq \Omega_1 | S_1(x) |^{\frac{1}{2}},$$

$$\Omega_1 > 0,$$

$$| \vartheta_{u2}(x, t) | \leq \Omega_2 | S_2(x) |^{\frac{1}{2}},$$

$$\Omega_2 > 0.$$

The control action is proposed as (6.39). To work out the control (u_i), ignoring uncertain terms and $\dot{z}_i$ in (6.48-6.49):-

$$
\begin{aligned}
\dot{S}_{o1} &= -\left(\frac{W_{comp}}{\tau}\right) - a\left(W_{comp} - k_e p_{im}\right) + bu_2 - au_1, \\
\dot{S}_{o2} &= k_2\left(k_e p_{im} + W_f^d\right) - k_2 u_1 - k_2 u_2.
\end{aligned}
$$

Taking $u_i, \ i = 1, 2$ as:-

$$
\begin{aligned}
u_1 &= \frac{1}{a+b}\left[-W_{comp}\left(a + \frac{1}{\tau}\right) + (a+b)k_e p_{im} + bW_f^d - \bar{u}_1 - \frac{b}{k_2}\bar{u}_2\right], \\
u_2 &= \frac{1}{a+b}\left[W_{comp}\left(a + \frac{1}{\tau}\right) + aW_f^d + \bar{u}_1 - \frac{a}{k_2}\bar{u}_2\right].
\end{aligned}
$$

$\dot{z}_i, \ i = 1, 2$ are taken as (6.40) where $z_i(0) = -S_{oi}(x_i(0))$ and $\bar{u}_i$ components of $u_i, \ i = 1, 2$ are ignored:-

$$
\begin{aligned}
\dot{z}_1 &= \left(\frac{W_{comp}}{\tau}\right) + a\left(W_{comp} - k_e p_{im}\right) - bu_2 + au_1, \\
\dot{z}_2 &= -k_2\left(k_e p_{im} + W_f^d\right) + k_2 u_1 + k_2 u_2.
\end{aligned}
$$

This choice of $\dot{z}_i$ and $z_i(0)$ will ensure that SM has been enforced from the initial time instant. For the left out system (6.42) with unstructured uncertainties as (6.43) and structured uncertainties as (6.50-6.51), the $\bar{u}_i, \ i = 1, 2$ are chosen as proposed in (6.44). Adaptation laws are chosen as (6.47). Gains M_i of $\bar{u}_i$ are chosen ensuring $M_i > \Omega_i$.

When continuous disturbances are present in the system, like very high frequency vibrations, tracking errors or actuator faults, the error may get added up in the sliding surfaces due to the integral term z_i. To avoid buildup of error Ioannou's σ-term [104] is used, widely referred to as forgetting term:-

$$
\dot{z}_i = \dot{z}_i - \sigma z_i.
$$

6.4.6 Results and Discussion

The proposed FTC algorithm has been checked on full order model of a diesel engine as defined in Section 4.4. A non-linear input transformation [99] is employed by reversing the EGR flow model and VGT flow model which have position of actuators as the inputs and gas flows as the outputs. These inversions have given the new control inputs u_{egr} and u_{vgt} corresponding to u_1 and u_2, as explained in Section 4.6. The results of controller based on ISM extended with adaptive part are compared with standard ISM based controller where uncertainties in (6.35) are assumed to be bounded as $\mid F_i(x,t) \mid \leq \varsigma_i \mid S_i(x) \mid^{\frac{1}{2}}$ with $\varsigma_i > 0$. The structure of the controller is taken as (6.39), where $\bar{u}_i = -M_i \mid S_i \mid^{\frac{1}{2}} \text{sign}(S_i)$. The gains are selected as $M_i > \varsigma_i$.
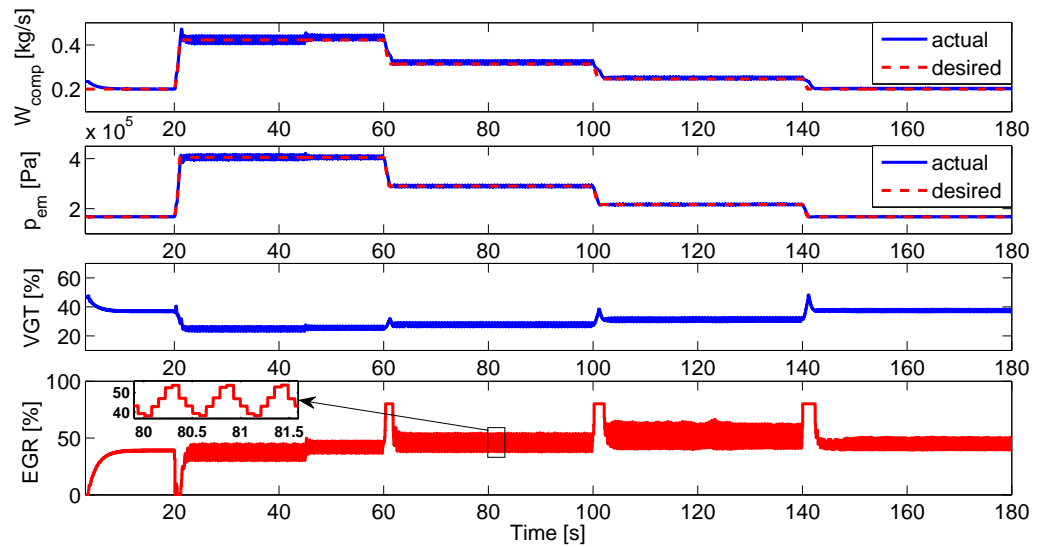
FIGURE 6.10: Results of standard ISM, 15% error has been introduced in EGR flow rate at $t \geq 45$ seconds
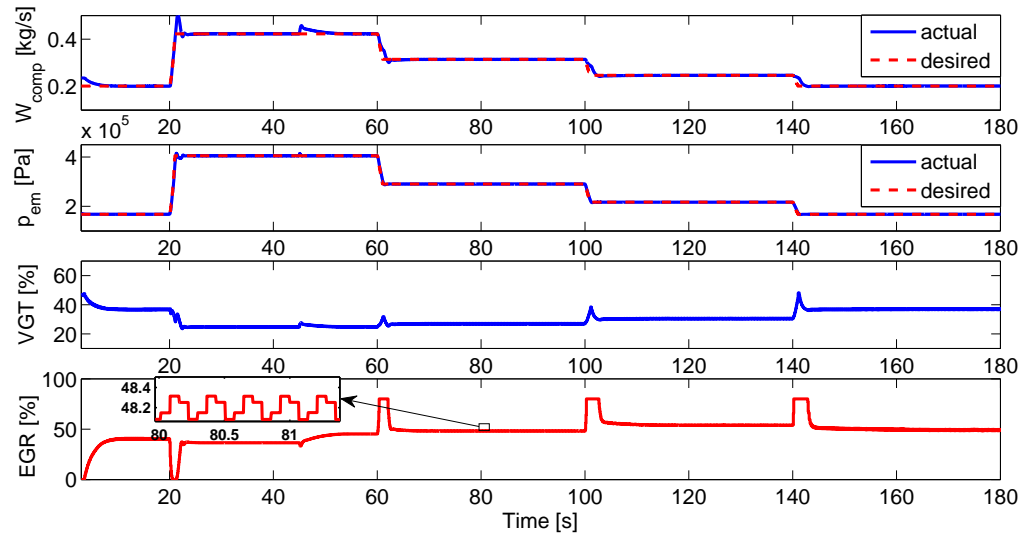
FIGURE 6.11: Results of ISM extended with adaptive part, 15% error has been
introduced in EGR flow rate at $t \geq 45$ seconds

The simulation results are shown by inducing a 15% error in EGR flow rate at $t \geq 45$ seconds, that depicts an over-flow case. Figure 6.10 and 6.11 show the tracking performance of standard ISM and ISM extended with an adaptive part based controllers respectively. The controller inputs u_{egr} and u_{vgt} are made to track W^d_{comp} and p^d_{em} respectively. In both cases, the controllers tracked the desired set-points successfully, however, in case of standard ISM based controller it has been observed that as the bounded fault is introduced in the system chattering increases. On the other hand ISM extended with an adaptive part based controller rejects the induced fault without creating excessive chattering, this is because, the presence of FDI module made fault detection, diagnoses and estimation possible, without any requirement of *apriori* knowledge. The fault effects are minimized by re-positioning the actuators. The unstructured uncertainties are dealt with the fixed controller gains.
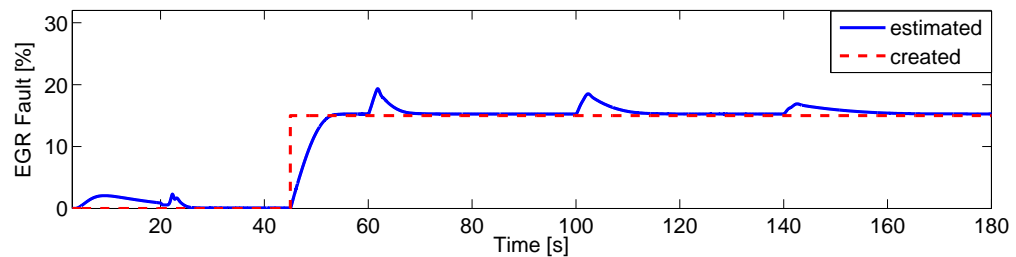
FIGURE 6.12: Results of ISM extended with adaptive part, 15% error has been introduced in EGR flow rate at $t \geq 45$ seconds

Figure 6.12, with the same over-flow fault of 15% in EGR system, illustrate the estimated fault. "+ive" or "-ive" sign provides the information regarding fault type i.e., over-flow or under-flow. Jumps in the result after every T seconds are visible. Changes in rpm or torque requirements affect the injected fuel quantity. This change desires for the new air and exhaust gas fractions. Controller repositions EGR and VGT actuators to fulfill new requirements. The algorithm estimates this deficit or excess of exhaust gas fraction or air and take it as a fault. Same is depicted as spikes in the plot. This phenomenon has been observed even in no fault case. A small error between actual and estimated fault is the result of assumptions made while reducing the system's order for ease in controller development. It has been handled by controller gains.

Figure 6.13 and 6.14 illustrate the tracking results of ISM based controller extended with an adaptive part with 20% under-flow fault has been induced in EGR flow rate at $t \geq 65$ seconds and 10% over-flow fault has been induced in VGT flow rate at $t \geq 120$ seconds. The occurrence of fault has been detected, its magnitude has been estimated. The fault effects are compensated, consequently, reducing the unwanted chattering. Re-positioning of actuators is evident form the Figure 6.15. Figure 6.16 depicts the sliding surfaces, clearly the reaching phase has been eliminated by the use of ISM based controller.
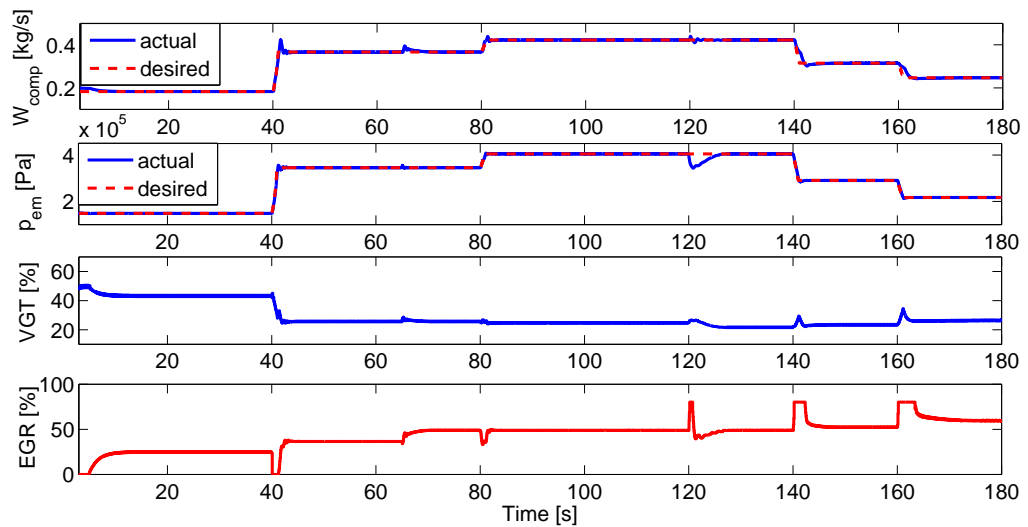
FIGURE 6.13: Results of ISM extended with adaptive part, 20% error has been introduced in EGR flow rate $t \geq 65$ seconds and 10% in VGT flow rate at $t \geq 120$ seconds
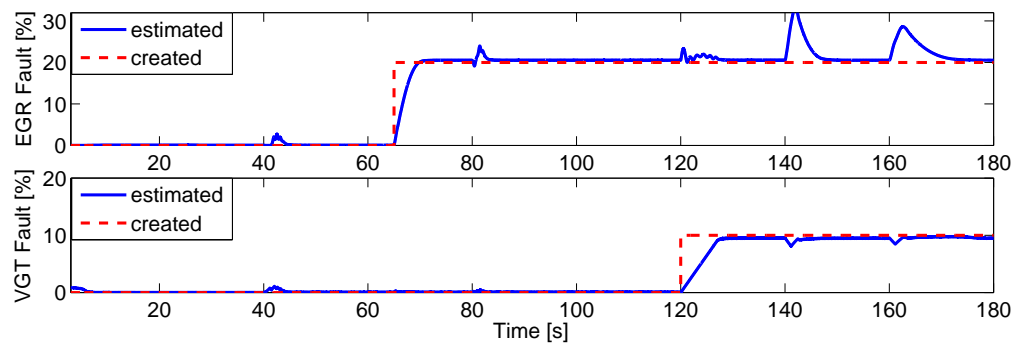
FIGURE 6.14: Results of ISM extended with adaptive part, 20% error has been introduced in EGR flow rate $t \geq 65$ seconds and 10% in VGT flow rate at $t \geq 120$ seconds
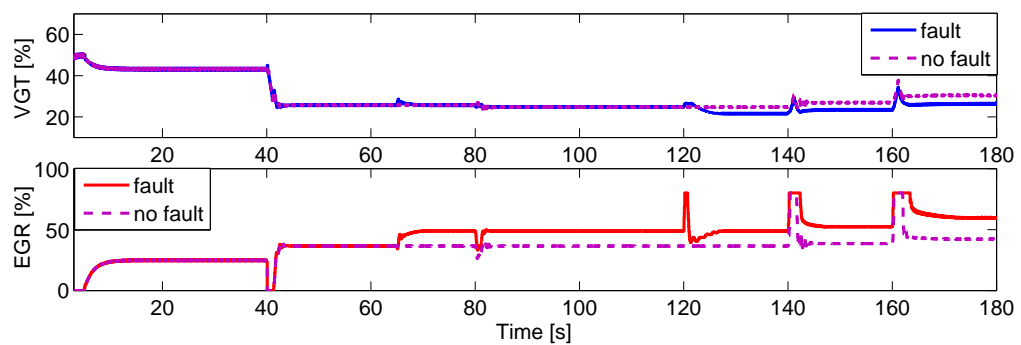
FIGURE 6.15: Results of ISM extended with adaptive part, 20% error has been introduced in EGR flow rate $t \geq 65$ seconds and 10% in VGT flow rate at $t \geq 120$ seconds
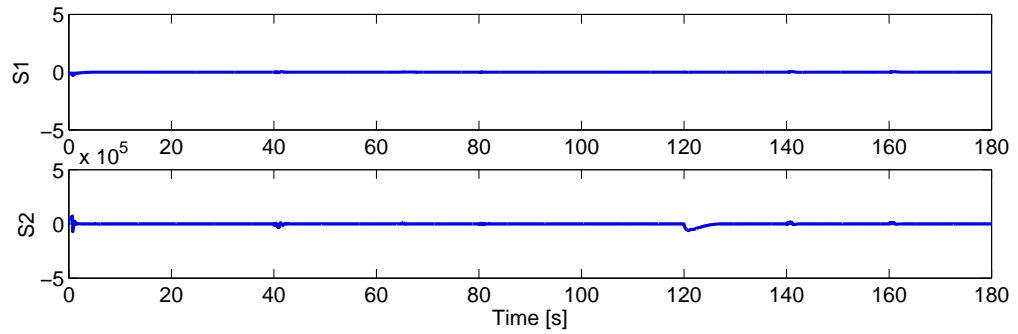
FIGURE 6.16: Results of ISM extended with adaptive part, 20% error has been introduced in EGR flow rate $t \geq 65$ seconds and 10% in VGT flow rate at $t \geq 120$ seconds
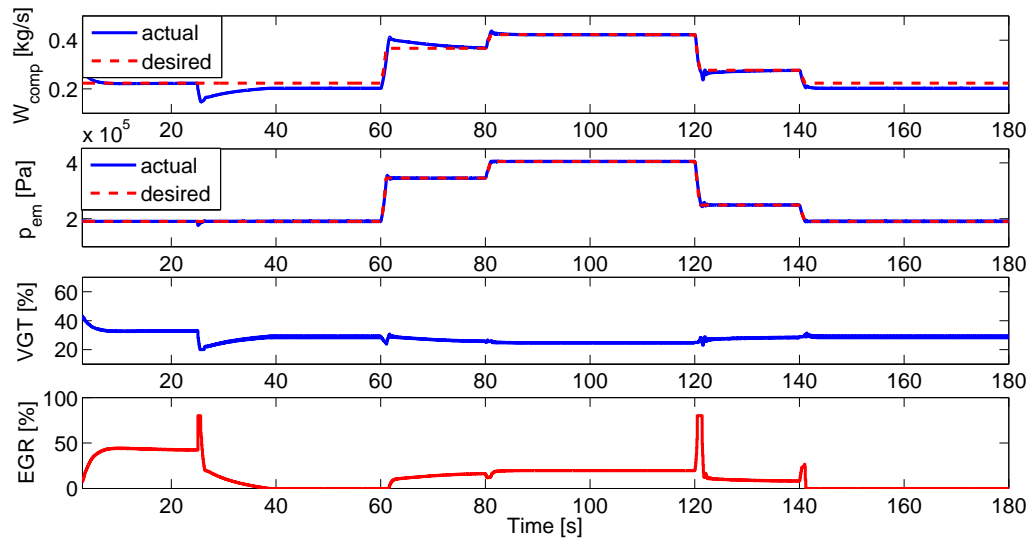
FIGURE 6.17: Results of ISM extended with adaptive part, over-flow fault of .07 kg/s has been introduced in EGR flow rate at $t \geq 25$ seconds

The controller will carry on with the compensation of the fault effects until actuators physical extremes, i.e., 0% or 100%, have been attained. Same is shown in Figure 6.17, where the fault depicting the EGR actuator leakage has been introduced. The actuator re-positions to nullify the effects of the fault, but it could not close lower than 0% position. Hence, could not track W_{comp}^d. However, effects of the fault are minimized by the controller. As the engine rpm rises (60-140 seconds), EGR actuator tracks the W_{comp} set-point successfully.

6.5   Chapter Summary

In this Chapter two FTC schemes for air management system of a diesel engine have been formulated, basing on the system's mathematical model. Initially CESTA based FTC approach has been discussed in detail. It has been seen that the adaptation law successfully estimated the induced structured faults with no requirement of *apriori* information for an upper bound on the fault. The effects of the induced faults have been compensated by the proposed controller. However, the CESTA based controller does not guarantee system's invariance to uncertainties during reaching phase. In order to overcome this short coming, an ISM based algorithm extended with an adaptive term has been proposed to develop a MIMO control law for EGR and VGT actuators. The performance of the controller is found satisfactory. The use of ISM ensured robustness throughout the system response starting from the initial time instance by eliminating the reaching phase. The simulation results have shown that in spite of simple structure, both the proposed controllers can meet strict emission regulations, even in the event of system faults with much less chattering as compared to the passive FTC schemes.

Chapter 7

Summary, Conclusion and Recommendations

We have proposed to investigate model based FTC for emission management of diesel engine. SM frame work based schemes are used to develop MIMO fault tolerant algorithms to control VGT and EGR actuators. The control structures have been discussed in detail with implementation, analysis and results. In spite of simplicity, the proposed control structures have the capability to fulfill strict emission standards even in the event of system faults. The faults include actuator getting chocked with soot or tar, leakages in the system resulting in exhaust gas escape, faulty actuation mechanisms that result in offset in actuator positions, wearing of actuator components due to erosion or corrosion and components getting coated with exhaust PM etc. These faults introduce a permanent error in actuators which can affect tracking of set-points. It has been observed that if the system functions with passive FTC schemes, minor additive or multiplicative faults in the actuators or process can be handled by introducing robustness properties in the control action. As the magnitude of fault increases, the passive schemes fail to provide the desired objectives, as the increased chattering makes implementation of such schemes impractical. Though the use of VGSTA based controller has reduced the chattering as compared to STA based controller, still chattering exists. Secondly, the requirement of *apriori* knowledge about the fault

bound is one of the major constraints in the passive schemes. On the other hand, the use of FDI module with FTC scheme helps in fault detection, estimation and compensation with no requirement of prior knowledge about an upper bound on the fault. Especially, the use of unified FDI and FTC schemes give the desired objectives swiftly with much less chattering as compared to the passive FTC schemes. Same has been investigated in CESTA and ISM extended with adaptive part based controllers, where the controllers have estimated the induced faults and successfully eliminated the fault effects by re-positioning the actuators. Some of the features of designed controllers and their comparison with existing diesel engine air management system FTC schemes are compared in the Table 7.1. The comparison validates the superior performance of CESTA and ISM extended with adaptive part based controllers, being active schemes.

The designed controllers have effectively tracked the desired set-points. Few observations are:-

1. Chattering is higher in cases of passive schemes, which further increases with the increase in fault magnitude. Thus passive schemes are only useful if fault magnitudes are relatively lower.

2. *Apriori* knowledge about fault bound is essentially required for implementation of passive schemes, as they do not use FDI module.

3. The use of FDI module in support of FTC scheme helps in fault detection, diagnosis and estimation with no requirement of any prior information about the faults or fault bounds.

4. The use of unified approach guarantees swift integration of FDI and FTC schemes, thus ensuring desired system performance under all situations.

5. The estimation of faults help compensating their effects by re-organizing the control effort, thus, reducing the chattering.

6. The use of ISM based technique guarantees robustness throughout the system response starting from the initial time instance by eliminating the reaching phase.

TABLE 7.1: Comparison of FTC approaches.

Technique	Type of FTC	Controller Gains	Controllers	FDI	Fault Estimation	Fault Bound	Fault Types	Chattering
STA [4]	passive	fixed	u_{egr}, u_{vgt}	no	no	yes	minor	high
VGSTA [5]	passive	variable	u_{egr}, u_{vgt}	no	no	yes	minor	moderate
CESTA [6]	active	fixed	u_{egr}, u_{vgt}	yes	yes	no	medium	low
ISM extended [7]	active	fixed	u_{egr}, u_{vgt}	yes	yes	no	medium	low
STA [55]	passive	fixed	W_{egr}, W_{vgt}	no	no	yes	minor	high
AISMC [52]	passive	adaptive	W_{egr}, W_{vgt}	no	no	yes	minor	moderate
STA [54]	passive	fixed	W_{egr}, W_{vgt}	no	no	yes	minor	high
STA [53]	passive	adaptive	W_{egr}, W_{vgt}	no	no	no	minor	moderate

7.1 Future Works

Some of the works that are not addressed in this manuscript are:-

1. Reduced order diesel engine model is used for development of FDI-FTC schemes. Use of full order model for development of these schemes will definitely improve results. However, this will be requiring re-establishment of stability of hidden dynamics, which may be higher in case of full order model.

2. Only actuator faults have been addressed. It has been assumed that rest of the system is fault free. Effect of sensor faults on overall system performance needs further exploration. This can be done by combining fault detection techniques with supervisory control and on-line controller re-configuration to accommodate faults. There is an abundance of literature on fault diagnosis that ranges from analytical approaches to statistical methodologies including artificial intelligence. The approaches as proposed in [1, 9–11] may be helpful in this direction.

3. Permanent failure cases of actuators i.e., jammed actuators have not been addressed, same may be explored. This can be done by re-planing the tracking set-points so as to track a new controlled variable i.e., oxygen concentration in the intake manifold instead of the compressor flow. Fundamental thermodynamic laws can be used to work out new set-points. The approach as proposed in [105] may be useful for further work in this direction.

4. In this work it has been assumed that fuel is available from a separate controller. Quantity of injected fuel contributes in exhaust emissions, for instance, rich mixture produces PM and unburnt HCs. Design of a fuel controller with an aim of ensuring fuel economy and minimized emissions especially in cases of faults, may be explored in conjunction with FTC design for air path actuators.

Bibliography

[1] Y. Zhang and J. Jiang, "Bibliographical review on reconfigurable fault-tolerant control systems," *Annual reviews in control*, vol. 32, no. 2, pp. 229–252, 2008.

[2] R. Isermann, *Combustion engine diagnosis.* Springer Berlin, pp. 109-111, 2016.

[3] "Partially chocked actuator, downloaded 11 jan 2016, (available from URL: https://axleaddict.com/auto-repair/bad-egr-valve-symptoms-and-what-to-do-about-them)."

[4] G. Murtaza, Y. A. Butt, and A. I. Bhatti, "Higher order sliding mode based control scheme for air path of diesel engine," in *International Conference on Emerging Technologies (ICET), Isb, Pak*, Oct 2016, pp. 1–6.

[5] G. Murtaza, A. I. Bhatti, and Y. A. Butt, "FTC for air path actuators of a diesel engine using VGSTA," in *13th International Conference on Emerging Technologies (ICET), Isb, Pak.* IEEE, 2017, pp. 1–6.

[6] G. Murtaza, A. I. Bhatti, and Y. A. Butt, "Super twisting controller-based unified FDI and FTC scheme for air path of diesel engine using the certainty equivalence principle," *Proceedings of the Institution of Mechanical Engineers, Part D: Journal of Automobile Engineering*, vol. 232, no. 12, pp. 1623–1633, 2018.

[7] G. Murtaza, A. I. Bhatti, and Y. A. Butt, "Unified FDI and FTC scheme for air path actuators of a diesel engine using ISM extended with adaptive part," *Asian Journal of Control (Accepted)*, 2019.

[8] I. Hwang, S. Kim, Y. Kim, and C. E. Seah, "A survey of fault detection, isolation, and reconfiguration methods," *IEEE transactions on control systems technology*, vol. 18, no. 3, pp. 636–653, 2010.

[9] V. Venkatasubramanian, R. Rengaswamy, K. Yin, and S. N. Kavuri, "A review of process fault detection and diagnosis: Part I: Quantitative model-based methods," *Computers & chemical engineering*, vol. 27, no. 3, pp. 293–311, 2003.

[10] V. Venkatasubramanian, R. Rengaswamy, K. Yin, and S. N. Kavuri, "A review of process fault detection and diagnosis: Part II: Quantitative model-based methods," *Computers & chemical engineering*, vol. 27, no. 3, pp. 313–326, 2003.

[11] V. Venkatasubramanian, R. Rengaswamy, S. N. Kavuri, and K. Yin, "A review of process fault detection and diagnosis: Part III: Process history based methods," *Computers & chemical engineering*, vol. 27, no. 3, pp. 327–346, 2003.

[12] R. Isermann, "Fault diagnosis of machines via parameter estimation and knowledge processingtutorial paper," *Automatica*, vol. 29, no. 4, pp. 815–835, 1993.

[13] Z. Gao, C. Cecati, and S. X. Ding, "A survey of fault diagnosis and fault-tolerant techniques part I: Fault diagnosis with model-based and signal-based approaches," *IEEE Transactions on Industrial Electronics*, vol. 62, no. 6, pp. 3757–3767, 2015.

[14] K. Watanabe, S. Hirota, L. Hou, and D. Himmelblau, "Diagnosis of multiple simultaneous fault via hierarchical artificial neural networks," *AIChE Journal*, vol. 40, no. 5, pp. 839–848, 1994.

[15] R. Vaidyanathan and V. Venkatasubramanian, "Representing and diagnosing dynamic process data using neural networks," *Engineering Applications of Artificial Intelligence*, vol. 5, no. 1, pp. 11–21, 1992.

[16] J. V. Kresta, J. F. MacGregor, and T. E. Marlin, "Multivariate statistical monitoring of process operating performance," *The Canadian journal of chemical engineering*, vol. 69, no. 1, pp. 35–47, 1991.

[17] J. F. MacGregor and T. Kourti, "Statistical process control of multivariate processes," *Control Engineering Practice*, vol. 3, no. 3, pp. 403–414, 1995.

[18] B. M. Wise and N. B. Gallagher, "The process chemometrics approach to process monitoring and fault detection," *Journal of Process Control*, vol. 6, no. 6, pp. 329–348, 1996.

[19] R. Dunia, S. J. Qin, T. F. Edgar, and T. J. McAvoy, "Identification of faulty sensors using principal component analysis," *AIChE Journal*, vol. 42, no. 10, pp. 2797–2812, 1996.

[20] W. J. Staszewski, K. Worden, and G. R. Tomlinson, "Time–frequency analysis in gearbox fault detection using the wigner–ville distribution and pattern recognition," *Mechanical systems and signal processing*, vol. 11, no. 5, pp. 673–692, 1997.

[21] P. M. Frank, "Advanced fault detection and isolation schemes using nonlinear and robust observers," *IFAC Proceedings Volumes*, vol. 20, no. 5, pp. 63–68, 1987.

[22] P. M. Frank, "Enhancement of robustness in observer-based fault detection," *International Journal of control*, vol. 59, no. 4, pp. 955–981, 1994.

[23] R. Patton and J. Chen, "Observer-based fault detection and isolation: Robustness and applications," *Control Engineering Practice*, vol. 5, no. 5, pp. 671–682, 1997.

[24] R. J. Patton, P. M. Frank, and R. N. Clarke, *Fault diagnosis in dynamic systems: theory and application.* Prentice-Hall, Inc., pp. 325-333, 1989.

[25] R. Patton and J. Chen, "A review of parity space approaches to fault diagnosis," in *IFAC/IMACS safeprocess conference, Baden, Germany*, 1991, pp. 65–81.

[26] J. Gertler, "Fault detection and isolation using parity relations," *Control engineering practice*, vol. 5, no. 5, pp. 653–661, 1997.

[27] R. Isermann, "Process fault detection based on modeling and estimation methodsa survey," *automatica*, vol. 20, no. 4, pp. 387–404, 1984.

[28] X. Ding and P. M. Frank, "Fault detection via factorization approach," *Systems & control letters*, vol. 14, no. 5, pp. 431–436, 1990.

[29] P. M. Frank and X. Ding, "Frequency domain approach to optimally robust residual generation and evaluation for model-based fault diagnosis," *Automatica*, vol. 30, no. 5, pp. 789–804, 1994.

[30] S. Ding, *Model-based fault diagnosis techniques: design schemes, algorithms, and tools.* Springer Science & Business Media, pp. 144-148, 2008.

[31] J. Gertler, *Fault detection and diagnosis in engineering systems.* CRC press, pp. 45-55, 1998.

[32] D. Upadhyay, V. I. Utkin, and G. Rizzoni, "Multivariable control design for intake flow regulation of a diesel engine using sliding mode," *IFAC Proceedings Volumes*, vol. 35, no. 1, pp. 277–282, 2002.

[33] J. Wahlström, L. Eriksson, L. Nielsen, and M. Pettersson, "PID controllers and their tuning for EGR and VGT control in diesel engines," *IFAC Proceedings Volumes*, vol. 38, no. 1, pp. 212–217, 2005.

[34] J. Wahlstrom, L. Eriksson, and L. Nielsen, "EGR-VGT control and tuning for pumping work minimization and emission control," *IEEE Transactions on Control Systems Technology*, vol. 18, no. 4, pp. 993–1003, 2010.

[35] J. Wahlström and L. Eriksson, "Nonlinear EGR and VGT control with integral action for diesel engines," *Oil & Gas Science and Technology–Revue d'IFP Energies nouvelles*, vol. 66, no. 4, pp. 573–586, 2011.

[36] M. Jankovic and I. Kolmanovsky, "Robust nonlinear controller for turbocharged diesel engines," in *American Control Conference, Philadelphia, USA*, vol. 3. IEEE, 1998, pp. 1389–1394.

[37] M. Jankovic and I. Kolmanovsky, "Constructive Lyapunov control design for turbocharged diesel engines," *IEEE Transactions on Control Systems Technology*, vol. 8, no. 2, pp. 288–299, 2000.

[38] P. Ortner, P. Langthaler, J. V. G. Ortiz, and L. del Re, "MPC for a diesel engine air path using an explicit approach for constraint systems," in *IEEE Conference on Computer Aided Control System Design, IEEE International Conference on Control Applications, IEEE International Symposium on Intelligent Control, Munich, Germany.* IEEE, 2006, pp. 2760–2765.

[39] M. Herceg, T. Raff, R. Findeisen, and F. Allgowe, "Nonlinear model predictive control of a turbocharged diesel engine," in *IEEE Conference on Computer Aided Control System Design, IEEE International Conference on Control Applications, IEEE International Symposium on Intelligent Control, Munich, Germany.* IEEE, 2006, pp. 2766–2771.

[40] G. Stewart and F. Borrelli, "A model predictive control framework for industrial turbodiesel engine control," in *47th IEEE Conference on Decision and Control, CDC, Cancun, Mexico.* IEEE, 2008, pp. 5704–5711.

[41] P. Ortner, R. Bergmann, H. J. Ferreau, and L. Del Re, "Nonlinear model predictive control of a diesel engine airpath," *IFAC Proceedings Volumes*, vol. 42, no. 2, pp. 91–96, 2009.

[42] M. Karlsson, K. Ekholm, P. Strandh, R. Johansson, and P. Tunestål, "Multiple-input multiple-output model predictive control of a diesel engine," *IFAC Proceedings Volumes*, vol. 43, no. 7, pp. 131–136, 2010.

[43] J. Wahlström and L. Eriksson, "Output selection and its implications for MPC of EGR and VGT in diesel engines," *IEEE Transactions on Control Systems Technology*, vol. 21, no. 3, pp. 932–940, 2013.

[44] J. Richalet, "Industrial applications of model based predictive control," *Automatica*, vol. 29, no. 5, pp. 1251–1274, 1993.

[45] D. Q. Mayne and H. Michalska, "Receding horizon control of nonlinear systems," *IEEE Transactions on automatic control*, vol. 35, no. 7, pp. 814–824, 1990.

[46] V. Utkin, H. C. Chang, I. Kolmanovsky, and J. A. Cook, "Sliding mode control for variable geometry turbocharged diesel engines," in *American Control Conference, Chicago, USA*, vol. 1, no. 6. IEEE, 2000, pp. 584–588.

[47] J. Wang, "Hybrid robust air-path control for diesel engines operating conventional and low temperature combustion modes," *IEEE Transactions on Control Systems Technology*, vol. 16, no. 6, pp. 1138–1151, 2008.

[48] S. Larguech, S. Aloui, O. Pagès, A. El Hajjaji, and A. Chaari, "Adaptive sliding mode control for a class of nonlinear MIMO systems: application to a turbocharged diesel engine," in *22nd Mediterranean Conference of Control and Automation (MED), Palermo, Italy*. IEEE, 2014, pp. 1205–1210.

[49] M. Ammann, N. P. Fekete, L. Guzzella, and A. Glattfelder, "Model-based control of the VGT and EGR in a turbocharged common-rail diesel engine: theory and passenger car implementation," *SAE Technical Paper*, pp. 865–875, 2003.

[50] X. Wei and L. del Re, "Gain scheduled control for air path systems of diesel engines using lpv techniques," *IEEE transactions on control systems technology*, vol. 15, no. 3, pp. 406–415, 2007.

[51] M. Jung and K. Glover, "Calibratable linear parameter-varying control of a turbocharged diesel engine," *IEEE Transactions on control systems technology*, vol. 14, no. 1, pp. 45–62, 2006.

[52] S. A. Ali and N. Langlois, "Passive fault tolerant control strategy using adaptive sliding mode control. application to diesel engine air path," in *Australian Control Conference (AUCC), Sydney, Australia*. IEEE, 2012, pp. 186–191.

[53] S. A. Ali and N. Langlois, "Sliding mode control for diesel engine air path subject to matched and unmatched disturbances using extended state observer," *Mathematical Problems in Engineering*, vol. 1, pp. 1–11, 2013.

[54] S. A. Ali, N. Langlois *et al.*, "Fault tolerant control design based higher-order sliding mode control for Internal Combustion engine," in *3rd International Symposium on Environmental Friendly Energies and Applications (EFEA),St. Ouen, France.* IEEE, 2014, pp. 1–6.

[55] S. A. Ali, M. Guermouche, and N. Langlois, "Fault-tolerant control based Super-Twisting algorithm for the diesel engine air path subject to loss-of-effectiveness and additive actuator faults," *Applied Mathematical Modelling*, vol. 39, no. 15, pp. 4309–4329, 2015.

[56] M. Guermouche, S. A. Ali, and N. Langlois, "An Adaptive Integral Sliding Mode Control Design for Internal Combustion Engine Air Path," *IFAC Proceedings Volumes*, vol. 46, no. 25, pp. 87–94, 2013.

[57] I. Djemili, A. Aitouche, and V. Cocquempot, "Fault tolerant control of internal combustion engine subject to intake manifold leakage," *IFAC Proceedings Volumes*, vol. 45, no. 20, pp. 600–605, 2012.

[58] J. Burton and A. S. Zinober, "Continuous approximation of variable structure control," *International journal of systems science*, vol. 17, no. 6, pp. 875–885, 1986.

[59] K. D. Young, V. I. Utkin, and U. Ozguner, "A control engineer's guide to sliding mode control," in *IEEE International Workshop on Variable Structure Systems, Tokyo, Japan.* IEEE, 1996, pp. 1–14.

[60] H. Sira-Ramirez, O. Llanes-Santiago, and N. A. Fernandez, "On the stabilization of nonlinear systems via input-dependent sliding surfaces," *International Journal of Robust and Nonlinear Control*, vol. 6, no. 8, pp. 771–780, 1996.

[61] M. L. Tseng and M. S. Chen, "Chattering reduction of sliding mode control by low-pass filtering the control signal," *Asian Journal of control*, vol. 12, no. 3, pp. 392–398, 2010.

[62] V. I. Utkin, "Sliding mode control design principles and applications to electric drives," *IEEE transactions on industrial electronics*, vol. 40, no. 1, pp. 23–36, 1993.

[63] G. Bartolini, A. Levant, A. Pisano, and E. Usai, "Higher-order sliding modes for the output-feedback control of nonlinear uncertain systems," in *Variable structure systems: towards the 21st century*. Springer, 2002, pp. 83–108.

[64] T. Gonzalez, J. A. Moreno, and L. Fridman, "Variable gain super-twisting sliding mode control," *IEEE Transactions on Automatic Control*, vol. 57, no. 8, pp. 2100–2105, 2012.

[65] M. K. Bera, B. Bandyopadhyay, and A. Paul, "Variable Gain Super-Twisting Control of GMAW Process for Pipeline Welding," *Journal of Dynamic Systems, Measurement, and Control*, vol. 137, no. 7, p. 074501, 2015.

[66] A. Barth, M. Reichhartinger, J. Reger, and et al., "Lyapunov-design for a super-twisting sliding-mode controller using the certainty-equivalence principle," *IFAC-PapersOnLine*, vol. 48, no. 11, pp. 860–865, 2015.

[67] G. Bartolini, "A robust control design for a class of uncertain non-linear systems featuring a second-order sliding mode," *International Journal of Control*, vol. 72, no. 4, pp. 321–331, 1999.

[68] A. Levant, "Sliding order and sliding accuracy in sliding mode control," *International journal of control*, vol. 58, no. 6, pp. 1247–1263, 1993.

[69] L. Fridman and A. Levant, "Higher order sliding modes," *Sliding mode control in engineering*, vol. 11, pp. 53–102, 2002.

[70] J. J. Slotine and J. Coetsee, "Adaptive sliding controller synthesis for nonlinear systems," *International Journal of Control*, vol. 43, no. 6, pp. 1631–1651, 1986.

[71] D. S. Yoo and M. J. Chung, "A variable structure control with simple adaptation laws for upper bounds on the norm of the uncertainties," *IEEE Transactions on Automatic Control*, vol. 37, no. 6, pp. 860–865, 1992.

[72] B. L. Walcott and S. H. Zak, "Combined observer-controller synthesis for uncertain dynamical systems with applications," *IEEE Transactions on systems, man, and cybernetics*, vol. 18, no. 1, pp. 88–104, 1988.

[73] R. Aguilar-López and R. Maya-Yescas, "State estimation for nonlinear systems under model uncertainties: a class of sliding-mode observers," *Journal of Process Control*, vol. 15, no. 3, pp. 363–370, 2005.

[74] L. Jiang and Q. Wu, "Nonlinear adaptive control via sliding-mode state and perturbation observer," *IEE Proceedings-Control Theory and Applications*, vol. 149, no. 4, pp. 269–277, 2002.

[75] D. Yoo, S. T. Yau, and Z. Gao, "Optimal fast tracking observer bandwidth of the linear extended state observer," *International Journal of Control*, vol. 80, no. 1, pp. 102–111, 2007.

[76] T. H. Chang and Y. Hurmuzlu, "Sliding control without reaching phase and its application to bipedal locomotion," *Transactions-American Society of Mechanical Engineers Journal of Dynamic Systems Measurement and Control*, vol. 115, pp. 447–447, 1993.

[77] S. B. Choi, D. W. Park, and S. Jayasuriya, "A time-varying sliding surface for fast and robust tracking control of second-order uncertain systems," *Automatica*, vol. 30, no. 5, pp. 899–904, 1994.

[78] V. I. Utkin and J. Shi, "Integral sliding mode in systems operating under uncertainty conditions," in *Proceedings of the 35th IEEE Conference on Decision and Control, Kobe, Japan*, vol. 4.   IEEE, 1996, pp. 4591–4596.

[79] V. Utkin, J. Guldner, and J. Shi, *Sliding mode control in electro-mechanical systems*.   CRC press, pp. 75-77, 2009.

[80] A. Isidori, *Nonlinear control systems.* Springer Science & Business Media, pp. 509-511, 2013.

[81] S. Emalyanov, S. Korovin, and L. Levantovsky, "Higher order sliding modes in the binary control system," in *Soviet Physics, Doklady*, vol. 31, no. 4, 1986, pp. 291–293.

[82] H. Sira-Ramírez, "On the sliding mode control of nonlinear systems," *Systems & control letters*, vol. 19, no. 4, pp. 303–312, 1992.

[83] G. Bartolini, A. Pisano, E. Punta, and E. Usai, "A survey of applications of second-order sliding mode control to mechanical systems," *International Journal of control*, vol. 76, no. 9-10, pp. 875–892, 2003.

[84] L. Fridman and A. Levant, "Higher order sliding modes as a natural phenomenon in control theory," in *Robust Control via variable structure and Lyapunov techniques.* Springer, 1996, pp. 107–133.

[85] S. Emel'Yanov, S. Korovin, and A. Levant, "High-order sliding modes in control systems," *Computational mathematics and modeling*, vol. 7, no. 3, pp. 294–318, 1996.

[86] S. Emelyanov, S. Korovin, and L. Levantovskiy, "A drift algorithm in control of uncertain processes." *Prob. Control Info. Theory.*, vol. 15, no. 6, pp. 425–438, 1986.

[87] D. Upadhyay, "Modeling and model based control design of the VGT-EGR system for intake flow regulation in diesel engines," Ph.D. dissertation, The Ohio State University, pp. 45-49, 2001.

[88] M. Jung and K. Glover, "Control-oriented linear parameter-varying modelling of a turbocharged diesel engine," in *Proceedings of IEEE Conference on Control Applications, Istanbul, Turkey*, vol. 1. IEEE, 2003, pp. 155–160.

[89] B. Unver, Y. Koyuncuoglu, M. Gokasan, and S. Bogosyan, "Modeling and validation of turbocharged diesel engine airpath and combustion systems,"

International Journal of Automotive Technology, vol. 17, no. 1, pp. 13–34, 2016.

[90] J. Wahlström and L. Eriksson, "Modelling diesel engines with a variable-geometry turbocharger and exhaust gas recirculation by optimization of model parameters for capturing non-linear system dynamics," *Proceedings of the Institution of Mechanical Engineers, Part D: Journal of Automobile Engineering*, vol. 225, no. 7, pp. 960–986, 2011.

[91] "Software packages from vehicular systems, 2010, downloaded 5 march 2015, (available from URL: http://www.fs.isy.liu.se/software)."

[92] J. Wahlström, "Control of EGR and VGT for emission control and pumping work minimization in diesel engines," Ph.D. dissertation, Institutionen för systemteknik, pp. 117-144. 2009.

[93] Heywood and J. B, *Internal combustion engine fundamentals.* Mcgraw-hill New York, pp. 34-36, 1988, vol. 930.

[94] J. Wahlström, "System analysis of a diesel engine with VGT and EGR," Ph.D. dissertation, Institutionen för systemteknik, pp. 79-110, 2009.

[95] R. Skelton, M. Oliveira, and J. Han, "Systems modeling and model reduction," *Invited chapter in the handbook of smart systems and materials*, 2004, Paper downloaded 17 June 2015, (available from URL: http://maeweb.ucsd.edu/skelton/publications).

[96] S. Volkwein, "Proper orthogonal decomposition: Theory and reduced-order modelling," *Lecture Notes, University of Konstanz*, vol. 4, no. 4, pp. 114–124, 2013.

[97] Z. Bai, "Krylov subspace techniques for reduced-order modeling of large-scale dynamical systems," *Applied numerical mathematics*, vol. 43, no. 1-2, pp. 9–44, 2002.

[98] D. J. Lucia, P. S. Beran, and W. A. Silva, "Reduced-order modeling: new approaches for computational physics," *Progress in Aerospace Sciences*, vol. 40, no. 1, pp. 51–117, 2004.

[99] J. Wahlström and L. Eriksson, "Nonlinear input transformation for EGR and VGT control in diesel engines," *SAE International Journal of Engines*, vol. 3, no. 2010-01-2203, pp. 288–305, 2010.

[100] A. Pisano and E. Usai, "Sliding mode control: A survey with applications in math," *Mathematics and Computers in Simulation*, vol. 81, no. 5, pp. 954–979, 2011.

[101] A. G. Stefanopoulou, I. Kolmanovsky, and J. S. Freudenberg, "Control of variable geometry turbocharged diesel engines for reduced emissions," *IEEE transactions on control systems technology*, vol. 8, no. 4, pp. 733–745, 2000.

[102] A. Barth, M. Reichhartinger, J. Reger, M. Horn, and K. Wulff, "Certainty-equivalence based super-twisting control using continuous adaptation laws," in *14th International Workshop on Variable Structure Systems (VSS), 2016, Nanjing, China.* IEEE, 2016, pp. 92–97.

[103] V. I. Utkin and H. Lee, "Chattering problem in sliding mode control systems," in *International Workshop on Variable Structure Systems, 2006. VSS'06, Alghero, Italy.* IEEE, 2006, pp. 346–350.

[104] P. A. Ioannou and P. V. Kokotovic, "Adaptive systems with reduced models," *Volume 47 of Lecture Notes in Control and Information Sciences*, pp. 23–25, 1983.

[105] R. Nitsche, M. Bitzer, M. El Khaldi, and G. Bloch, "Fault tolerant oxygen control of a diesel engine air system," *IFAC Proceedings Volumes*, vol. 43, no. 7, pp. 578–583, 2010.